



ADVANCED MASTERS IN STRUCTURAL ANALYSIS
OF MONUMENTS AND HISTORICAL CONSTRUCTIONS

Master's Thesis

Juan Murcia

**Seismic Analysis of Santa Maria
del Mar Church in Barcelona.**



UNIVERSITAT POLITÈCNICA
DE CATALUNYA



University of Minho



Education and Culture

Erasmus Mundus



ADVANCED MASTERS IN STRUCTURAL ANALYSIS
OF MONUMENTS AND HISTORICAL CONSTRUCTIONS



Master's Thesis

Juan Murcia

Seismic Analysis of Santa Maria del Mar Church in Barcelona.

This Masters Course has been funded with support from the European Commission. This publication reflects the views only of the author, and the Commission cannot be held responsible for any use which may be made of the information contained therein.

DECLARATION

Name: Juan Murcia Delso
Email: jmurciad@yahoo.com
ID nº: 46765139K

Title of the Msc Dissertation: Seismic Analysis of Santa Maria del mar Church in Barcelona
Supervisor(s): Pere Roca Fabregat
Year: 2008

I hereby declare that the MSc Consortium responsible for the Advanced Masters in Structural Analysis of Monuments and Historical Constructions is allowed to store and make available electronically the present MSc Dissertation.

University: Technical University of Catalonia (UPC)
Date: 20th July 2008
Signature:

A Mercedes

Acknowledgement

I would like to acknowledge the support I got from my supervisor Professor Pere Roca Fabregat, who gave me the opportunity to work in this incredibly beautiful building in a very interesting subject.

Many thanks go to Luca Pelà, who helped me a lot using COMET.

I would like to express my gratitude to the Msc Consortium and the Erasmus Mundus Programme for the opportunity to participate in this Master and the financial support.

Last but not least, I would like to sincerely thank to all the friends I made in Guimarães and Barcelona for all the moments we shared.

ABSTRACT

Seismic Analysis of Santa Maria del Mar Church in Barcelona

Author: Juan Murcia Delso
Supervisor: Pere Roca Fabregat

Santa Maria del Mar is an architectural jewel built in only 50 years in a pure and sober Gothic style. Built in the 14th Century, the building includes very interesting structural innovations shared only, among all Gothic construction, by the Barcelona and Mallorca cathedrals. This building is characterized by having 3 naves and no transept, creating a very big internal space due to very slender columns and large span vaults.

The church has experienced some damage in the past due to two earthquakes (1373 and 1428), causing the collapse of some elements: rose window and upper part of one of the towers. Besides this, the structure is not thought to have suffered considerable damages due to past earthquakes. Due to these past damages, to the slender characteristics of the structure and the cultural relevance of this construction, the seismic behaviour of Santa Maria del Mar Church has already been analysed. The previous structural analysis have pointed out that the structure might show only limited seismic strength due to the slenderness of the structural members and the large dimension of its vaults. According to the static nonlinear pushover analysis, the typical bay would be able to stand a ground acceleration of 0.09g to 0.14g (depending on the author and method used). However, only slight to moderate damages would be expected in the structure due to the design earthquake in Barcelona.

A more accurate structural analysis has been carried out in this work, taking advantage of the availability of new precise data about the morphology of the structure. A tension-compression damage model has been used to carry out a nonlinear Finite Element Analysis (FEA) in the typical bay of the building. Based in the theory of continuum damage, it takes into account the different behaviour of masonry under tension and compression.

The FEA of the structure subjected to gravity load revealed that the typical bay shows almost no damage and that it has an elevated safety margin (it could stand a load up to 3 times its self weight). The seismic behaviour of the structure was studied by means of a static nonlinear pushover analysis. According to this simplified method, the structure would be able to resist a ground acceleration of 0.12g. As a result of a sensitivity analysis, assuming a realistic value for the fracture energy was found necessary to estimate accurately the capacity of the structure. In addition, possible light and respectful strengthening strategies were simulated, but no improvement was found in the seismic performance of the structure.

The Capacity Spectrum Method was applied in order to evaluate the expected damage of the structure. The FEA didn't work well for applying this method as it didn't provide a complete capacity spectrum up to the ultimate displacement. The treatment of the structure as a continuum didn't permit to monitor the capacity curve when it is already a mechanism that rotates. In any case, the performance point was found next to the linear range, so only slight to moderate damages would be expected.

As a conclusion of this study, the structure of Santa Maria del Mar Church can be considered as safe and strong enough to resist the seismic action with acceptable levels of damage. The historical evidence and the inspection reflect not important damages due to earthquakes in the past. The numerical analysis showed that the structure could resist perfectly the seismic action in Barcelona, and the damages would be reduced and assumable.

RESUM

Anàlisi Sísmica de l'Església de Santa Maria del Mar a Barcelona

Autor: Juan Murcia Delso
Tutor: Pere Roca Fabregat

Santa Maria del Mar és una joia arquitectònica construïda en només 50 anys en un estil gòtic pur i sobri. Acabada a finals del segle XIV, l'edifici inclou innovacions estructurals molt interessants compartides només, entre totes les construccions gòtiques, amb les catedrals de Barcelona i Mallorca. Aquest edifici es caracteritza per tenir 3 naus i no tenir creuer, creant un espai interior molt ampli gràcies a uns pilars molt esvelts i unes voltes amb grans llums.

L'església ha experimentat algun dany en el passat a causa de dos terratrèmols (1373 i 1428), que provocaren la caiguda d'alguns elements: la rosassa i la part superior d'una de les torres. A banda d'això, l'estructura no ha patit danys considerables per l'efecte dels terratrèmols. Degut als danys anteriors, a l'esveltesa de l'estructura i a la seva rellevància cultural, el comportament sísmic de Santa Maria del Mar ha estat ja estudiat. Les anàlisis estructurals prèvies han posat de relleu que l'estructura té una resistència sísmica limitada, com a causa de l'esveltesa dels seus membres estructurals i les dimensions de les voltes. D'acord amb una anàlisi no lineal de l'empenta (*pushover*), la crugia tipus podria suportar una acceleració del terreny entre 0.09g i 0.14g (depenent dels autors i del mètode emprat). Tanmateix, només danys lleugers a moderats estan previstos a l'estructura pel sísmic de disseny de Barcelona.

En aquest treball s'ha dut a terme una anàlisi estructural més acurada, aprofitant noves dades més precises sobre la morfologia de l'estructura. S'ha utilitzat un model de dany de tracció – compressió per a realitzar una Anàlisi per Elements Finites en la crugia tipus de l'edifici. Basat en la teoria del dany, té en compte el comportament diferenciat de l'obra de fàbrica a tracció i compressió.

L'Anàlisi per Elements Finites de l'estructura sota càrrega gravitatòria mostra que la crugia tipus pràcticament no pateix gairebé dany i té un marge de seguretat elevat (podria resistir fins a càrrega 3 cops el seu propi pes). El comportament sísmic de l'estructura ha estat estudiat amb una anàlisi estàtica no lineal de l'empenta (*pushover*). D'acord amb aquest mètode simplificat, l'estructura seria capaç de resistir una acceleració del terreny de 0.12g. Com a resultat d'una anàlisi de sensibilitat, es conclou que és necessari assumir un valor realista de la energia de fractura per tal d'estimar de forma precisa la capacitat de l'estructura. A més a més, s'han simulat possibles tècniques de reforç lleugeres i respectuoses amb els principis moderns de conservació; però no s'ha trobat cap que millorés el comportament sísmic de l'estructura.

El Mètode de l'Espectre de Capacitat ha estat aplicat per tal d'avaluar el dany previst a l'estructura. L'Anàlisi per Elements Finites no ha funcionat bé per aplicar aquest mètode ja que no proporciona una corba de capacitat completa fins al desplaçament últim. El fet de tractar l'estructura com un continu no permet monitorar el corba de capacitat quan aquesta ja és un mecanisme que rota. En qualsevol cas, el punt de funcionament es troba a prop del rang lineal, de manera que només es preveu un dany de lleuger a moderat.

Com a conclusió de l'estudi, l'estructura de l'Església de Santa Maria del Mar es pot considerar segura i prou resistent com per suportar l'acció sísmica amb un nivell de dany acceptable. Les evidències històriques i la inspecció realitzada reflecteixen danys poc importants a causa de terratrèmols en el passat. L'anàlisi numèrica mostra que l'estructura pot resistir perfectament l'acció sísmica a Barcelona, essent els danys reduïts i assumibles.

RESUMEN

Análisis Sísmico de la Iglesia de Santa María del Mar en Barcelona

Autor: Juan Murcia Delso
Tutor: Pere Roca Fabregat

Santa María del Mar es una joya arquitectónica construida en sólo 50 años en un estilo gótico puro y sobrio. Construida en el siglo XIV, el edificio incluye innovaciones estructurales muy interesantes compartidas sólo, entre todas las construcciones góticas, con las catedrales de Barcelona y Mallorca. Este edificio se caracteriza por tener 3 naves y no tener crucero, creando un espacio interior muy amplio gracias a unos pilares muy esbeltos y unas bóvedas de grandes luces.

La iglesia ha experimentado algún daño en el pasado a causa de dos terremotos (1373 y 1428), que provocaron la caída de algunos elementos: el rosetón y la parte superior de una de las torres. A parte de esto, la estructura no ha sufrido daños considerables por efecto de los terremotos. Debido a los daños anteriores, a la esbeltez de la estructura y a su relevancia cultural, el comportamiento sísmico de Santa María del Mar ha sido ya estudiado. Los análisis estructurales previos han puesto de manifiesto que la estructura tiene una capacidad sísmica limitada, a causa de la esbeltez de sus miembros estructurales y las dimensiones de las bóvedas. De acuerdo con un análisis estático no lineal de empuje (*pushover*), la cruja tipo podría soportar una aceleración del terreno de entre 0.09g y 0.14g (dependiendo del autor y el método usado). Sin embargo, sólo daños leves a moderados están previstos en la estructura para el sismo de diseño de Barcelona.

En este trabajo se ha llevado a cabo un análisis estructural más exacto, aprovechando nuevos datos más precisos sobre la morfología de la estructura. Se ha utilizado un modelo de daño de tracción – compresión para realizar un Análisis por Elementos Finitos de la cruja tipo del edificio. Basado en la teoría del daño, tiene en cuenta el comportamiento diferenciado de la obra de fábrica a tracción y compresión.

El Análisis por Elementos Finitos de la estructura bajo carga gravitatoria muestra que la cruja tipo prácticamente no sufre ningún daño y tiene un margen de seguridad elevado (podría resistir hasta 3 veces su peso propio). El comportamiento sísmico de la estructura ha sido estudiado a través de un análisis estático no lineal del empuje (*pushover*). De acuerdo con este método simplificado, la estructura sería capaz de resistir una aceleración del terreno de 0.12g. Como resultado de un análisis de sensibilidad, se concluye que es necesario asumir un valor realista de la energía de fractura para estimar de forma precisa la capacidad de la estructura. Además, se han simulado posibles técnicas de refuerzo ligeras y respetuosas con los principios modernos de conservación; pero no se ha encontrado ninguna que mejorase el comportamiento sísmico de la estructura.

El Método del Espectro de Capacidad ha sido aplicado para evaluar el daño previsto en la estructura. En Análisis por Elementos Finitos no ha funcionado bien para aplicar este método ya que no proporciona una curva de capacidad completa hasta el desplazamiento último. El hecho de tratar a la estructura como un continuo no permite monitorizar la curva de capacidad cuando esta ya es un mecanismo que rota. En cualquier caso, el punto de funcionamiento se encuentra cerca del rango lineal, de manera que sólo se prevén daños leves a moderados.

Como conclusión del estudio, la estructura de la Iglesia de Santa María del Mar se puede considerar segura y suficientemente resistente como para soportar la acción sísmica con un nivel de daño aceptable. Las evidencias históricas y la inspección realizada reflejan daños poco importantes a causa de terremotos en el pasado. El análisis numérico muestra que la estructura puede resistir perfectamente la acción sísmica en Barcelona, siendo los daños reducidos y asumibles.

INDEX

1. Introduction and goals.....	3
1.1 Introduction	3
1.2 Objectives	4
2. State of the art in the study of the structure	7
2.1 General description of the building	7
2.2 History and past seismic performance.....	12
2.3 Morphology	15
2.4 Damage.....	20
2.5 Previous studies on the seismic performance	24
3. Tension-compression damage model for masonry.....	39
3.1 Damage theory.....	39
3.2 Tension – compression scalar damage model	42
3.3 Software and examples	44
3.4 FEA of masonry buildings with damage models.....	51
4. Finite Element Analysis of Santa Maria del Mar Church.....	55
4.1 Characteristics of the model	55
4.2 Verification and calibration: Linear Elastic and Modal analysis	56
4.3 Gravity load	59
4.4 Seismic analysis: nonlinear static pushover	65
4.5 Sensitivity analysis	72
4.6 Simulation of possible reinforcement techniques	81
5. Capacity Spectrum Method applied to Santa Maria del Mar Church	87
5.1 Capacity Spectrum Method.....	87
5.2 Capacity spectrum	90
5.3 Demand spectra.....	91
5.4 Performance point and damage estimation	92

6. Conclusions	97
6.1 State of the art in the study of the structure	97
6.2 Finite Element Analysis	98
6.3 Capacity Spectrum Method.....	99
6.4 Final conclusion on the seismic performance of the structure.....	100
6.5 Future developments	101
References	103

CHAPTER 1

Introduction and goals

1.1 Introduction

Santa Maria del Mar is an architectural jewel built in only 50 years in a pure and sober Gothic style. The building includes very interesting structural innovations shared only, among all Gothic construction, by the Barcelona and Mallorca cathedrals. Built in the XIV, it is a together with the Cathedral a reference of the Catalan Medieval History in Barcelona. While the outside of the building gives a sense of robustness, the interior is a big clear space due to the large spans and height of the vaults and the slenderness of the columns (figures 1.1 and 1.2).



Figure 1.1 - External view of the church



Figure 1.2 - Internal view of the church

The church has experienced some damage in the past due to two earthquakes: 1373 (still under construction) and 1428. Due to these past damages, to the slender characteristics of the structure and the cultural relevance of this construction, the seismic behaviour of Santa Maria del Mar Church has already been analysed. Irizarry (2004) studied the seismic performance of the typical bay using the Capacity Spectrum Method combined with Limit Analysis and Finite Element Analysis (FEA) techniques. The conclusion was that the structure was safe enough as only slight damages were expected due to seismic action. In the scope of an inter-disciplinary study done to assess the structural condition of the church, Roca (2007) carried out a similar study for all the macro-elements of the building, using more accurate data about the structure and the actions. Some of the new data available could place the structure in a more delicate situation. The seismic capacity of the structure was found to be slightly lower than in the

previous study but the expected damages for an earthquake were still found to be slight to moderate.

1.2 Objectives

The *general objective* of this dissertation is to analyze and conclude about the seismic performance of Sta. Maria del Mar Basilica in Barcelona. The previous structural analysis have pointed out that the structure might show only limited seismic strength due to the slenderness of the structural members and the large dimension of its vaults. A more refined seismic analysis is needed to understand the true seismic performance of the building and the possible need of a seismic strengthening. This new development takes advantage of the accurate data provided by Roca (2007) to carry out a Finite Element Analysis (FEA) of the typical bay using a tension-compression damage mode (Cervera, 2003), which has been satisfactorily used in similar studies of historical buildings.

In order to conclude about the seismic performance of this historical building, the ISCARSAH recommendations (ICOMOS, 2003) will be followed. Any practice related to the conservation of architectural heritage requires a multidisciplinary approach involving a variety of professionals and organisations. Studies and planning require both qualitative data, based on the direct inspection of material decay and structural damage, historical research etc., and quantitative data based on specific tests, monitoring and structural analysis (figure 1.3). Even though the main contribution of the present work will be the numerical simulation of the structure, the other levels of study (History, Inspection and Monitoring) will be also taken into account as part of a bibliographical research.

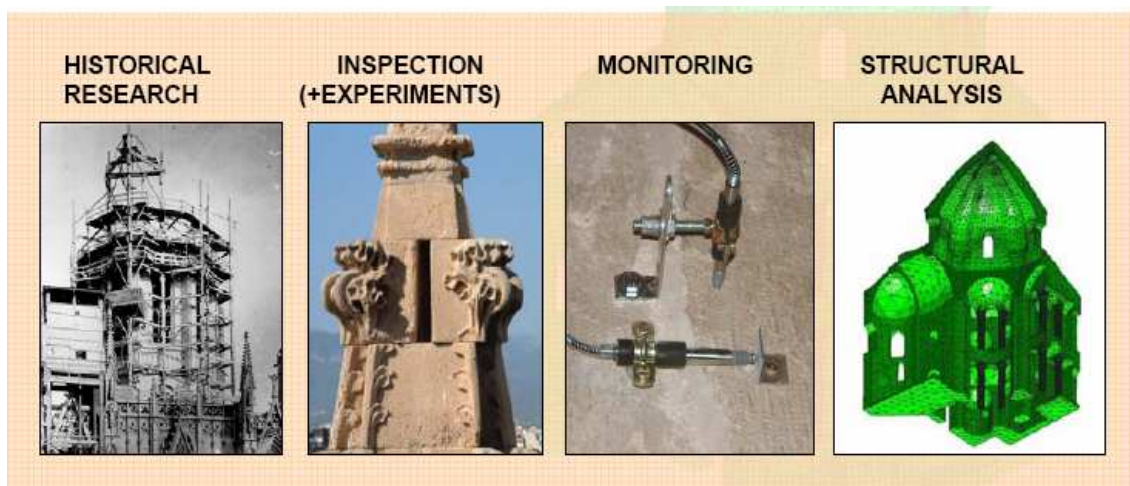


Figure 1.3 – Multidisciplinary approach to investigate historical constructions

As a result of this approach, the following secondary objectives (and related tasks) are defined to achieve the main goal.

Secondary Objective 1: Establish a state of the art in the study of the structure of Santa Maria del Mar Church and its seismic performance.

Related Tasks:

- Obtain an accurate description of the structure of Santa Maria del Mar Church, including morphology and damage (bibliographical research and inspection of the building)
- Gather Historical data and information about past seismic performance (bibliographical research).
- Review past studies on the seismic performance of the building (bibliographical research).

Secondary Objective 2: Simulate numerically the seismic behaviour of the structure of Santa Maria del Mar Church.

Related tasks:

- Investigate on the use of tension-compression damage model for masonry modelling (bibliographical research and FEA).
- Carry out a gravity load analysis and study the vertical load safety margin (FEA).
- Carry out a pushover analysis of the typical bay and obtain a capacity curve (FEA).
- Study the sensitivity of the numerical results to the variation of the main mechanical parameters: compressive strength, tensile strength, fracture energy (FEA).
- Simulate possible strengthening strategies (FEA).

Secondary Objective 3: Evaluation of the seismic capacity of Santa Maria del Mar by means of the Capacity Spectrum Method.

- Characterize the seismic action and obtain a demand curve (bibliographical research)
- Apply the Capacity Spectrum Method and evaluate the expected structural damage (calculations).

CHAPTER 2

State of the art in the study of the structure of Santa Maria del Mar Church

In this chapter the state of the art in the study of the structural performance of Santa Maria del Mar Church is reviewed. After a general description of church, the History of the building and its past seismic performance are summarized. Then, the morphology of the structure and the current damage patterns are described. Finally, the results of previous studies on the seismic performance of the structure of church are presented.

2.1 General description of the building

The building is composed of three naves, formed by four sections and an altar that consists of a polygon of seven sides, all covered by cross-vaults. The octagonal columns are 26m high and are separated by 13 meters from each other, forming four central sections of 13 by 13 meters. The Catalan gothic style uses buttresses instead of flying arches and the spaces between the end of the lateral naves and the end of the buttresses are included inside the structure, using them to locate little chapels. A top view and an internal view of the building are shown in figures 2.1 and 2.2.

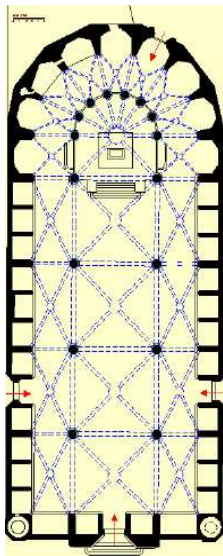


Figure 2.1 - Plan view of the church



Figure 2.2 - Internal view of the church

Santa Maria del Mar Church is placed in the Ribera area of Barcelona. Nowadays, it is almost an isolated building in the urban environment, having only in the North side some annexed buildings (as shown in figures 2.3 and 2.4). This configuration is quite new and a result of different urban changes starting in the 19th Century. It is known that in the past, two cemeteries were annexed to the church.

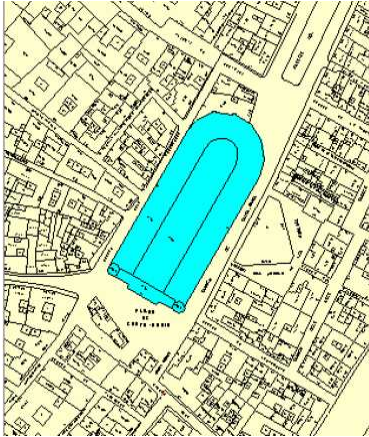


Figure 2.3 Plan view of the Church and surroundings



Figure 2.4 - External view of the Church from the Eastern side

The building is almost 85 meters long, 35.30 meters wide and has a maximum height of 34 meters from the ground to the roof. The plan view of the church is known as basilica plan, as no transept crosses the 3 naves (figure 2.1). In the Northern part of the building there is a semicircular apse and in the Southern façade one tower at each side (47m high the Western one and 46m high the Eastern one). The towers are integrated in the lower part of the perimeter of the façades. There are four entrances: one at each visible face of the building, two to the lateral naves at the lateral façades, one to the central nave at the main façade and one at the head.

All the faces of the building have similar characteristics, with a first level of walls around 16m high, defining the height of the lateral chapels (figure 2.5). In fact, the lower part of the buttresses is embedded in this wall, connecting them to make them work together. This wall has two levels: the first one is 6-7m high and the second 10m with windows at each lateral chapel of about 8x2m.



Figure 2.5 - View of the Eastern wall

In the main façade there is the main entrance to the Church with a big portal 12 high (figure 2.6). It is built out of the plane of the walls and has sculptures on it. The other entrances are similar but smaller and simpler.



Figure2.6 – Main portal

The upper part of the main façade is a vertical plan interrupted by two longitudinal buttresses (carrying the longitudinal thrust of the vaults) and the towers at the sides (figure 2.7). A 9m diameter rose window in the centre of the wall is the most representative element of the façade. The rest of the perimeter is composed by the walls, the lateral chapels and the transversal buttresses. The cover of the lateral chapels created a terrace level that is used for circulation of people (figure 2.8). By means of small doors in the buttresses it is possible to make it continuous along the perimeter. There are four buttresses at each side, two in the main façade and six at the head (figure 2.9). They are all 14m high (from the chapel cover level to the top), some of them are 1.50 wide and other 1.38m.



Figure 2.7 - Upper part of main façade and rose window



Figure 2.8 – circulation at the chapel cover level and door in buttress

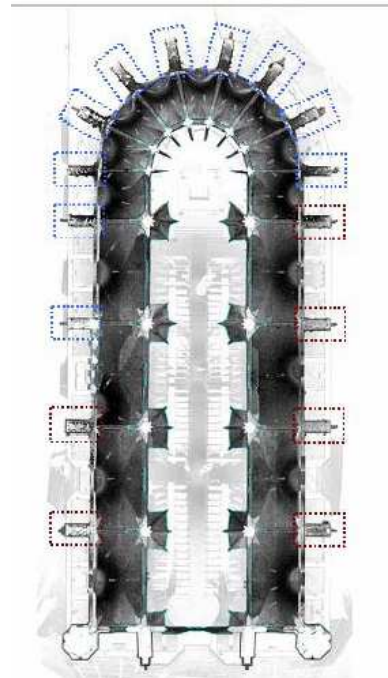


Figure 2.9 - Plan view at the level of the chapel cover

Next level is the lateral nave cover. The roof is composed of tiles and has a shape that enables water drainage. The roof is only interrupted by triangular walls aligned with the diaphragmatic

arches that can have both structural and drainage functions (figure 2.10). In the top of these walls a channel enables the drainage of the central nave cover (figure 2.11).



Figure 2.10 – View of the roof of the lateral nave

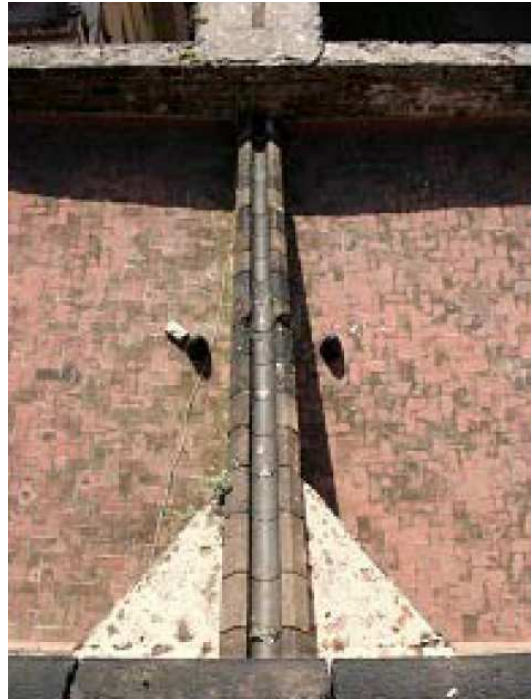


Figure 2.11 – Drainage channel on the top of the triangular wall

At the last level, the cover of the central nave is done with a tiled surface with different slopes adapted to the vault shape and enabling drainage (figure 2.12). In fact, it is possible to identify the 4 vaults and the vault with palm shape at the head of the church. Another important element is the existence of a triangular wall which is in fact the upper part of the diaphragmatic arch. It is thought that this wall was used in the early times to support the provisional roof of the church.



Figure 2.12 – View of the roof of the central nave

The interior of the church shows the characteristics of the Southern Gothic: a very clear volume creating almost a single space, with a preference for the longitudinal orientation (no transept), as shown in figure 2.2. The church is composed by three naves with 13x13m square sections in the central nave and rectangular sections in the lateral naves (figures 2.13 and 2.14). The altar consists on a polygon of seven sides. Little chapels are found in the space created between buttresses. The columns have an octagonal shape and are 26m high and are 1.56m wide.

The squared sections are covered by cross vaults surrounded by diaphragmatic arches at a height of 32m (figure 2.13). The lateral vaults have a significant height compared to the central one (26m) and are also covered by rectangular cross vaults (figure 2.14). The altar of the church is covered with a vault with palm shape and has a big circular keystone in the centre (2m diameter), as shown in figure 2.15.



Figure 2.13 – Square cross vault at central nave



Figure 2.14 – Rectangular cross vault at lateral nave



Figure 2.15 – Vault with palm shape in altar

2.2 History and past seismic performance

History of construction and of damages

Santa Maria del Mar Church started to be built in 1329 and the works finished in 1383, when the last section was covered. However, there are evidences that in the 1340s the new Gothic

Church was already open to cult. Between 1339 and 1352, the majority of the lateral chapels were already built. The head chapels were built afterwards, between 1360 and 1370.

There is evidence of two events causing damage in the structure during construction. In 1373 an earthquake caused the partial collapse of the Eastern tower. In 1378 there was an important fire that caused important damages in the interior of the church.

No more information is available about the construction process, except that the last vault was closed in 1383. The existing towers were finished long time afterwards (1496 and 1902). In figures 2.16 and 2.17, Vendrell et al. (2007) draw the construction phases of the building.

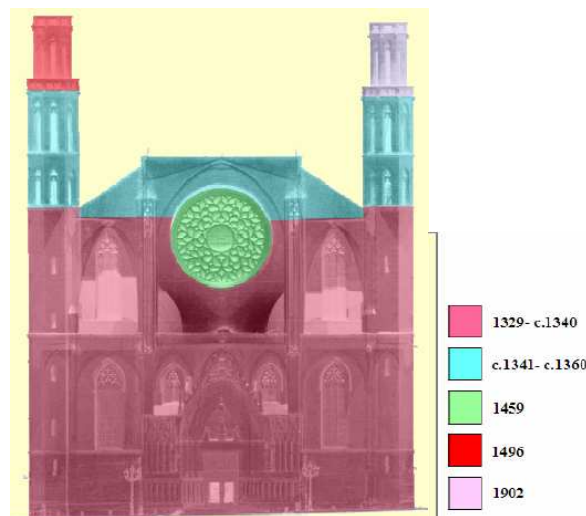


Figure 2.16 – Façade view of construction phases, according to Vendrell et al. (2007)

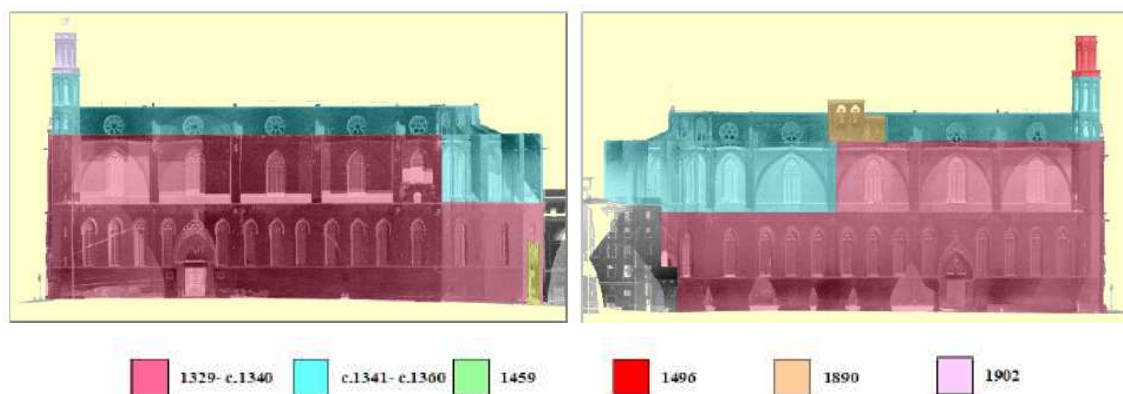


Figure 2.17 – Lateral view of construction phases, according to Vendrell et al. (2007)

There is also evidence of an important earthquake in 1428 that caused the partial collapse of the rose window of the façade, killing 25 people. This piece was restored in 1459.

Several interventions have been carried out afterwards: little architectural changes for functional reasons, repair interventions due to bombing 17th, 18th and 19th Centuries, restorations. In the 20th Century there was an important intervention after a big fire in 1936.

The three main important events causing damage were:

- Fire in 1378, affecting almost all the church. Some of the pathologies usually associated to 1936 fire could correspond in fact to this one. Mainly, this fire could have affected the vault of the second section, which was being built at this moment. In 1379 there were important works to repair the damages caused.

- Earthquake of 1428: it was an important earthquake causing damage to the façade and fall of the rose window (figure 2.18). The damage was however caused probably by a succession of events and not a single one, as between 1427 and 1428 the seismic activity in Barcelona was important. The existing cracks in the façade can be a consequence of these earthquakes (in the beginning of the 20th Century these cracks were described as stable).

- Fire in 1936: the most affected areas were the old presbiterium, the head of the church and the old organ. Nowadays the damage is still visible in some of the piers (figure 2.19).



Figure 2.18 Current view of the rose window built on 1459 after its collapse in 1428 earthquake



Figure 2.19 – Current view of the third pier at left side, damaged due to 1936 fire

Past earthquakes

The most important earthquakes that the building has experienced were in the 14th and 15th Century.

1. 1373 Earthquake with Epicenter in the Pyrenees and intensity VII-IX (MSK). In Barcelona, the assumed intensity is V-VI. The highest part of Eastern tower collapsed. It was rebuilt in the 20th Century.
2. In 1427 there is a long list of earthquakes in different places of Catalonia with intensities between III and VIII. Apparently no damage is produced in Barcelona.
3. February 1428 there is an earthquake with epicenter in the Pyrenees and intensity VIII. The estimated intensity on Barcelona is VI-VIII. The rose window of Santa Maria del Mar collapses killing some people. There are also damages in Sta. Maria del Pi church.
4. May 1448 there is an earthquake with epicenter near Barcelona and intensity V-VI, causing in Barcelona damage to houses and palaces, that were previously damaged by a flood.

Except some local damages (rose window and the tower), it is possible to conclude that Santa Maria del Mar has resisted earthquakes of some importance. The most important in 1373 (intensity V-VI) and 1428 (VI-VIII). Even though some damages could not be reported in the documents found, it is rare that they have omitted important damages or partial collapses (given the associated high costs of repair). Therefore the building resisted earthquakes without important problems. As a conservative estimation, an intensity of VI could be associated to the maximum earthquake that the building has resisted all along its history.

According to Roca (2007) and using the given correlation of an old Spanish Seismic Code it is possible to relate the intensity with an acceleration:

$$\text{Log}_{10} a = 0,30103 I - 0,2321 \quad (2.1)$$

Valid for $T=500$ years, being a the acceleration ($\text{gals}, 10^{-2}\text{m/s}^2$) and I the Intensity. Applying the formula the obtained acceleration for intensity VI is $0,375 \text{ m/s}^2 = 0,038\text{g}$. According to the Spanish seismic code, the seismic action in Barcelona has a basic acceleration of $0,04 \text{ g}$ (corresponding to $T=500$ years). This value is almost the same as the obtained one. This estimation has to be taken as an orientative value, but it is not possible to assure that the past earthquakes reached these values. However, the fact that the structure resisted earthquakes of this kind it will be taken into account when analysing the results of the numerical simulations.

2.3 Morphology

Vendrell et al. (2007) carried out a detailed study on the morphology of the structure, by means of a bibliographical research, inspection, Non Destructive Techniques (georadar, seismic tomography) and extraction of cores. As a result, it was possible to obtain detailed characteristics of the different elements of the structure, including the vault infill.

A geotechnical study was carried out to characterize the soil conditions. The existing soil is composed basically by sands, with an intermediate thin layer of clay. In the top, there is a layer of anthropic origin. As a result, the soil is characterized for calculations as a type II-IV in the classification of the Spanish Seismic Code.

By using georadar and opening some holes in the foundations, it was possible to identify the foundation type and a considerable number of pre-existing constructions (figures 2.20 and 2.21). Nowadays, these old constructions are integrated in the foundations. Their existence provided a pre-consolidation of the soil and makes the foundation condition heterogeneous.



Figure 2.20 Buttress Foundation at the head of the church



Figure 2.21 – Pier foundation

Walls and buttresses are three-leaf elements made of two external ashlar masonry layers and a rubble infill. This morphology can be seen from the holes made by bombing and shots from the 1714 and 1936 wars (figure 2.22). Therefore no NDT was needed to characterize them. As the ashlar masonry is very thin, the load-carrying capacity is provided by the irregular masonry of the infill (figure 2.23).



Figure 2.22 Hole in the wall (interior composition visible)

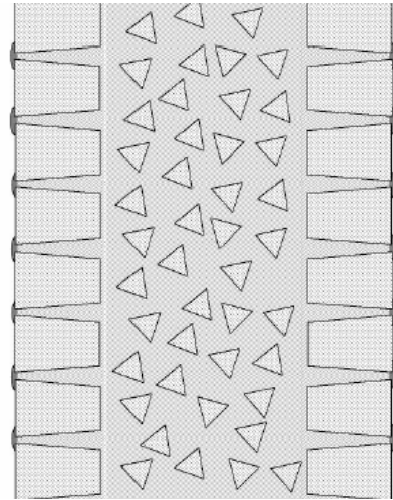


Figure 2.23 – Three-leaf wall composition

By means of seismic tomography, it was possible to identify the massif condition of the piers (figure 2.24). The section consists on one central squared ashlar of big dimensions surrounded by 4 hexagonal blocks giving an external octagonal shape (figure 2.25). The position of the internal block rotates 45° at each level in order to ensure stability, as it was found in Mallorca cathedral. Given the big dimensions of the stones, the thin layers of mortar and the massif condition of the pier, they are supposed to have a higher stiffness and strength than the rest of masonry elements of the structure. This hypothesis is in good agreement with their essential role in the global behaviour of the structure.



Figure 2.24 Pier base

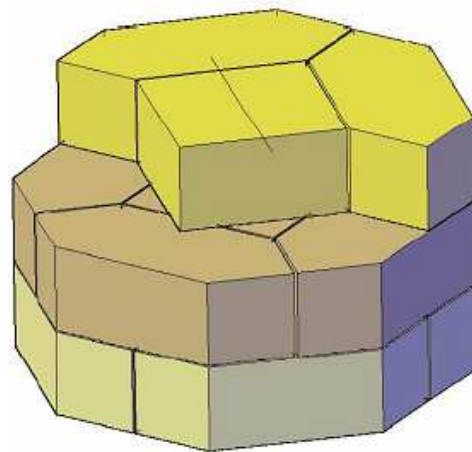


Figure 2.25 – Pier composition

The vaults morphology was characterized by means of information obtained from past interventions, combined with georadar and the opening of few holes. The vaults are made of blocks around 20cm thick. In the lateral vaults there is a supplementary layer of load-carrying

material made by rubble masonry linked with lime mortar (creating a medieval concrete). In the central vault there is a light infill made by ceramic pieces, which is 0.7 to 1m thick (figure 2.26). In the top, there is a pavement 12cm to 15cm thick. The central and lateral vaults have different morphology due to structural reasons. The light infill in the central vault reduces the vertical load carried by the piers and the thrust that the buttresses need to counteract. However, the lateral vaults do need this load-carrying infill as their structural function is similar to a flying arch: transfer the thrust of the central vault to the buttress. That is why they have almost the same height as the central vault. This is a very significant characteristic of Santa Maria del Mar design, which is shared with Barcelona cathedral. In this case, as the vaults are squared and cover a bigger area the piers were improved to carry a bigger load.



Figure 2.26 - Infill of the central vault (pictures done in the 1990s)

The arches supporting the vaults have been found to be diaphragmatic arches. They consist in vertical walls of load-carrying masonry up to the roof. It is thought their existence is justified by the need to support the timber beams of a previous temporary roof. However, previous calculations (Roca, 2007) showed that they also contribute in a significant way to the seismic capacity of the structure.

The towers are very light elements, compared to the rest of the building. Their interior is empty, except a cylindrical 20cm thick wall that supports the steps of the stairs (figures 2.27 and 2.28). The external wall is 40cm thick.



Figure 2.27 Central empty space and internal wall of the tower



Figure 2.28 – Stairs space between internal and external wall

Regarding the materials used, the masonry is mainly done with stones from Montjuic hill (siliceous gres) and lime mortar. The stone from Santa Maria del Mar Church has not been tested, but their mechanical properties are well characterized by previous studies and are listed below:

Specific weight: 22 kN/m³

Compressive strength: 30 MPa

Elastic modulus: 10 GPa

From this information it is possible to obtain the design values for masonry, as a material composed by stone and mortar. The same specific weight will be assumed. The compressive strength is obtained by applying the formula from Eurocode 6 (CEN, 2005):

$$f_k = K f_b^{0.65} f_m^{0.25}, f_m \leq 10 \text{ N/mm}^2, f_m \leq 2 f_b, \text{ with } K=0.6 \quad (2.2)$$

where f_c would be the resulting compressive strength of masonry, f_b the compressive strength of stone block and f_m the compressive strength of mortar. As a result, and assuming $f_m = 5 \text{ MPa}$, the compressive strength for masonry would be 8 MPa. All the values used are conservative, therefore this is a conservative strength. The elastic modulus can be estimated from the formula $E=1000 f_c$ (CEN, 2005), which will result in a modulus from 8 to 10 GPa.

2.4 Damage

A damage survey was carried out by Vendrell et al. (2007) by complementing an inspection with NDT techniques. In the following lines a summary of the main structural damages is done.

Perimeter walls

The perimeter walls show diverse slight and punctual damages: loss of mortar in joints, opening of construction joints, holes due to bombing. Behind them, there is a crack damage pattern associated to the openings of windows. Cracks starting from the base of the opening going down vertically or slightly inclined (figure 2.29). Some of them can be associated to differential settlements and other to the existence of tension stresses below the opening resulting from a deviation of the load as an arch. In addition, there are some cracks in the wall associated to the tower. The cracks start from the upper part of the first window from the corner towards the tower and there is no continuity of the crack below the window (figure 2.30). These cracks could be caused by the leaning of the tower (possibly caused by an earthquake).



Figure 2.29 – Vertical crack below window



Figure 2.30 – Inclined crack from window towards tower

Façade

The façade also shows the same kind of vertical cracks associated to the windows and the towers, in both the East and West sides (figures 2.31 to 2.33). Other cracks appear near the rose window, but they could be related to construction joints (figures 2.33 and 2.34). Finally, in the towers the stone presents damage due to the corrosion and expansion of steel pieces.

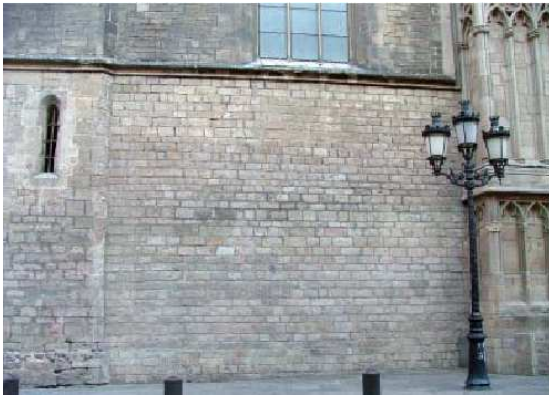


Figure 2.31 – Vertical crack in the façade



Figure 2.32 – Vertical crack in the upper wall of façade

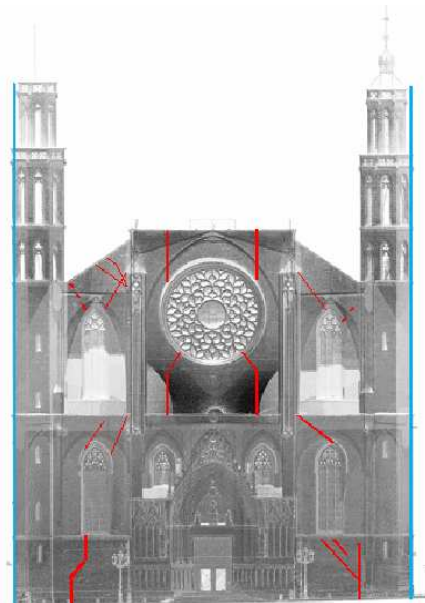


Figure 2.33 – Crack pattern in façade



Figure 2.34 – cracks near rose window

Upper walls

Some cracks are also observed in the upper walls (in the upper perimeter walls and walls of central nave). The most characteristic pattern is the crack starting at the arches and going up inclined to the circle opening, that can be seen both from outside and inside (figure 2.35). It can be caused by the existence of a relieving arch caused by the opening. As a result, the central part wouldn't be loaded.

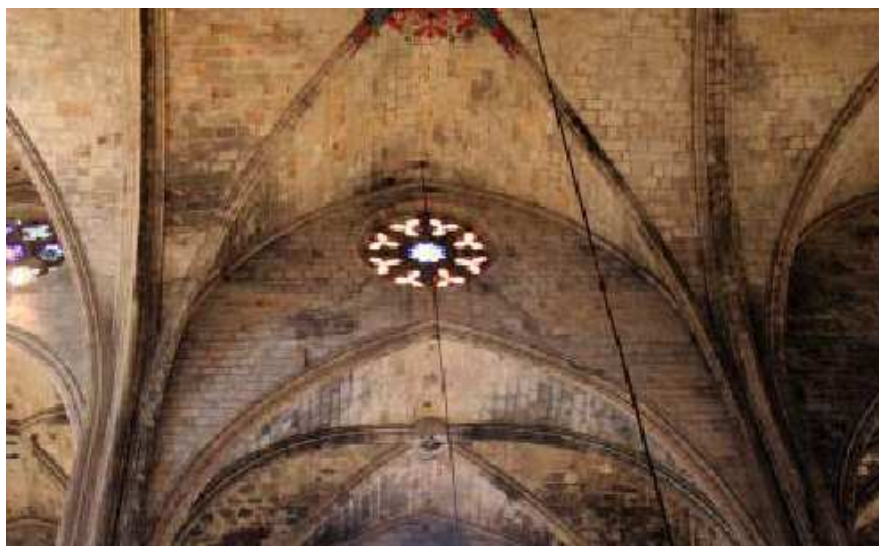


Figure 2.35 – Crack in the wall of the central nave

Vaults and arches

Some lateral vaults show loss of material and fissures, also in the arches and nervures (figure 2.36). This can be result of the fires of 1379 and 1936. In fact, the central vaults were repaired but some lateral vaults still show this damage. Another damage that can be seen in the keys of some vaults and arches are longitudinal cracks and even relative displacements (figure 2.37). This could be due to the 1379 fire, when part of the structure was still under construction. Some workforms were burned and destroyed, while the mortar didn't still set. As a result there was a loss of mortar and big deformations.

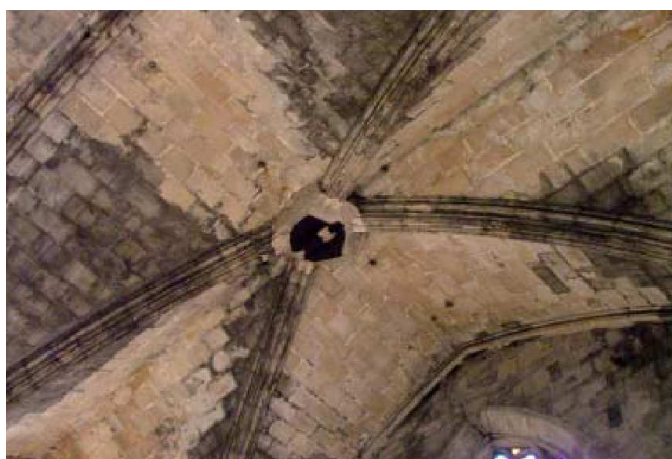


Figure 2.36 – Loss of material in vaults



Figure 2.37– Relative displacement in arch and vault key

Piers

The piers are probably the most damage and vulnerable elements of the church. Their damage was mainly caused by the 1379 and/or 1936 fires. Some piers show an important loss of material (stone and mortar), for example the third pier at the Western side (figure 2.38). There is also some splitting of material in the corner of some piers (figure 2.39). This could be caused by a high compressive stress concentration. However, the stresses are not expected to be so high. As the piers showing this problem are also in the affected area of the fire, it is thought that fire was the cause of this damage.



Figure 2.38 – Loss of material in pier 3 West



Figure 2.39– Splitting of material in pier

Deformations and settlements

The leaning of the piers and towers has been measured. The piers showed a horizontal displacement between 2 and 8cm in the transversal direction and between 4 and 7cm in the longitudinal direction. The Eastern tower presented a longitudinal leaning of 6cm and the Western tower 15cm longitudinally and 13cm transversally (to the exterior of the building in all cases). The movements can be considered as small for an ancient structure like this one: for the piers equal or less than 1/200 and for the towers below 1/300.

The cracks in the wall near the tower could be associated to the leaning. However, it is important to notice that the upper part of the Western tower rebuilt in 1496 doesn't show a leaning. This would mean that the movement stabilized before that date. Therefore, the movement could be associated to the 1427 earthquake.

The existence of some cracks point out possible differential settlements. However, it is difficult to justify them, as the structure has been found to transfer the vertical load to the foundation in a uniform way. Possible reasons for differential settlements could be the heterogeneity of the soil conditions due to pre-existing constructions and the construction process. In fact, the perimeter walls were built before the piers. Even though the settlement could be similar in both elements, the difference of time between one and the other could cause the cracks in the structure. In other words, the settlement already existed in the wall when the rest of elements were built, so that the structure suffered this differential settlement due to the late settlement of the piers.

Material damage

In addition to the aforementioned damage, Santa Maria del Mar Church shows other damages at the material level, namely: loss of material in stone and mortar, cracking due to steel corrosion, dirt, biological colonisation, vegetal growth, moist spots and graffiti.

2.5 Previous studies on the seismic performance

Two studies exist regarding the seismic performance of Sta. Maria del Mar. In the scope of the RISK-UE project, Irizarry (2004) applies the Capacity Spectrum Method to the transversal section of the church, using two different approaches to obtain the capacity curve: Equilibrium Limit Analysis and Finite Element Analysis (FEA). In the scope of an inter-disciplinary study done to assess the structural condition of the church, Roca (2007) carries out a similar study but using more accurate data about the structure, the actions and the foundations. In addition, the seismic performance of the other macro-elements of the church (façade, tower) is studied.

Risk-UE project

In the scope of the European project RISKUE (Lagomarsino et al., 2002), Irizarry (2004) studied the seismic risk associated to Santa Maria del Mar church. This study is the first one of this kind devoted to Santa Maria del Mar and it is very useful for a further seismic studies. First, from the seismologic point of view, as it defines both deterministic and probabilistic hazard parameters which are more precise for the church location than the obtained from the Spanish Seismic code. Second, it is a first attempt to characterize the seismic behaviour of the church by using the Capacity Spectrum Method, even though the data available from the structure and foundations is not very precise.

Irizarry et al. (2003) studied the seismic response of the typical transversal section of the church, as it is considered a priori the most vulnerable macro-element of this structure (the spans of the vaults are large and the piers slender). The capacity curve is obtained by both Limit Analysis and FEA.

A static nonlinear FEA of a representative 3D model of the central and lateral vaults was carried out (figure 2.40). This model includes half of the vaults at each side of the piers with appropriated boundary conditions. Shell elements are used and a damage constitutive law is considered for masonry. A modal analysis was carried out, obtaining as fundamental period of the structure $T=0.81s$. A pushover analysis was carried out with 3 different models: a) dead load + 0.14g horizontal acceleration, together; b) same analysis with lower E-modulus in the vaults; c) considering load history: first dead load and then incremental horizontal acceleration.

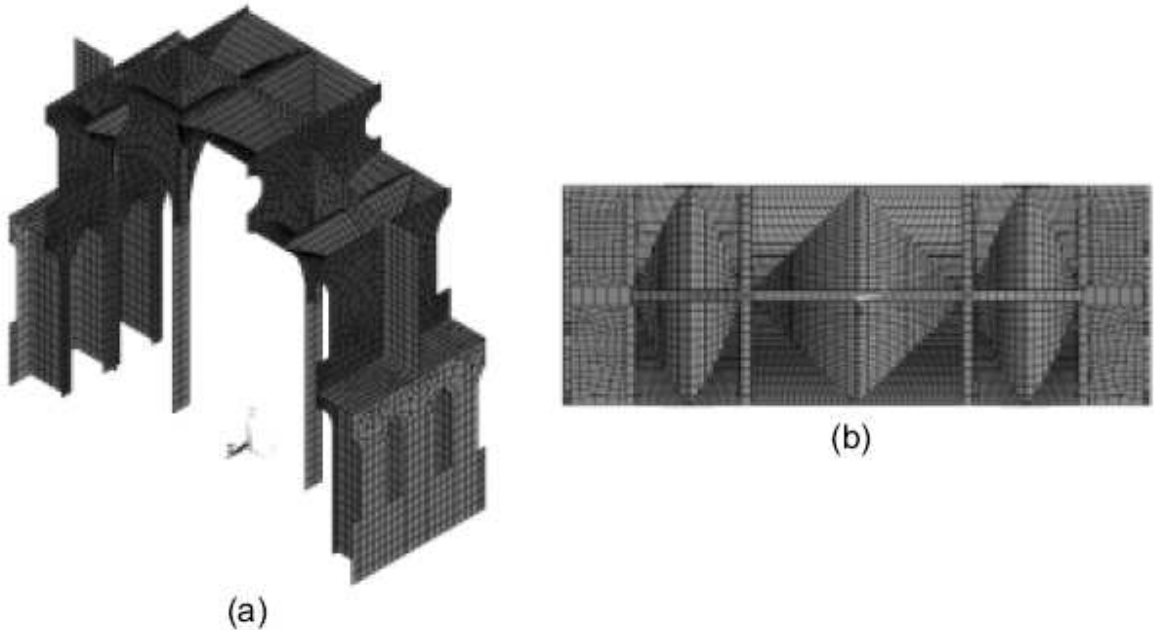


Figure 2.40 - FE model used by Irizarry et al. (2003)

The resulting capacity curves and inelastic deformations are shown in figures 2.41 and 2.42.

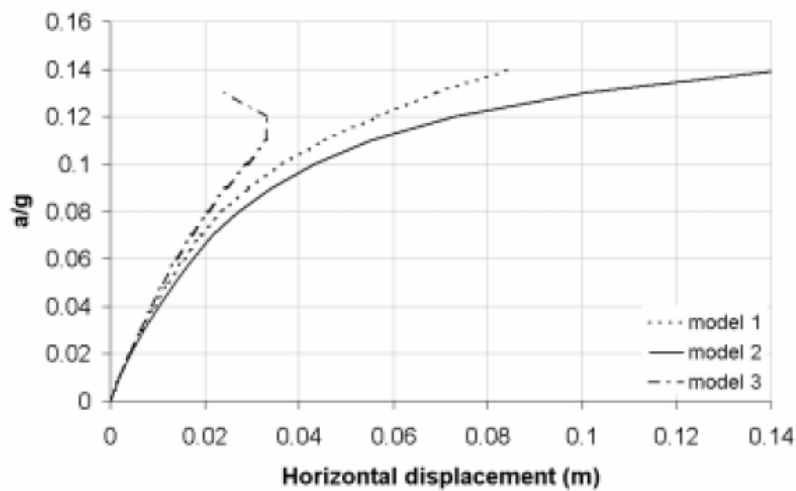


Figure 2.41 – Capacity curve for each model done by Irizarry et al. (2003)

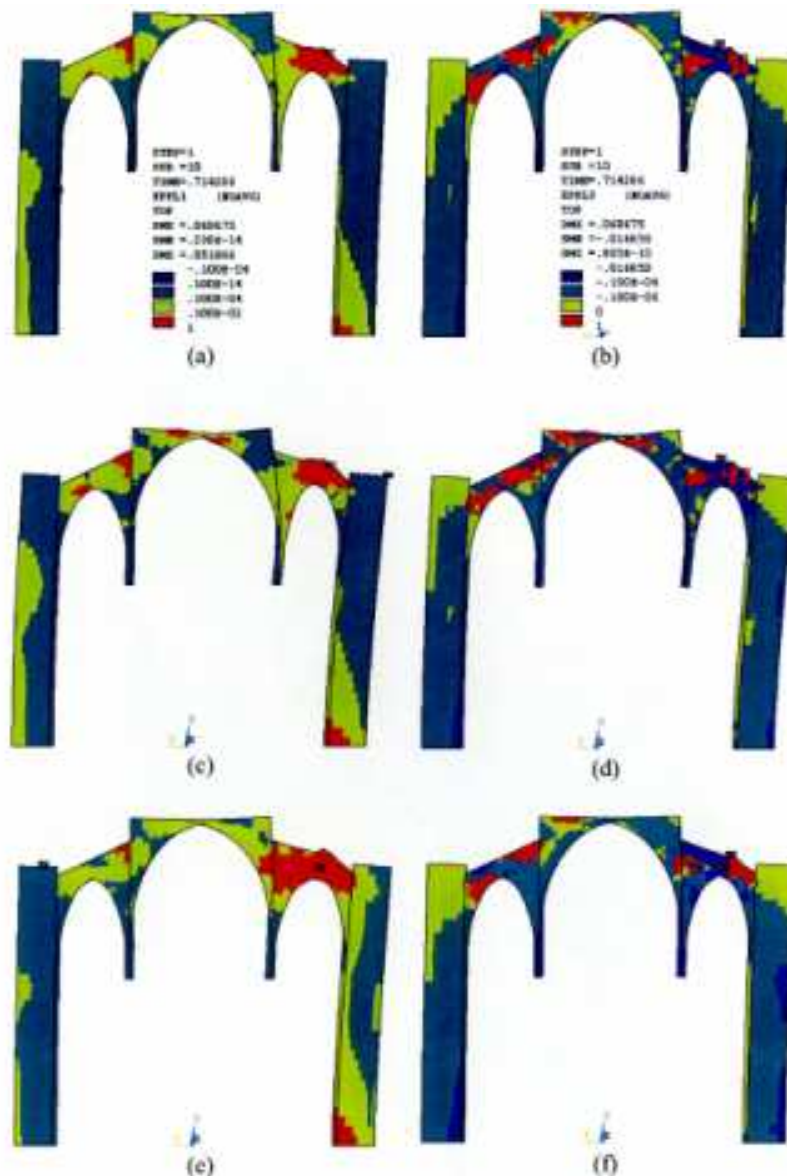


Figure 2.42 - Principal inelastic deformations. Maximum deformations: (a) Model 1, (c) Model 2, (e) Model 3; and Minimum deformations: (b) Model 1, (d) Model 2, (f) Model 3 (Irizarry, 2004)

From the FEA, the church is able to resist up to an acceleration of 0.14g with models 1 and 2. Model 3 is a more realistic representation of the load, but convergence problems were encountered at 0.13g. Therefore only models 1 and 2 were considered in order to identify a possible collapse mechanism for the kinematic model.

The Equilibrium Limit Analysis was carried out in a kinematic model defined by an aleatoric position of the hinges dividing the structure in 7 rigid bodies. The hinges are moved in order to find a minimum load factor. One of the possible mechanisms is shown in figure 2.43.

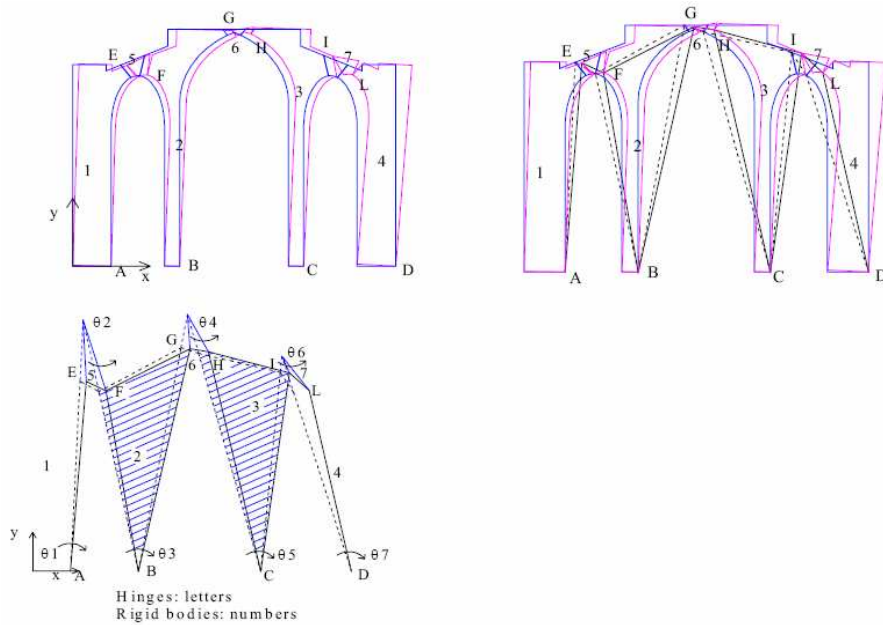


Figure 2.43- Possible mechanism and diagram of rigid blocks (Irizarry, 2003)

The information obtained from the FEA was very useful to define the location of hinges (section with high tensile strains in one face and concentrated compressions in the other). The process is repeated for different rotation angle of one of the blocks in order to obtain the capacity as the mechanism evolves. The load factor vs horizontal displacement is plotted in figure 2.44 for two different mechanisms, depending on the FE model which inspired the mechanism. The seismic coefficient is estimated as 0.12g.

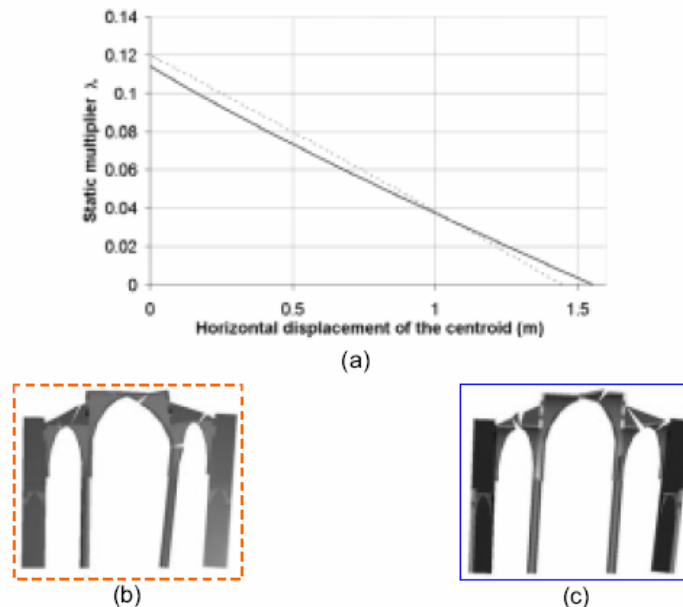


Figure 2.44 - a) load factor vs horizontal displacement graph for mechanism b) and c) (Irizarry, 2003)

A simplified capacity curve of Sta.Maria del Mar was built from the obtained results in the Equilibrium Limit Analysis. An elastic region is defined with a slope defined by:

$$slope = \frac{4\pi}{9.8T_0^2} \tag{2.3}$$

The elastic region is defined until tension appears in the section. This phase is considered as a level of damage 0. The level of damage 1 is defined until the intersection of the extension of the elastic line and the line obtained with the Equilibrium Limit Analysis. The rest of damage levels are defined as a fraction of the ultimate displacement. The resultant capacity curve is plotted in figure 2.45.

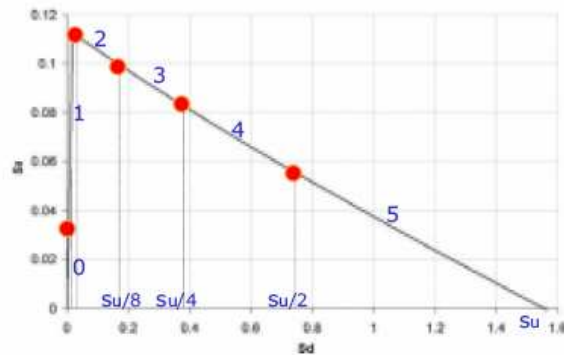


Figure 2.45 - Capacity curve obtained with limit analysis (Irizarry, 2004)

A good correspondence was found between FEA and Limit Analysis capacity curves, even if in one case the evolution is continuous and in the other discrete (figure 2.45).

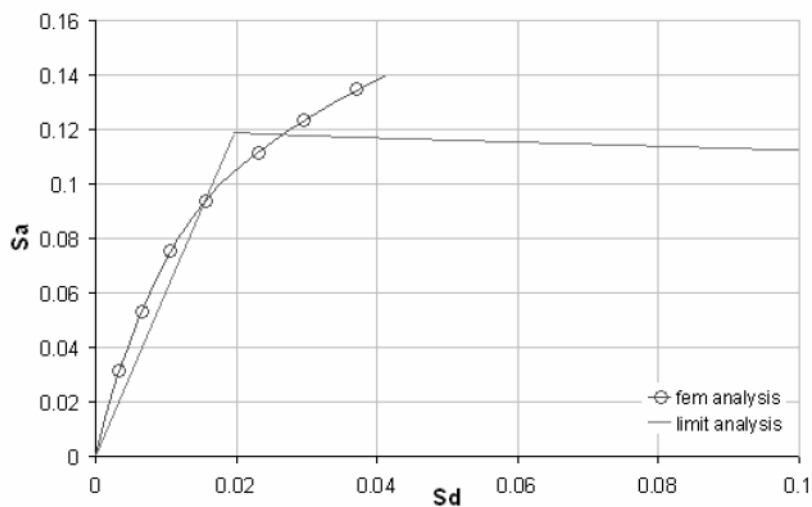


Figure 2.45 – Comparison between capacity curves obtained by Limit Analysis and FEA (Irizarry, 2004)

Once defined the capacity curve and the demand spectrum the damage of Sta.Maria del Mar was defined by obtaining the performance point, that is the intesection between the demand and capacity curves. In figures 2.46 to 2.48 this point is found fo the determinstic demand spectra, the probabilistic demand spectra and the demand spectra coming from the Spanish Seismic Code (NCSE-02, 2002). When intersecting out of the linear range a reduction of the demand spectrum has to be done in order to consider the same level of damping.

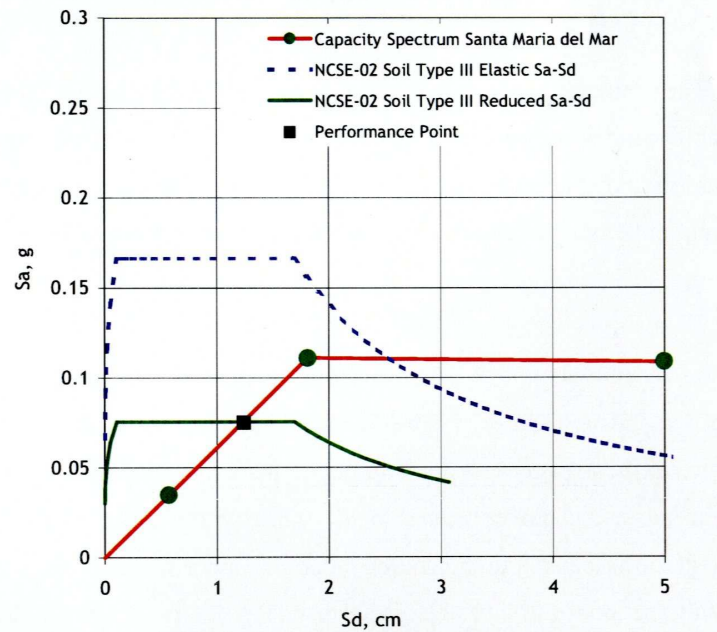


Figure 2.46 – Performance point considering a demand spectrum from Spanish Seismic Code (Irizarry, 2004)

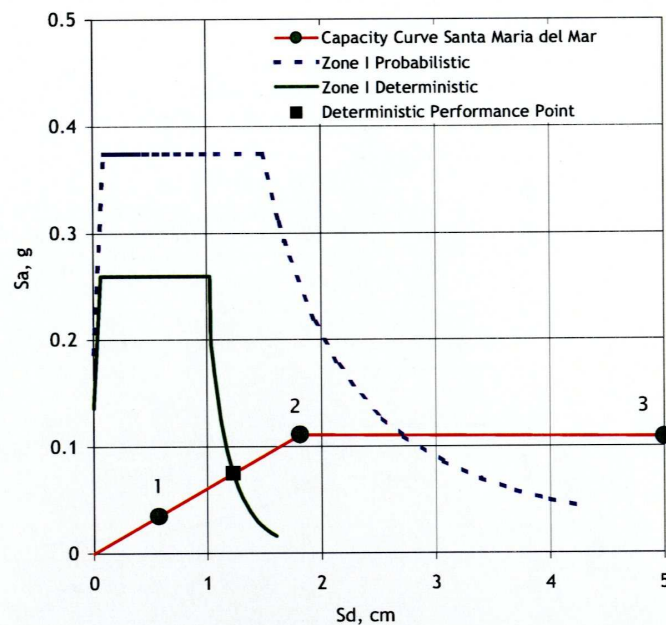


Figure2.47 – Performance point considering a demand spectrum from deterministic scenario (Irizarry, 2004)

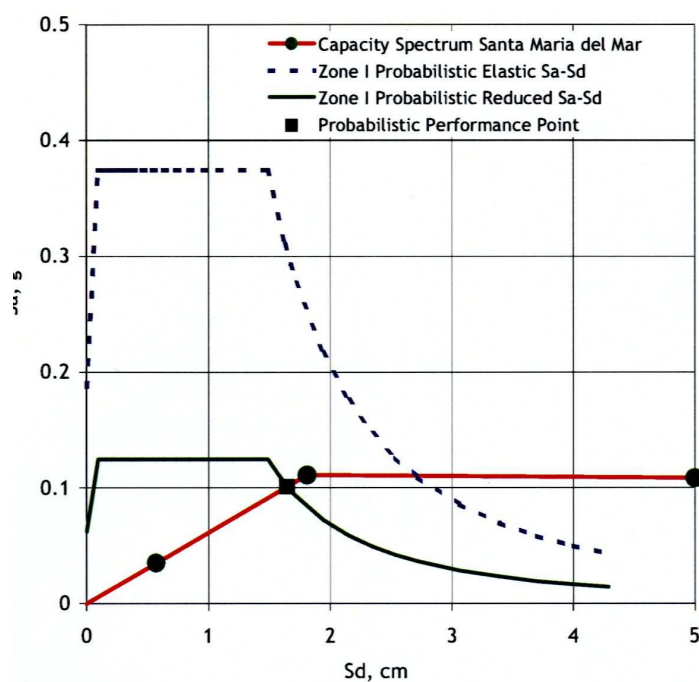


Figure 2.48 – Performance point considering a demand spectrum from probabilistic scenario (Irizarry, 2004)

With all the demand spectra, the performance point was found to be very close to the limit between the elastic and inelastic range of the capacity spectrum. This would correspond to slight to moderate damages.

Multidisciplinary study of Santa Maria del Mar (2007)

As a result of the inspection, Non Destructive Techniques and historical research in the scope of a multi-disciplinary study of Santa Maria del Mar, more accurate data is available about the structure. Roca (2007) considers that the new information places the church in a more disfavoured situation regarding seismic conditions, mainly due to the following facts:

- Better information about the foundation conditions, which has been found to be placed in a poor soil.
- Better information about the rubble fill of the vaults (meaning increment of mass), which were not considered by Irizarry (2004).

Therefore, the seismic performance of the church was studied again with a more precise data. The objectives of the structural analysis carried out by Roca (2007) were: a) characterize the behaviour and safety of the structure under gravity load b) characterize the dynamic and seismic behaviour of the structure c) relate the observed damage with possible causes by means of numerical simulation. For this purpose both Limit Analysis and Finite Element Analysis were used.

The numerical models were built using the information gathered from the inspection and NDT campaign done in this project: geometry, morphology and mechanical properties of materials. A FE model was built of half of a typical bay, considering appropriate boundary conditions to simulate symmetry (figure 2.49). The elastic properties of model have been validated using the dynamic test results, varying the stiffness of the materials until matching the experimental and numerical fundamental frequency. It was also verified that the stresses in the pier base from the model were similar to the real ones, found out by means of the NDT “holle drilling” test. Nonlinear material properties have been considered to take into account cracking in tension and crushing in compression of masonry. A smeared cracking model (simulating tensile behaviour) combined with a Drucker-Prager plasticity model (simulating compressive behaviour) have been used.

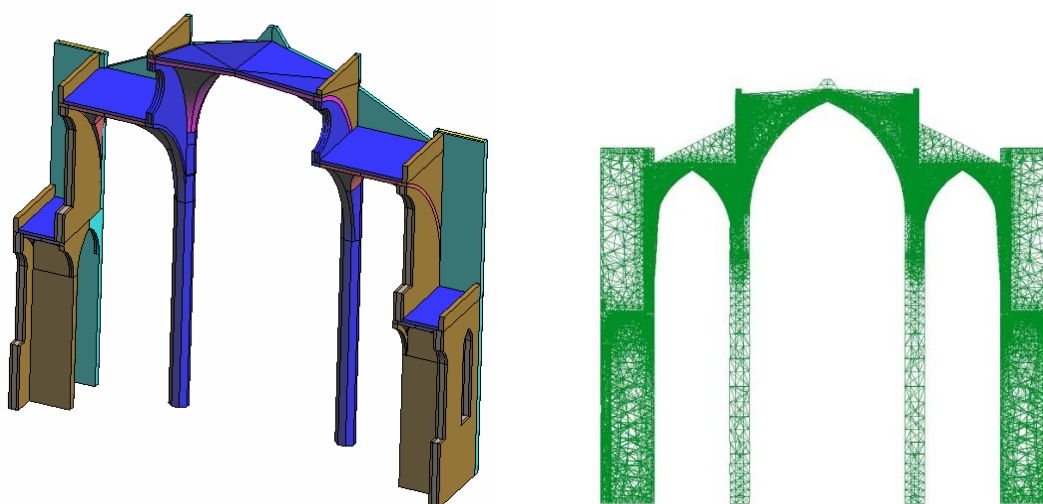


Figure 2.49 - FE model of typical bay: volumetric representation (left) and element discretisation (right) used by Roca (2007)

Three different analysis have been carried out with FEM: gravity load, differential settlement and seismic load.

As expected, the gravity load doesn't create important damage or deformation. There is however one order of magnitude of difference between the real and the expected deformations. This is a common trend in historical constructions, due to phenomena not considered in the instantaneous numerical analysis: construction process, long-term effects, environmental cycles, etc. From the Limit Analysis it has been proofed the importance of the rubble infill in the stability of the structure, and the need of considering it in the models.

Regarding the differential settlements, the structure would fail for a differential settlement of 12mm, in the case of immediate action. In real conditions, the structure can accomodate higher settlements due to creep and the corrections done during construction.

However, our main interest is focused in the seismic analysis carried out. For that purpose the following demand spectra have been considered: the deterministic and probabilistic demand spectra defined by Irizarry (2004) and the one obtained from the Spanish Seismic Code (NCSE-02, 2002). They are plotted in figure 2.50.

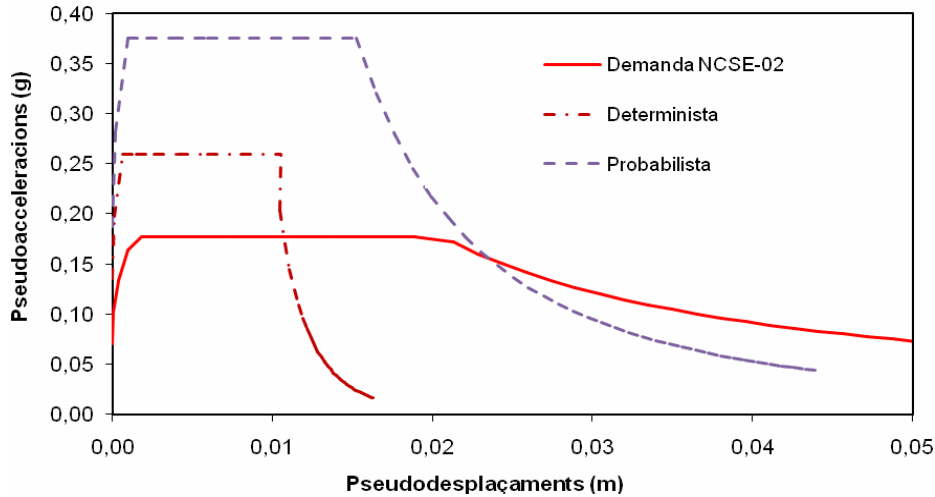


Figure 2.50- Demand spectra for the seismic study of Sta. Maria del Mar (Roca, 2007)

The study has been done for different macroelements independently: typical bay, principal façade, towers. Other elements (longitudinal façade, absis) have been considered stiff enough to avoid their study. The capacity of each macroelements were expressed in terms of seismic coefficients, defined as the maximum base shear divided by the self weight. In table 2.1 the seismic coefficients for each macroelement are shown considering different methods (static limit analysis, kinematic limit analysis, FEA). The values obtained by Irizarry (2004) are also tabulated. In general the equivalent horizontal forces have been applied according to mass distribution, except in the case of the transversal bay that has been done also according to the first mode of vibration.

For the typical bay the results from the static limit analysis and kinematic limit analysis is the same as expected. In figures 2.51 and 2.52 are plotted the obtained collapse mechanisms. The difference is that with the kinematic approach is possible to obtain the unload curve (figure 2.53). The FEA gives higher values (30%) due to the consideration of the tension capacity. In this case is also possible to obtain the complete load-unload curve (figure 2.54), and obtain at each step the distribution of inelastic deformations equivalent to the damage of the structure (figure 2.55).

Table 2.1 – Seismic coefficient for different macroelements and methods used (Roca, 2007)

Element	Analysis	Seismic coefficient (a/g)
Typical bay	FEA (load according to 1st mode)	0,12 / 0,15 ¹
	FEA (load according to mass)	0,13
Typical bay	Static Limit Analysis (load according to 1st mode)	0,09 / 1,12 ¹
	Static Limit Analysis (load according to mass)	0,10
	Kinematic Limit Analysis (load according to mass)	0,10
Typical bay (no rubble infill in vaults)	Static Limit Analysis (load according to mass)	0,12
	Kinematic Limit Analysis (load according to mass)	0,11
	FEA (load according to mass) – Irizarry (2004)	0,13-0,14
	Kinematic Limit Analysis (load according to mass) - Irizarry (2004)	0,11-0,12
Tower	Static Limit Analysis (load according to mass)	0,12
Upper part of tower	Kinematic Limit Analysis (load according to mass)	<0,08
Façade	Static Limit Analysis (load according to mass)	0,11
Upper part Of façade	Kinematic Limit Analysis (load according to mass)	0,07

1 – corrected to the effective participation of mass in the mode

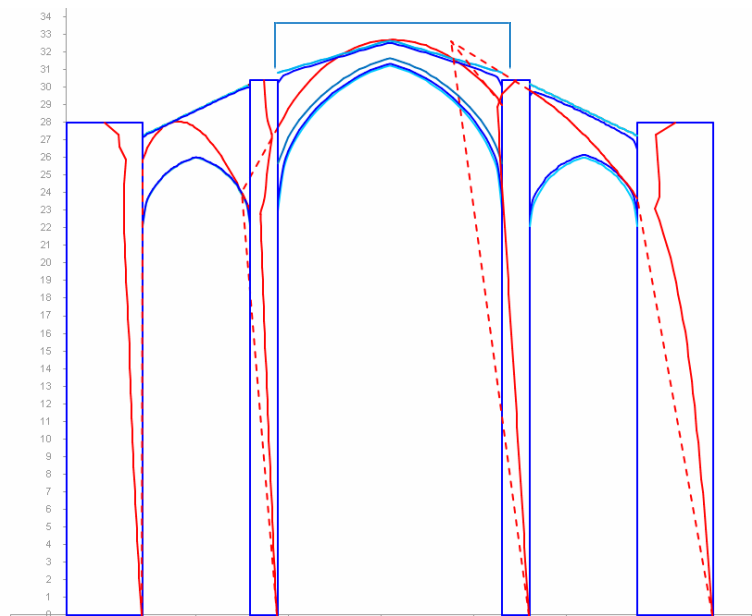


Figure 2.51- Collapse mechanisms of typical bay obtained by Static Limit Analysis (Roca, 2007)

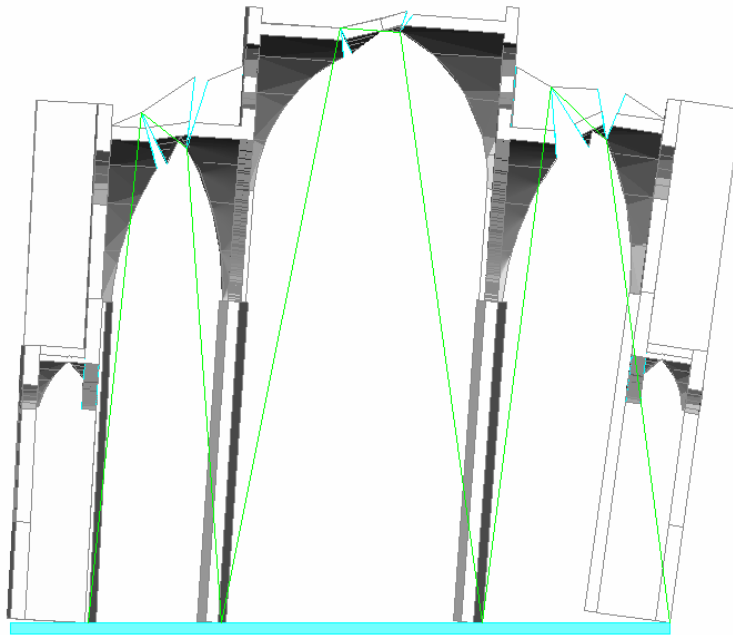


Figure 2.52 - Collapse mechanisms of typical bay obtained by Kinematic Limit Analysis (Roca, 2007)

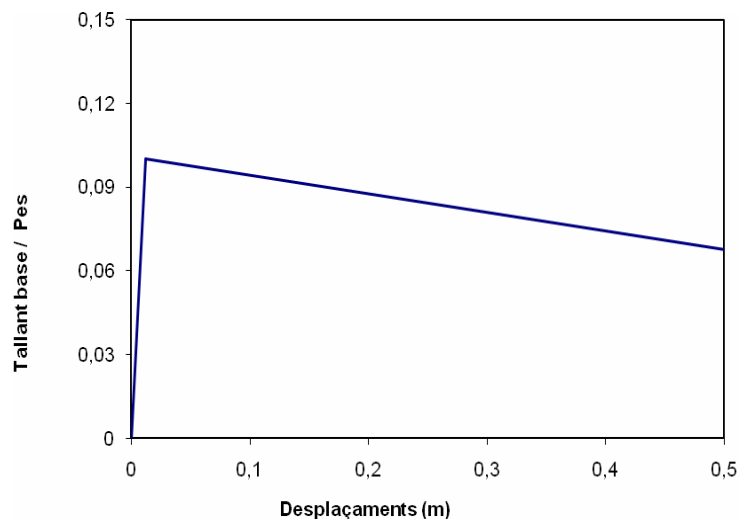


Figure 2.53– Capacity curve of the typical bay obtained with Kinematic Limit Analysis (Roca, 2007)

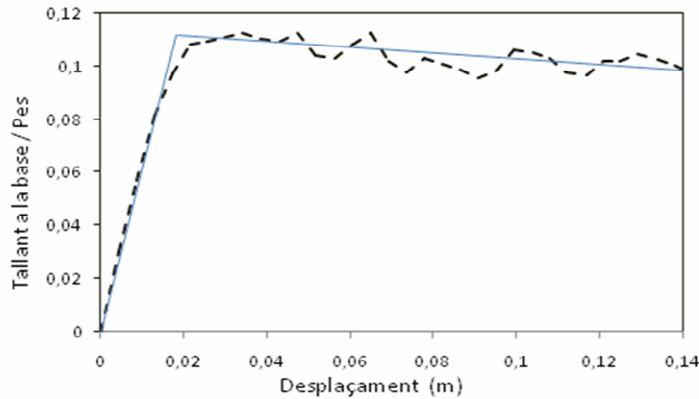


Figure 2.54 – Capacity curve of the typical bay obtained with FEA: real and idealized curve (Roca, 2007)

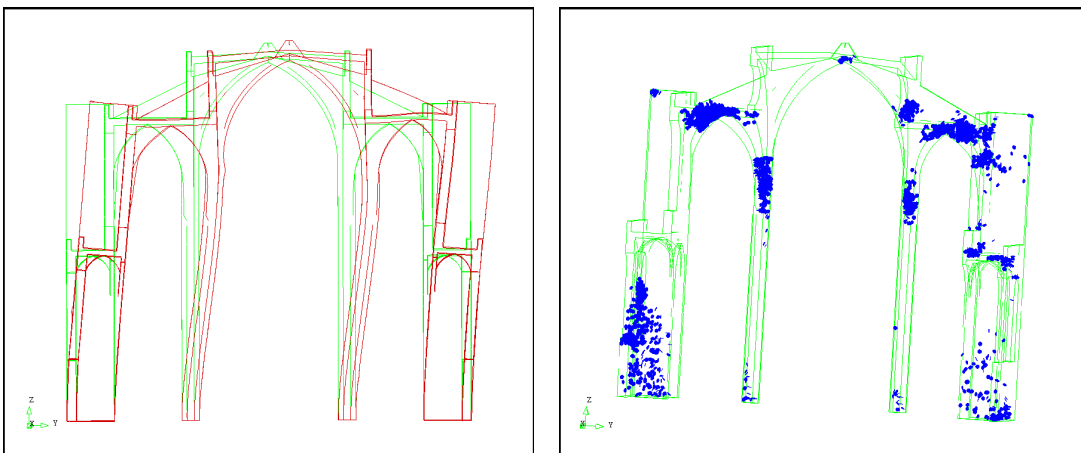


Figure 2.55 – Deformation and damage distribution for pushover in FEA (Roca, 2007)

The effect of not considering the rubble fill of the vaults has been also studied. On the one hand, the mass is reduced as the seismic capacity increases. On the other hand, for gravitational load would change the equilibrium path and excentricities would appear in the piers. Not considering also the triangular walls above the lateral vaults would reduce the seismic capacity. It is not so clear that these walls contribute to the resistance of the transversal section.

The Capacity Spectrum method was applied with the obtained demand and capacity spectra. Intersecting the capacity and demand curves it is possible to obtain the level of damage expected for an earthquake. The damage is expected to be reduced or moderate as the intersection point is near the elastic limit. Considering ductility, the curves are scaled and the damage is reduced, as shown in the figure 2.56.

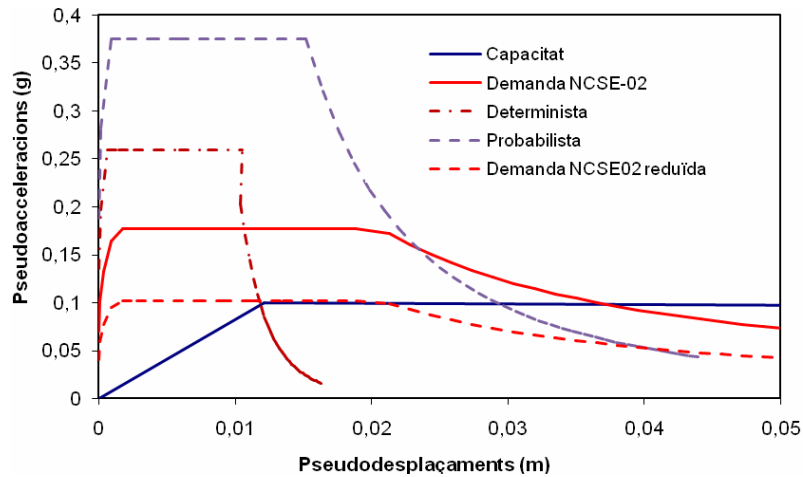


Figure 2.56 – Capacity and different demand spectra: deterministic, probabilistic and Seismic code (Roca, 2007)

The collapse mechanisms and seismic coefficients obtained by Roca (2007) are similar to Irizarry (2004). The seismic capacity is a little bit lower because the existing infill of the vaults has been taken into account. This new results should be more reliable because they are based on more accurate data.

In the rest of elements (tower, façade) the seismic coefficient has been found using Static and Kinematic Limit Analysis. The results are plotted in figures 2.57 to 2.61.

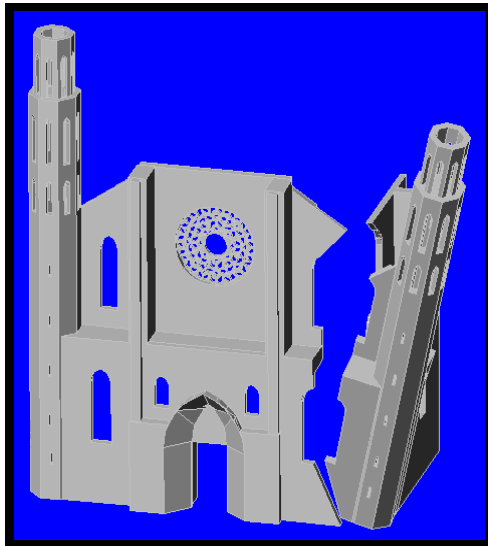


Figure 2.57 – Collapse mechanism for tower $s=0,14$ (Roca, 2007)

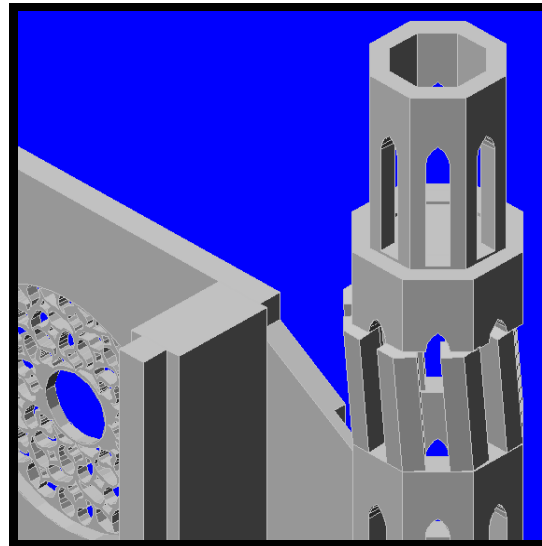


Figure 2.58 – Collapse mechanism for higher part of the tower, $s < 0,08$ (Roca, 2007)

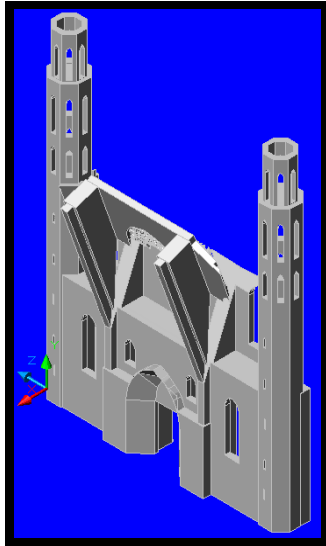


Figure 2.59 – Collapse mechanism for upper wall of façade, $s=0,22$ (Roca, 2007)

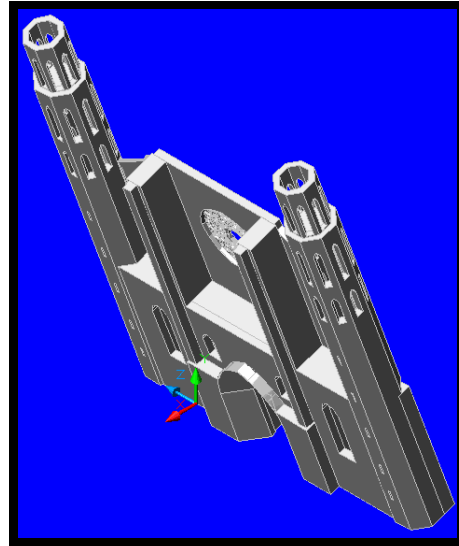


Figure 2.60 – Collapse mechanism for façade, $s=0,105$ (Roca, 2007)

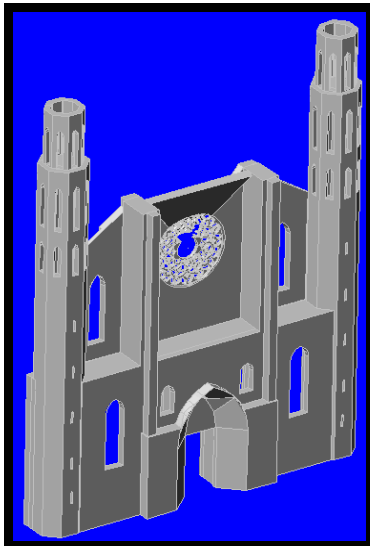


Figure2.61 – Collapse mechanism for wall above rose window, $s= 0,07$ (Roca, 2007)

CHAPTER 3

Tension-compression damage model for masonry

In this chapter the tension-compression damage model used to study numerically Santa Maria del Mar Church is presented. First, the basis of the damage theory is reviewed and the tension-compression damage model used for masonry is described. Then, some numerical examples are tested to understand the model and validate the program. Finally, some studies on masonry buildings using this material constitutive model of are presented.

3.1 Damage theory

The damage phenomenon can be interpreted as a nonlinear strain-stress relationship where the stiffness of the material degrades as a result of a given load. The formulation needs of an internal damage variable, which can be a scalar or a tensor.

In 1 dimension this phenomenon can be defined as:

$$\sigma = E_d \varepsilon \quad (3.1)$$

where E_d is written as:

$$E_d = (1-d)E \quad (3.2)$$

being d the damage variable (scalar in this case) and E the Young modulus.

Physically, the material degradation can be interpreted as the result of an initiation of microcracks or microvoids. In this context, the damage variable can be defined as the relation between the ratio of damaged surface and the total surface of the section as shown in figure 3.1

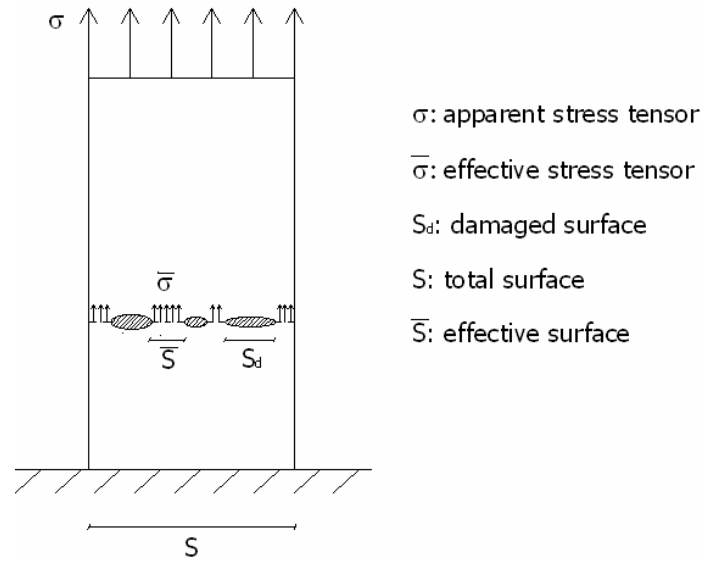


Figure 3.1 – Physical interpretation of damage

The effective surface is defined as the area that is carrying the stresses $\bar{\sigma} = S - S_d$ and the damage variable as $d = \frac{S_d}{S}$. For undamaged state $d=0$ ($S_d=0$) and for complete damaged $d=1$ ($S_d=S$).

$$\sigma \cdot S = \bar{\sigma} \cdot \bar{S} \rightarrow \sigma = \bar{\sigma} \cdot \frac{\bar{S}}{S} = \bar{\sigma} \cdot \frac{S - S_d}{S} = \bar{\sigma} \left(1 - \frac{S_d}{S}\right) = \bar{\sigma} (1 - d) \quad (3.3)$$

Then, the stress-strain relationship can be established as follows:

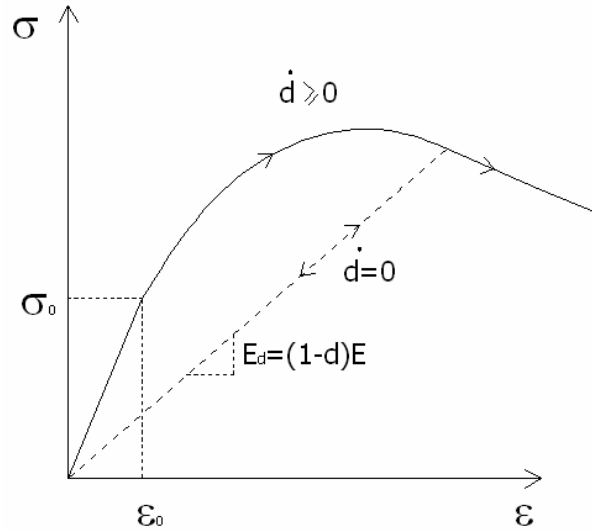
$$\sigma = (1 - d)\bar{\sigma} = (1 - d)E\varepsilon = E_d \varepsilon \quad (3.4)$$

where $0 < d < 1$, as stated before.

The variable d has to fulfil the following conditions:

- The damage surface cannot be diminished: $\dot{S}_d > 0 \rightarrow \dot{d} > 0$
- The damage is initiated when the stress (or strain) exceeds the initial damage threshold $(\varepsilon_0, \sigma_0)$.
- when unloading there is not evolution of damage, keeping d constant and an elastic behaviour.

These conditions are represented in figure 3.2.


 Figure 3.2 – Evolution of variable d in the strain-stress diagram

It is possible to define a varying damage threshold, as a function of the evolution of the stress state. This is established by means of hardening or softening laws. As shown in figure 3.2 there is a reduction of the stiffness but the stresses can still increase, called a hardening behaviour. Afterwards, the stresses start to be reduced, called a softening. When unloading there is an elastic unloading with the damaged stiffness (but strains are recovered).

In 3D, the problem would be formulated in a tensorial way:

$$\boldsymbol{\sigma} = \mathbf{D}_d : \boldsymbol{\varepsilon} \quad (3.5)$$

where the 4th order constitutive tensor \mathbf{D}_d is defined in terms of damage in specific point. There are many ways to characterize the damage and therefore the variability of the constitutive matrix. One of the simplest is the scalar damage, as shown before, \mathbf{D}_d is defined by:

$$\mathbf{D}_d = (1 - d)\mathbf{D} \quad (3.6)$$

This model implies same damage in all the directions and is called isotropic damage. More complex models exist having the damage variables defined in a tensor way, affecting the elastic tensor \mathbf{D} . In any case, the damage variables have to fulfil the aforementioned conditions.

In the case of isotropic scalar damage a norm r in the stress space (or a norm in the strain space) is defined to control the evolution of the damage variable. In addition an internal variable r is needed to establish the damage threshold. When the norm is higher than a given threshold, the damage variable increases and the threshold moves to a new value. If that is not the case, d and r remain constant.

3.2 Tension – compression scalar damage model

In the present work, an isotropic damage model, with two scalar internal variables to monitor the local damage under tension and compression (Cervera, 2003), is used. It provides a simple constitutive model which is able to capture the non-linear behaviour including strain hardening/softening, stiffness degradation under multiple stress reversals. This is a sufficient good model for masonry, as it takes into account a different behaviour in tension and compression and an independent control of the damage in each case. It has already been satisfactorily used in large-scale models of masonry buildings, which will be presented in following sections.

The model is based on the effective stress concept ($\bar{\sigma}$), defined as the stress associated to elastic strain $\boldsymbol{\epsilon}$; $\bar{\sigma} = \mathbf{D} : \boldsymbol{\epsilon}$, where \mathbf{D} is the elastic constitutive tensor. The tensor $\bar{\sigma}$ is divided into a positive or tensile part $\bar{\sigma}^+$ and a negative or compressive part $\bar{\sigma}^-$, in the following way:

$$\bar{\sigma}^+ = \sum_{i=1}^3 \langle \sigma_i \rangle \mathbf{p}_i \otimes \mathbf{p}_i \quad \text{and} \quad \bar{\sigma}^- = \bar{\sigma} - \bar{\sigma}^+ \quad (3.7)$$

where σ_i is the i -th principal stress of $\bar{\sigma}$; \mathbf{p}_i represents the unit vector associated with the principal direction i and $\langle \cdot \rangle$ are the Macaulay brackets, defined as $\langle x \rangle = \max(0, x)$.

Two internal variables of damage, each one associated with a sign of the stresses are defined: d^+ for tensile damage and d^- for compressive damage. Under these considerations, the constitutive equation is written as:

$$\boldsymbol{\sigma} = (1 - d^+) \bar{\sigma}^+ + (1 - d^-) \bar{\sigma}^- \quad (3.8)$$

These variables state the level of damage reached at each integration point, in such a way that $d^\pm = 0$ means that the material is intact and $d^\pm = 1$ indicates the total material failure. The use of a different variable for each sign of the stresses implies that, for example, a material previously damaged to tension would recover its original behaviour if it is put under compression, and vice versa.

Next, the equivalent effective stress norm is defined. This is a scalar positive value that is used to compare different stress states in three dimensions, and it is useful to unify load, unload and reload concepts. The equivalent norms for tensile effective stress (τ^+) and for compressive effective stress (τ^-) have the form:

$$\tau^{\pm} = (\bar{\sigma}^{\pm} : \mathbf{C}^{\pm} : \bar{\sigma}^{\pm})^{1/2} \quad (3.9)$$

where the two non-dimensional fourth order metric tensors \mathbf{C}^+ and \mathbf{C}^- are identical and equal to the inverse of tensor D/E , being E the Young's modulus of the material.

Starting from the previous definitions, two different criteria of damage can be introduced, namely, g_+^{\pm} and g_-^{\pm} , defined as:

$$g^{\pm}(\tau^{\pm}, r^{\pm}) = \tau^{\pm} - r^{\pm} \leq 0 \quad (3.10)$$

where r_+^{\pm} and r_-^{\pm} are internal variables that control the size of the damage surface in the stresses space in every time step. Their initial values are $r_0^{\pm} = f_e^{\pm}$ where f_e^+ and f_e^- are respectively the tensile and compressive strength of the material (the stresses at which the material fails and damage appears). In this sense, the explicit definition of these internal variables has the form:

$$r^{\pm} = \max[r_0^{\pm}, \max(\tau^{\pm})] \quad (3.11)$$

The criterion stated in equation 3.10 implies that damage evolution occurs when condition $g^{\pm} \leq 0$ is not satisfied. In this case, r^{\pm} is updated until damage criterion is satisfied again. Finally, the damage variables d^{\pm} are defined explicitly as a function of their respective internal variables r_+^{\pm} . They are monotonic increasing functions of the form $0 \leq d^{\pm}(r^{\pm}) \leq 1$. The post-peak behaviour is defined by means of the tensile and compressive fracture energy of the material G^{\pm} (explained graphically in figure 3.3). This parameter is normalized respect to the characteristic length of the finite elements, to ensure objectivity respect to the mesh size.

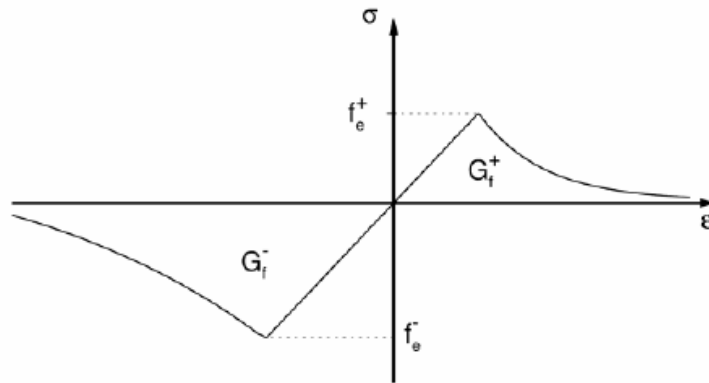


Figure 3.3 – Fracture Energy definition in the strain-stress diagram (Clemente, 2006)

3.3 Software and examples

The software used to run de FEA with the tension-compression damage model is COMET (Cervera et al., 2002). Its name means COupled MEchanical and Thermal problems solved by the Finite Element Method (FEM). It is a program developed at the International Center for Numerical Methods in Engineering of Barcelona (CIMNE). In our case we are going to use only the mechanical features for nonlinear static analysis. Implemented in COMET there is a tension compression scalar damage model based on the aforementioned theory. The material input data need the definition of elastic parameters (density, Young modulus and Poisson coefficient) and parameters related to the damage model (tensile strength, tensile fracture energy, compressive strength and compressive fracture energy).

The tension-compression scalar damage model has been tested in simple models before applying it to a complex reality as Santa Maria del Mar, in order to understand the influence of the different parameters and validate the program. Three examples are proposed to validate the program: 1) at the material level, 2) at the structural level, 3) at the structural level in a typical masonry element.

Example 1: Single element model (2D)

The first example to be tested is a single 2D plane stress square element in order to evaluate the tension – compression damage model at the material level. The square element is fixed in the bottom nodes and subjected to alternate positive and negative forces in the top nodes creating a specific compression and tension loading/unloading path, as shown in figure 3.4. In fact, what is controlled is not the load but the displacement.

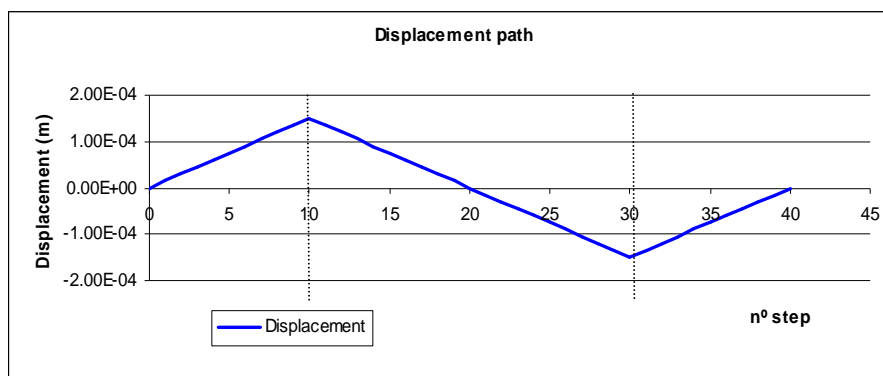


Figure 3.4 – Displacement loading path

Different values have been given in order to understand and verify the constitutive model, namely the ratio between compression / tension strength and the fracture energy. For the given loading path two different compression / tension strength ratios have been chosen. The results are plotted in figures 3.5 and 3.6.

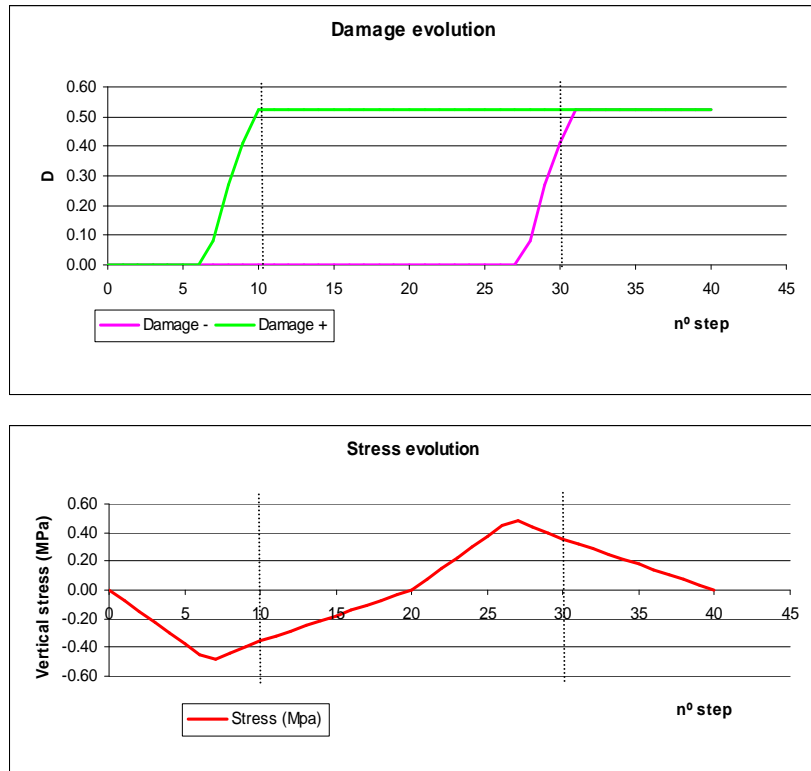


Figure 3.5 - Damage and vertical stress evolution for Compression / tension strength =1

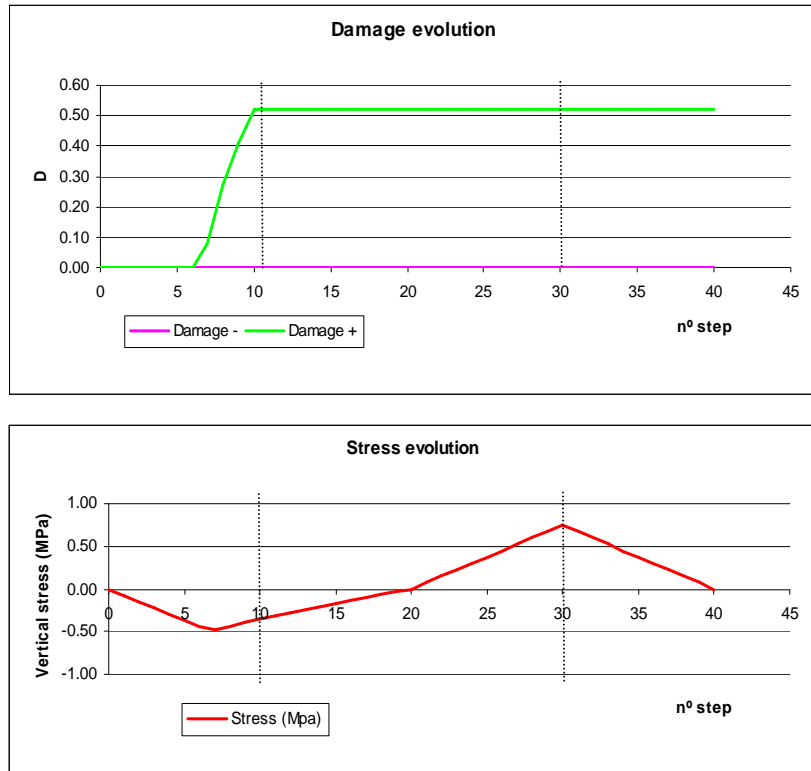


Figure 3.6 - Damage and vertical stress evolution for Compression / tension strength =2

The first case is considering same strength for compression and tension. In this case, the following trends can be observed in figure 3.5:

- Tensile loading: there is a linear relation between load and displacement until a maximum displacement (and a corresponding maximum load) is reached. This load corresponds to the tensile strength: 0.5MPa. After this moment, damage begins: the displacement keeps growing but the load decreases, as the compressive damage variable increases up to a maximum of 0.52.
- Tensile unloading: as the displacement decreases until the equilibrium point, the relationship between force and displacement is again linear, but this relation is based in the new damaged condition, as a result of a new stiffness $E_d = (1 - d)E$.
- Compressive loading: when the compressive loading begins, the original stiffness is recovered as the damage model is independent for compression and tension. This linear behaviour stops when the compressive strength is achieved. In this case as the ratio=1 the behaviour is symmetric to the tension. The same compressive damage is reached and the same loading/unloading path is followed.

When the compressive strength is higher than the tensile strength (ratio=2), the behaviour is not symmetric even if the loading path is. As shown in figure 3.6, while in tension damage is reached, in the compressive loading path the limit is not reached and no damage is achieved.

Regarding the fracture energy, it is a parameter defined to control the softening of the material (post-peak behaviour). Different values have been tested obtaining the curves plotted in figure 3.7.

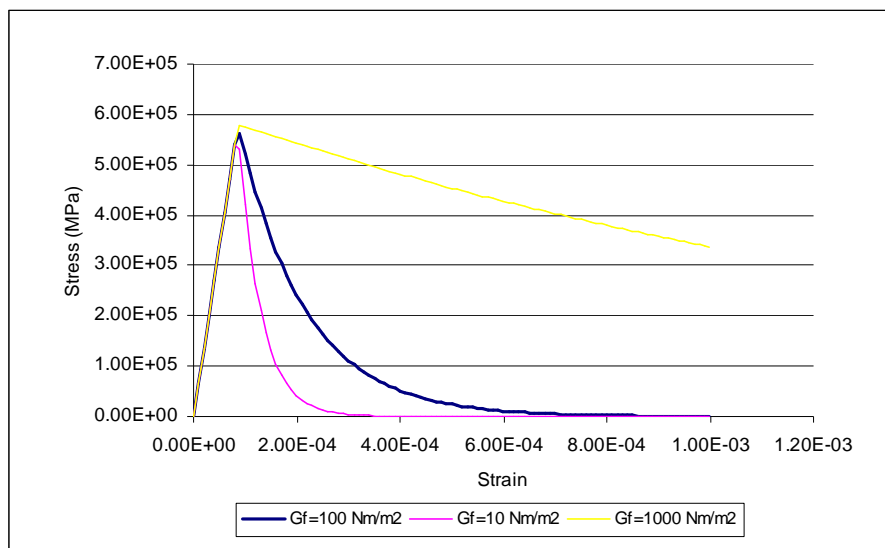


Figure 3.7 Strain-stress diagram for different fracture energy values

Graphically, the fracture energy is related to the area below the strain-stress graph. Therefore, the higher is that value the flatter is the curve.

Example 2: Cantilever (2D)

The second example is done in a real 2D plane stress cantilever (composed by many elements) to evaluate the nonlinear behaviour at the structural level. A vertical cantilever subjected to a horizontal force in the top has been studied with a tension – compression model. It has been studied with two hypotheses regarding the strength: a) compression/tension strength =1 and b) compression/tension strength =10.

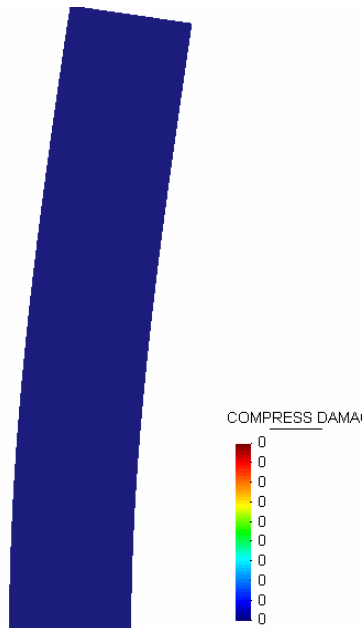


Figure 3.8 - Deformed shape and compressive damage (strength ratio=10)

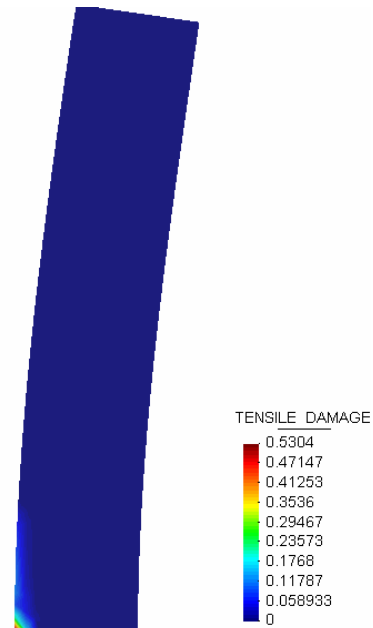


Figure 3.9 - Deformed shape and tensile damage (strength ratio=10)

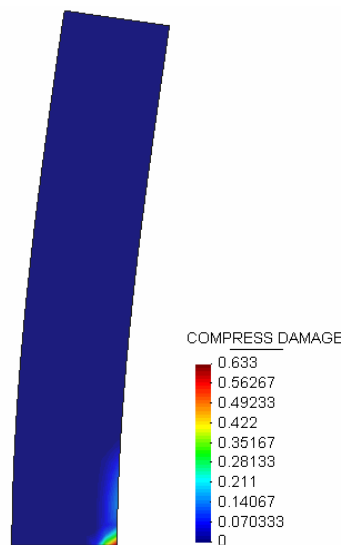


Figure 3.10 - Deformed shape and compressive damage (strength ratio=1)

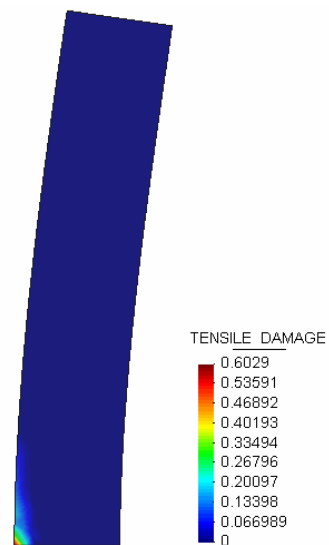


Figure 3.11 - Deformed shape and tensile damage (strength ratio=1)

As shown in figures 3.8 and 3.9, considering damage ratio=10 the damage occurs in the base of the section only in the tensile area. This reduces the stiffness of the section with respect to the linear model, reaching higher displacements. For the ratio=1 starts to damage the compression and tension areas of the base, where the bending moment is maximum, more or less at the same level (figures 3.10 and 3.11). This reduces even more the stiffness of the section obtaining higher deformation, as shown in figure 3.12.

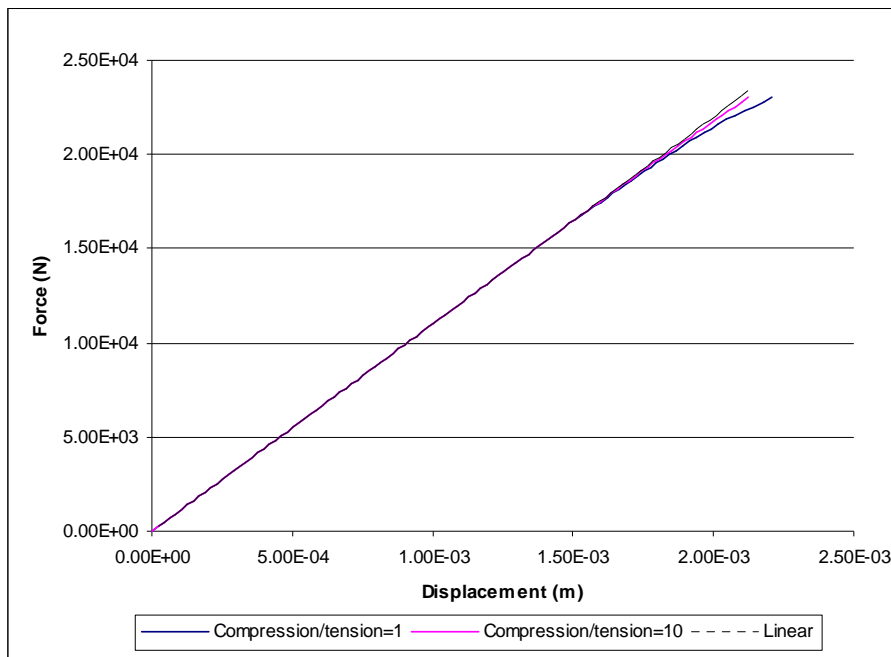


Figure 3.12 - Displacement- Force graph for cantilever subjected to horizontal force

Comparing both cases, for the same load, the tension/compression=1 is more damaged due to the lower compression strength. In addition, a higher redistribution of stresses causes higher stresses in tension area increasing also de tension damage. This leads to a higher deformation.

Example 3: arch (3D)

The third example is done with a 3D arch in order to evaluate the damage model in a common masonry element and to be able to identify its typical collapse mechanism. A three dimensional model of an arch has been tested with the tension-compression damage model in COMET. An arch is analysed for a self-weight load and an increasing concentrated load at $\frac{1}{4}$ of the span (taking as reference value 3000N). The same case has been already tested by Massanas (2003) using a similar damage model, but adapted to concrete. Two hypotheses have been made for the fracture energy:

- $G_f=1^{10} \text{ Nm/mm}^2$, which is equivalent to an infinite fracture energy. That means that after the damage threshold the curve is flat and the stress remains constant.

- $Gf=100 \text{ Nm/mm}^2$, which is a common value for masonry (the curve goes down quickly after the damage threshold).

As shown in figure 3.13, the relation deflection-load remains linear while the self-weight is being applied. In both cases the result is the same as the nonlinear range is not reached. As the arch starts to carry the point load at $\frac{1}{4}$ span the load curve becomes non linear (figure 3.14) because the arch starts to be damaged. The result for infinite fracture energy gives a higher strength (Load factor=1.52 against 1.35) because even if damaged the masonry can keep on carrying tension.



Figure 3.13 - Deflection – load factor for self weight

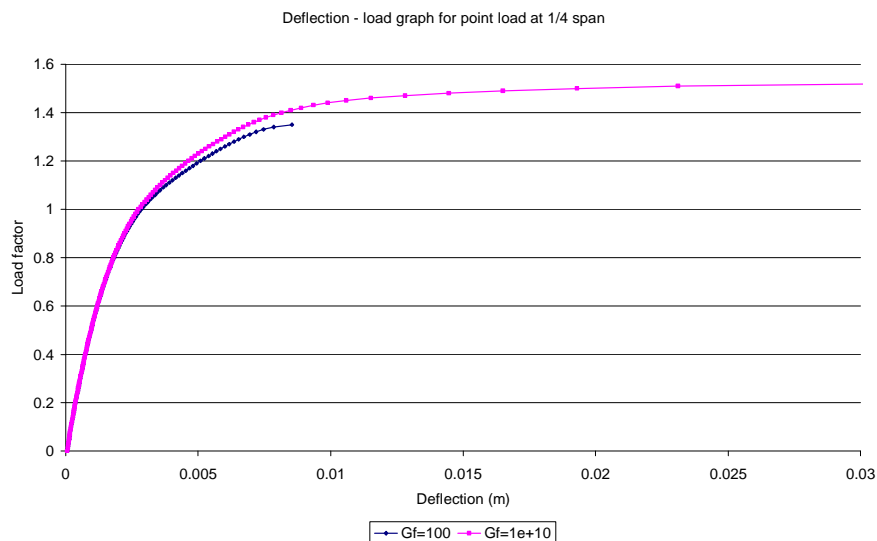


Figure 3.14- Deflection – load factor for $\frac{1}{4}$ span point load

In fact, the effect of the self weight in the arch already damages the arches a little bit in tension (figure 3.15 and 3.16). In both cases the damage is exactly the same in the extrados of the supports.

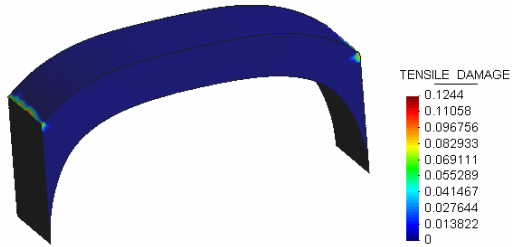


Figure 3.15 - Tensile damage and deformed shape for self-weight (infinite G_f)

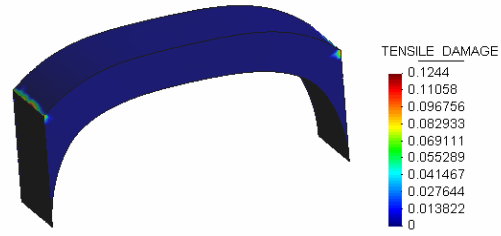


Figure 3.16 - Tensile damage and deformed shape for self-weight (finite G_f)

For a Load Factor equal to 1 of the point load ($F=30000N$) the damage is distributed in the way shown in figures 3.17 to 3.20. The compressive damage is due to the concentration of the load in that point. From the tensile damage we can observe that 4 hinges are being developed (also seen from the deformed shape where big rotations develop). Their progression will lead to collapse because, as they are not symmetrically placed, they will create a mechanism.

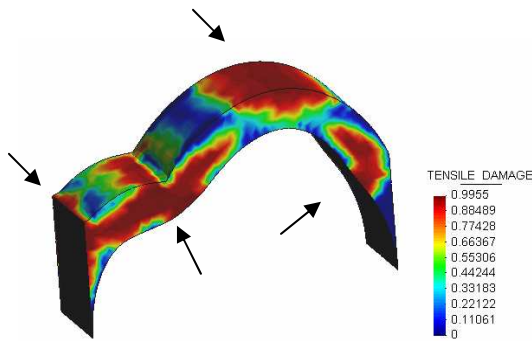


Figure 3.17 - Tensile damage and deformed shape point load LF=1 (infinite G_f)

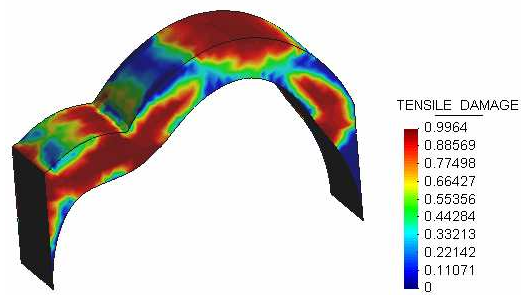


Figure 3.18 - Tensile damage and deformed shape point load LF=1 (finite G_f)

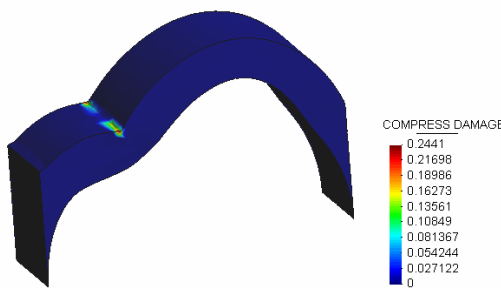


Figure 3.19 - Compressive damage and deformed shape point load LF=1 (infinite G_f)

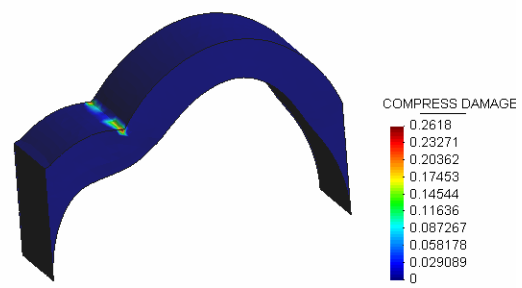


Figure 3.20 - Compressive damage and deformed shape point load LF=1 (finite G_f)

These results are in good agreement with the typical mechanism in arches subjected to an unsymmetrical load, as shown in figure 3.21. This mechanism has also been obtained for the

studied arch using limit analysis software (figure 3.22). In addition, the load factor is very similar ($LF=1.55$). In this case the value is a little bit higher as the arch has a wider section in the base to enclose the thrust line (the geometry is not exactly the same due to limitations of the software).

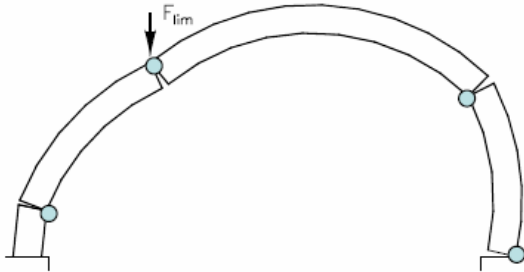


Figure 3.21 – Typical arch mechanism for $\frac{1}{4}$ span load

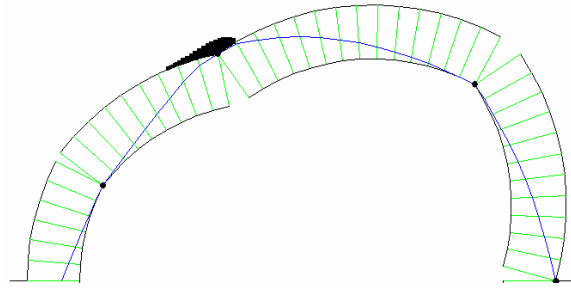


Figure 3.22 – Mechanism found by Limit Analysis ($LF=1.55$)

3.4 FEA of masonry buildings with damage models

Similar damage models have been used to carry out nonlinear FEA in several studies of masonry historical constructions, namely Girona cathedral (Mendoza, 2002), Küçük Ayasofya Mosque in Istanbul (Massanas et al., 2004), and Mallorca Cathedral (Clemente et al., 2006). The use of a continuum damage model has been found to be sufficiently accurate and relatively inexpensive in terms of computational cost for such a complex models.

Mendoza (2002) and Massanas et al. (2004) used a tension-compression damage model developed for concrete to carry out nonlinear FEA in Girona cathedral and Küçük Ayasofya Mosque, respectively (figures 3.23 and 3.24). The effects of the gravity load and differential settlements were studied and pushover analyses were carried out to evaluate the seismic performance of the structures. For instance, Girona cathedral was found to have a large safety margin for gravity loads, as it is able resist up to 3 times the self weight. The pushover analysis done with a horizontal force distributed according to the mass leads to collapse for a seismic coefficient of 0.18g (this value is far away from the seismic coefficient obtained from the Spanish Seismic Code for this location: 0.117g). Regarding Küçük Ayasofya Mosque, it was found to resist with moderate damage a horizontal acceleration of 0.30g. In both studies, the numerical analysis weren't able to predict the large deformations shown in the building. In historical buildings it is common to have deformations one or more order of magnitude superior to those than can be predicted by instantaneous numerical analyses, as many phenomena cannot be taken into account: construction process, long-term creep, thermal cycles, etc.

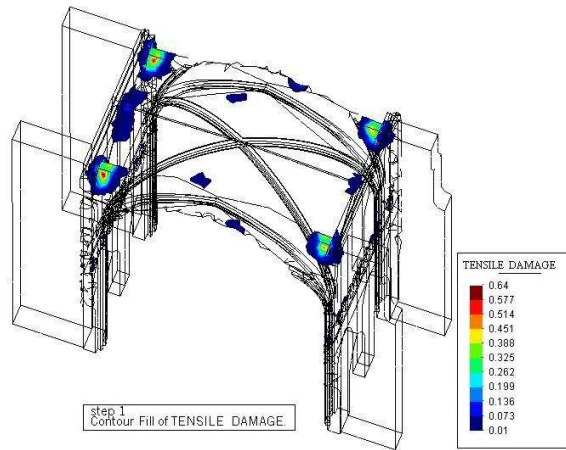


Figure 3.23 – Tensile damage distribution of Girona typical bay under gravity load (Mendoza, 2002)

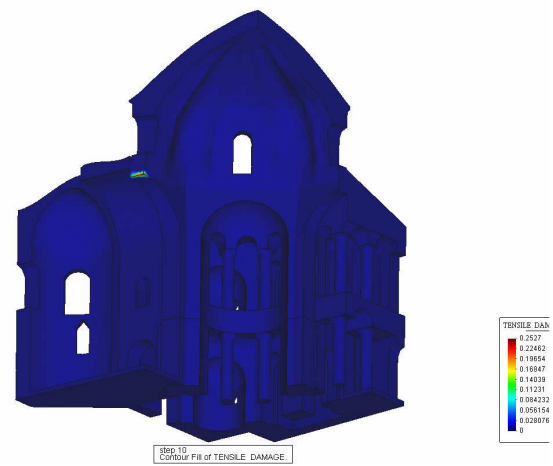


Figure 3.24 – Tensile damage distribution of Küçük Ayasofya Mosque under gravity load (Massanes, 2003)

In order to ensure numerical convergence, in both studies very high values were assumed for the fracture energy. It is shown that this parameter has a low influence in the results for gravity load, as the damage is reduced. However, considering high energy fracture is equivalent to assuming constant tensile strength while damage increases. Physically it would mean that there is a constant tensile capacity even if the material is cracked. Therefore, this assumption can lead to an overestimation of the capacity of the structure.

Clemente et al. (2006) improved the continuous tension-compression damage model or smeared-crack scalar damage model, modified in such a way that it can reproduce localized individual (discrete) cracks. This was achieved by means of a local crack tracking algorithm. The model was used to analyze the response of the structure of Mallorca Cathedral under gravity and seismic forces. Compared with the traditional smeared cracking approach, the tracking method showed a better capacity to predict realistic collapsing mechanisms; the resulting damage in the ultimate condition appears localized in individual cracks, which behave similarly to real plastic hinges; the computed ultimate loads become less sensitive to the variation of the tensile strength and other material parameter.

The structure was found to resist around 2 times its self weight, according to both models. The seismic performance of the building is assessed by means of a push-over analysis consisting of the gradual application of a system of lateral equivalent static forces on the structure distributed according to the mass. The continuous damage model predicts failure for a seismic coefficient of 0.10g while the localized damage model a between 0.12g and 0.14g depending on parameters related to the crack formation. The localized cracking model produces a higher failure load factor due to the restrictions that the model imposes to the propagation of damage (as compared in figures 3.25 and 3.26)

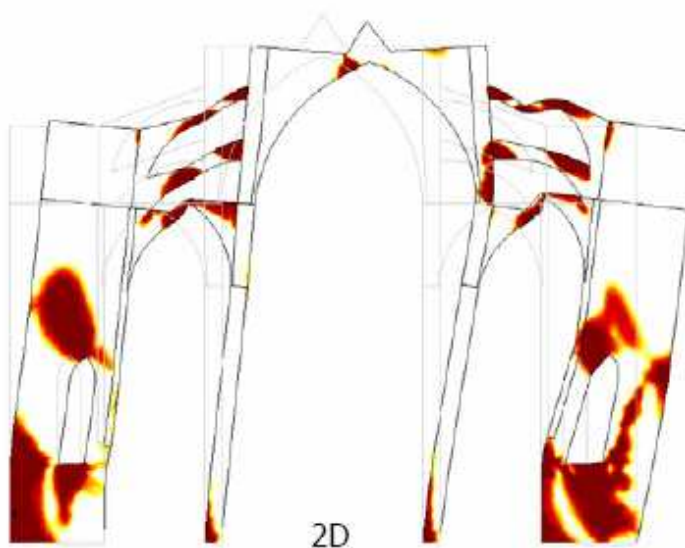


Figure 3.25– Collapse mechanism and tensile damage distribution for seismic load using a continuous damage model (Clemente, 2006)

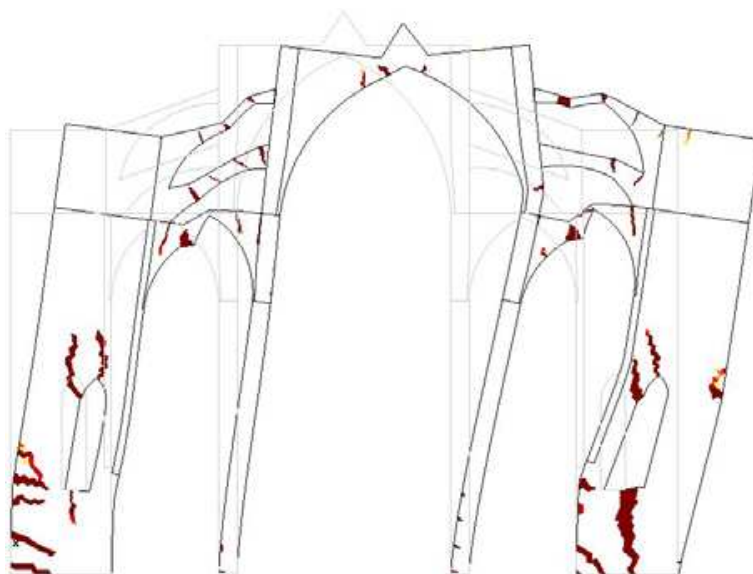


Figure 3.26– Collapse mechanism and tensile damage distribution for seismic load using a localized damage model (Clemente, 2006)

Again, a large value for the fracture energy is considered to ensure numerical convergence. This can affect in a significant way the collapse load factors and therefore the safety assessment of the structure.

CHAPTER 4

Finite Element Analysis of Santa Maria del Mar Church

In this chapter the results of a nonlinear FEA of the typical bay of Santa Maria del Mar Church are presented and discussed. First, the characteristics and calibration of the model and are described. Second, the results of analysing the structure subjected to gravity load and seismic load are presented and discussed. Then, the sensitivity of the model to specific mechanical parameters is studied. Finally, possible reinforcement techniques are simulated by numerical analysis.

4.1 Characteristics of the model

Both the geometry and FE meshing of the typical bay have been imported from the model used by Roca (2007). It consists in a 3 dimension model with 130.453 tetraedrical elements of 4 nodes representing half of the typical bay, introducing the convenient boundary conditions to consider symmetry (figure 4.1). Studying a portion of the building in a seismic analysis is a simplification, but it has been considered sufficiently accurate for the transversal behaviour of the structure. From the experimental modal analysis (Roca, 2007), the bays seemed to have similar dynamic behaviour independently from their position in the church (near the façade or the crossing).

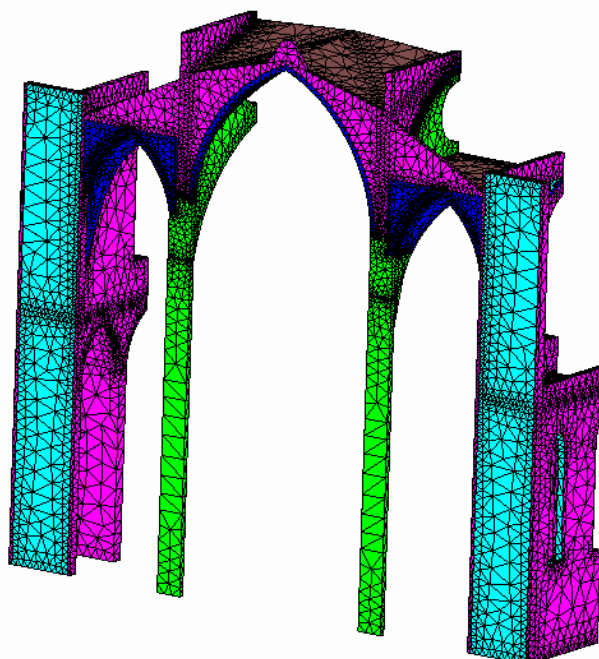


Figure 4.1 - FE model of Santa Maria del Mar

Same properties as Roca (2007) for every structural component were assumed. The nonlinear parameters were adapted to the new material constitutive model (tension-compression damage) for the masonry.

Table 4.1 – Mechanical properties of masonry

	Density (kg/m ³)	E (N/mm ²)	f_t (N/mm ²)	f_c (N/mm ²)
Columns	2200	12000	0.6	8.0
Central and lateral Vaults	2200	8000	0.4	8.0
Walls and buttresses	2200	8000	0.4	8.0
Wall infill	2200	4000	0.2	4.0
Heavy fill in vaults	2200	4000	0.2	4.0
Light fill in vaults	200	1000	0.2	4.0
Cover layer of vault	2200	1000	0.2	4.0

The Poisson's ratio was taken as 0.3 in all cases. All the masonry types had the same fracture energy. Two different fracture energies were assumed in the analysis. First, a typical value in masonry $G_{f,t}=0.1\text{Nmm/mm}^2$ for tension has been assumed; according to Lourenço (1996) the values for masonry range between 0.01 and 0.1Nmm/mm^2 . The compressive fracture energy would be automatically obtained as $G_{f,c} = G_{f,t} * (f_c / f_t)^2$. The variability of this and other mechanical parameters ($G_{f,t}$, f_t , f_c) is studied later.

4.2 Verification and calibration: Linear Elastic and Modal analysis

A linear elastic analysis with gravity load and a modal analysis have been carried out to test the model. The first one was done for verification of the model. The obtained results (deformed shape and stress distribution) give realistic values (figure 4.2 to 4.4). The maximum tensions in the vaults (0.65N/mm^2) are a little bit higher than their tensile strength (0.4N/mm^2), but this will be solved with the nonlinear analysis by developing little damage. The maximum deflection (almost 6mm in the key of the central vault) or the maximum vertical stress (3.3 N/mm^2 in the base of the columns), are realistic and assumable values. A nonlinear geometric analysis has been carried out and the obtained values for stresses and displacements are almost identical (difference <0.2%) as the structure is not so slender. As a result, this feature won't be taken into account in following analysis to simplify this analysis.

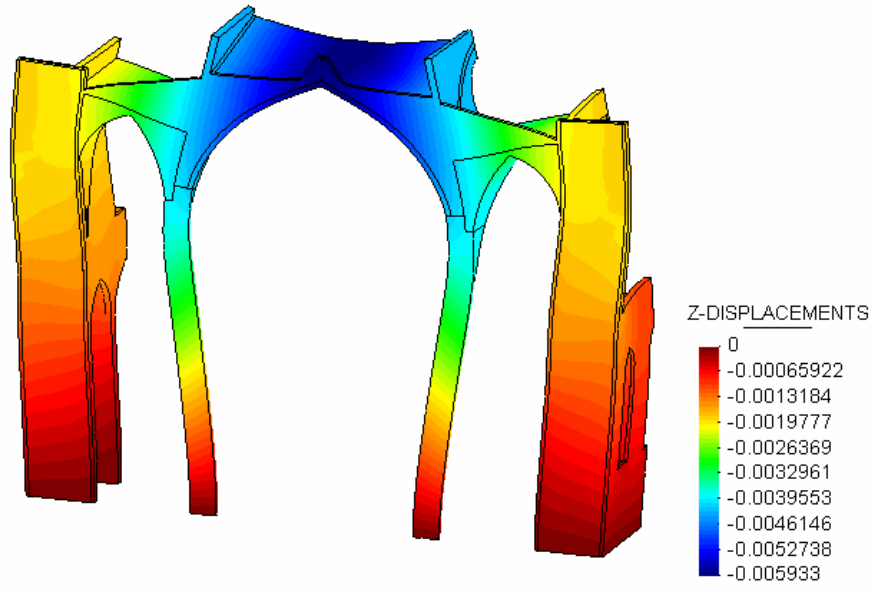


Figure 4.2 - Vertical displacement under self- weight in m (maximum deflection: 5.9 mm)

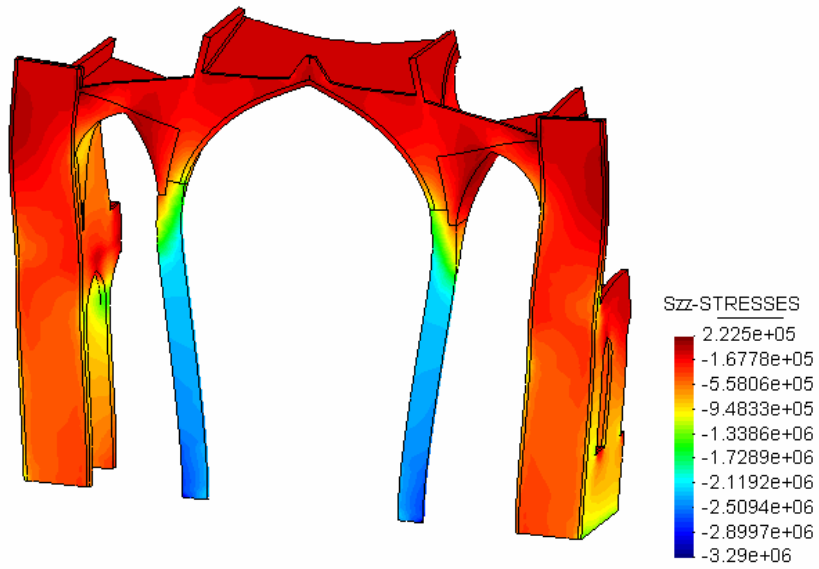


Figure 4.3 - Vertical stresses under self- weight in N/m^2 (maximum compression: 3.3 MPa)

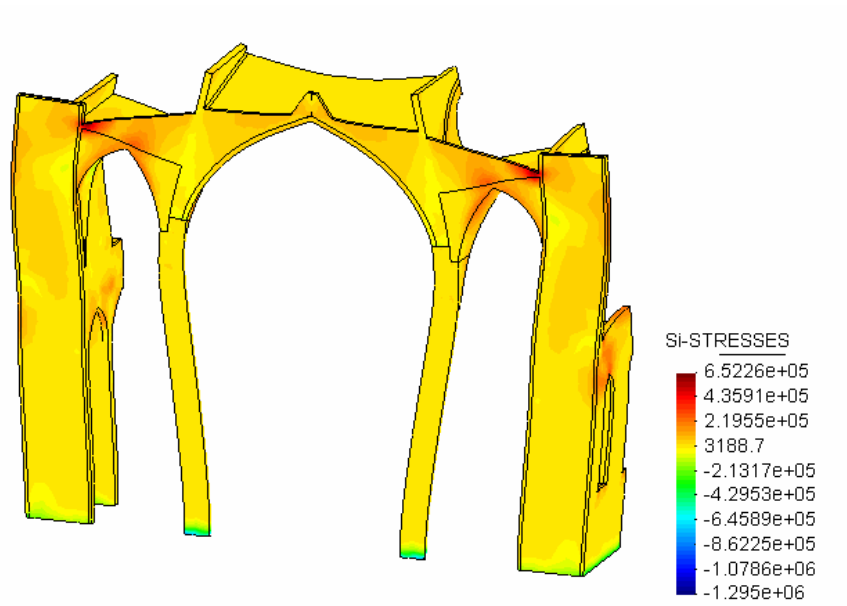
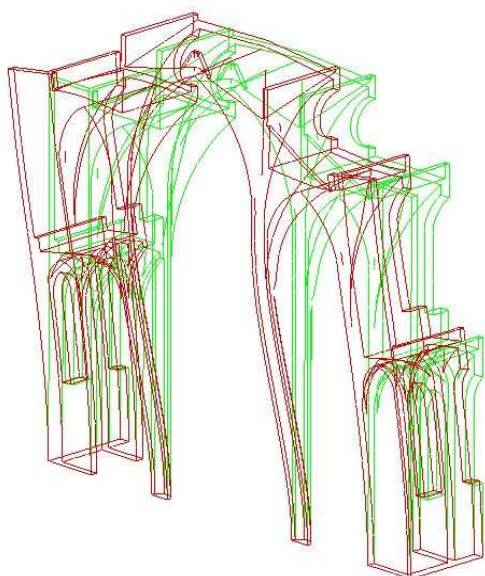


Figure 4-4 Maximum principal stresses under self- weight in N/m^2 (maximum tension: 0.65 MPa)

The elastic parameters used by Roca (2007) were defined according to the type of masonry used, but corrected to calibrate the model with modal analysis. The numerical 1st natural mode of the structure was approximated to the experimental one by varying the stiffness (E-modulus) of the different structural components. As a result of the modal analysis, the first 5 modes are listed in table 4.2 and the first two modes are shown in figures 4.5 and 4.6. The first mode is the most representative in the y-direction (with a mass participation ratio of 73.5%) and will be used for computing the load pattern in the pushover analysis and to apply to Capacity Spectrum Method in this direction.

Table 4.2 - Natural modes of the typical bay

Mode	Experimental (Hz)	Numerical (Hz)	Type	Mass participation Ratio (transversal direction)	Mass participation Ratio (vertical direction)
1st	1.45	1.43	Transversal	73.5%	0%
2nd	2.17	3.26	Vertical	0%	2.10%
3rd	-	6.7	Transversal	9.60%	0.20%
4th	-	6.72	Vertical	0.50%	5.40%
5th	-	8.4	-	2%	0%

Figure 4.5 - 1st mode (transversal)Figure 4.6 - 2nd mode (vertical)

Starting by the values used by Roca (2007), there was an attempt to adjust also the 2nd mode of the structure (vertical mode). However, it has been impossible to adjust the model for the 2nd mode and the 1st mode (transversal mode) at the same time.

As a result, the calibration done by Roca (2007) has been considered sufficient, keeping in mind that it is a simplification of the reality. The impossibility to calibrate the model to both the 1st and 2nd mode could be due to the soil heterogeneous characteristics and the interaction between the different macroelements of the structure. This could be solved by modelling the whole structure and a considerable portion of the soil were it is founded in a single numerical model. This task is out of scope of this study.

4.3 Gravity load

A material nonlinear FE analysis has been done for the gravity load. As shown in figure 4.7 there is a very slight difference between the deflection in a linear and a nonlinear analysis (vertical displacement distribution is shown in figure 4.8). This is due to the slight damage that appears in the corner of the triangular walls above the lateral vaults, as shown in figures 4.9 and 4.10. This damage is caused by the eccentricity of the thrust line, creating tension and cracking.

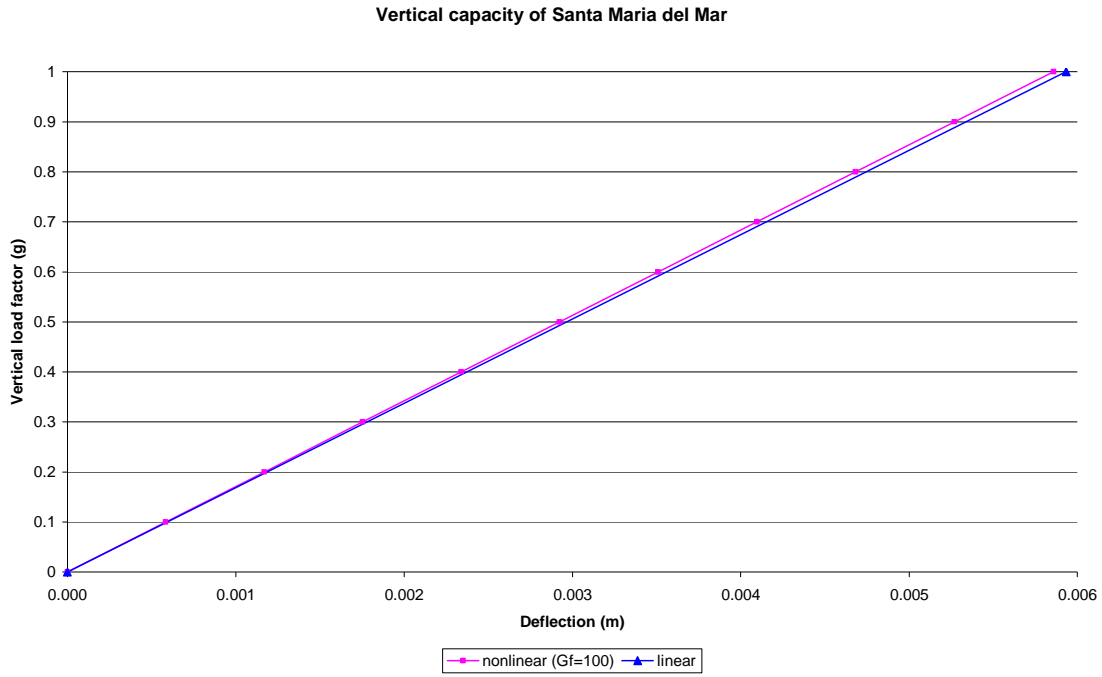


Figure 4.7 – Deflection in central vault – Load Factor graph

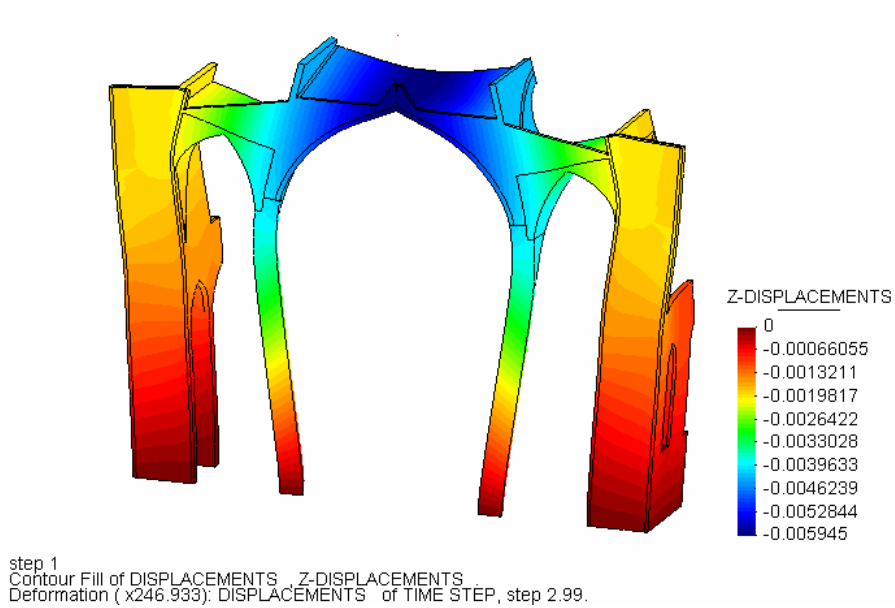


Figure 4.8 – Vertical displacements due to gravity load in m

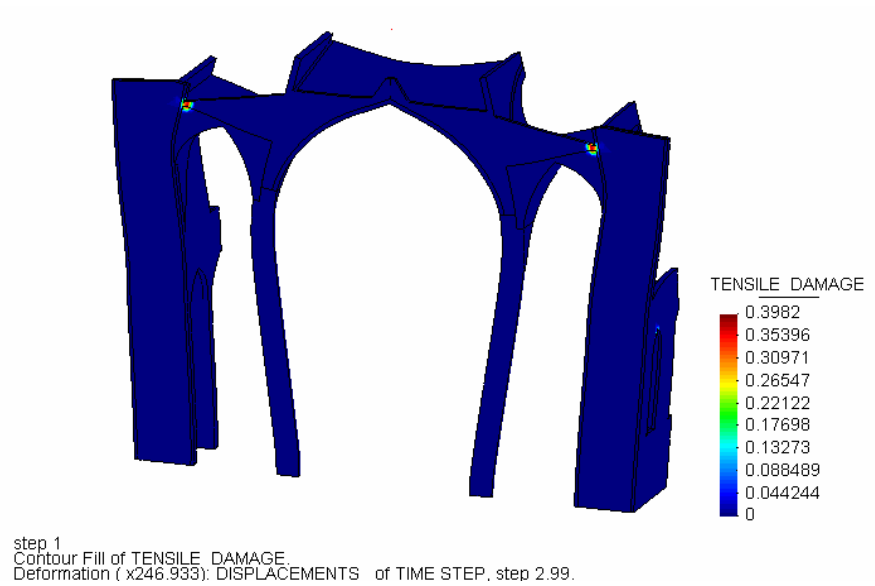


Figure 4.9– Tensile damage distribution due to gravity load

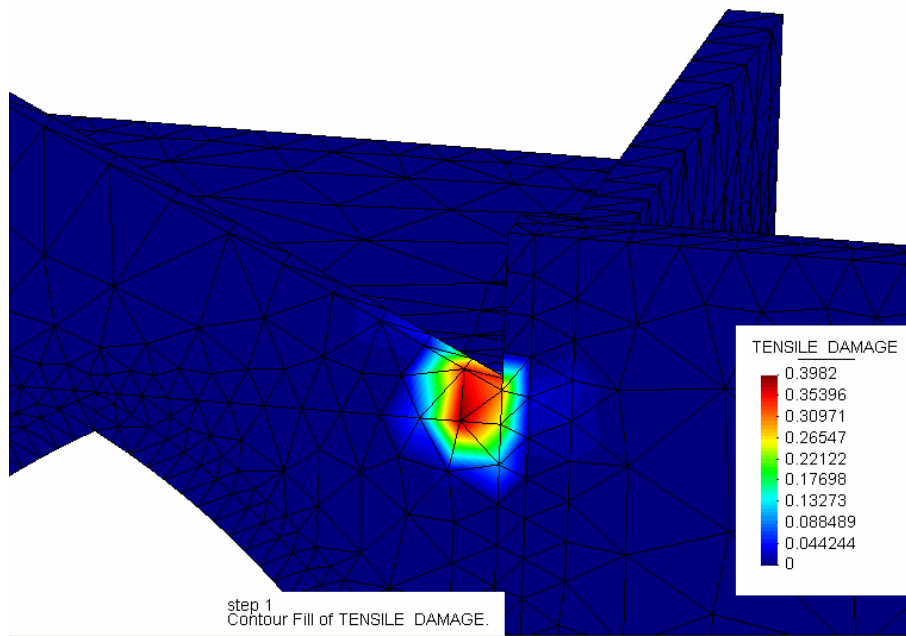


Figure 4.10– Detail of the tensile damage in the triangular wall

Regarding the stresses, we can observe that the higher tension stresses are concentrated in the damaged areas (figure 4.11). Of course, these stresses are equal or lower than the tensile strength: in the case of the vaults that means 0.4 MPa. The average vertical compression in the base of the piers is 2.8MPa, while the maximum is 3.3MPa (41% of their resistance), as shown in figure 4.12. These values are similar to the stresses measured with the “hole drilling” test: an average of 2.9MPa and a maximum of 3.8MPa (Roca, 2007). No damage is found in compression.

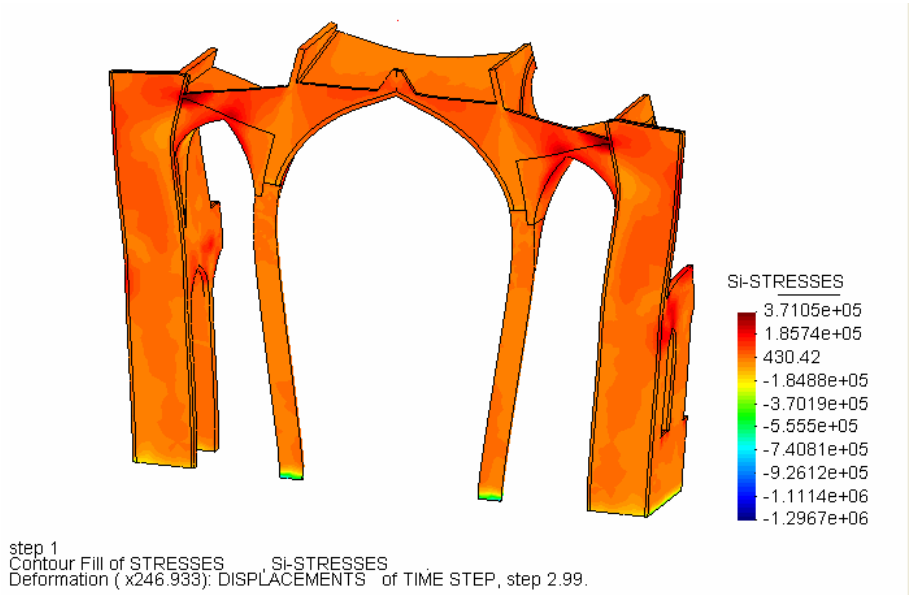


Figure 4.11 – Maximum principal stresses for gravity load in N/m^2 (maximum tensions)

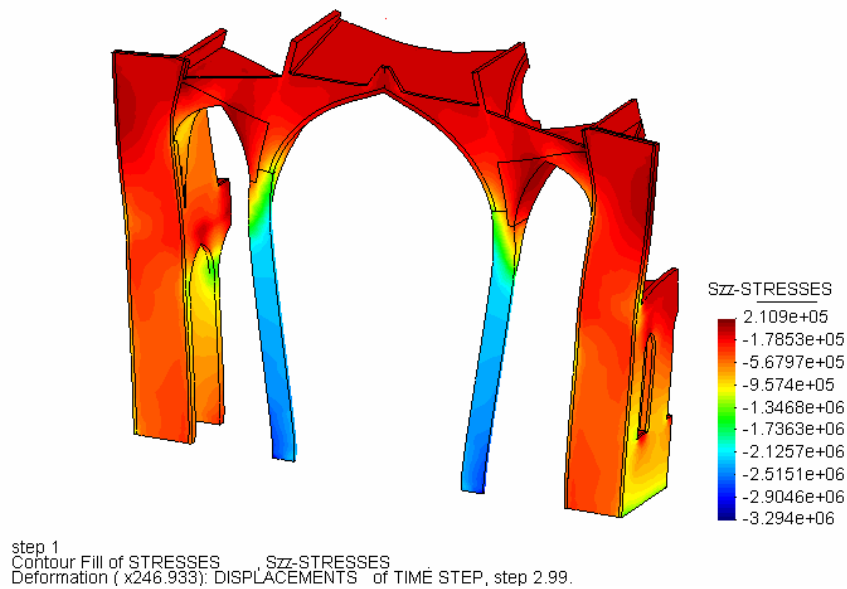


Figure 4.12 – Vertical stresses for gravity load in N/m^2

Roca (2007) obtained very similar values using the graphic static method: average compression of 2.9MPa. By means of this technique, the function of the lateral vault infill was also studied. The conclusion was that this infill is placed to compensate the thrust of the central vault and centre the load in the pier. Reducing its weight would reduce significantly the average compression in the base to 2.15MPa (and also collaborate for a better seismic resistance, as mass in height would be reduced). However, this situation could lead to an eccentric load in the pier, having an elevated risk of cracking and/or crushing.

In order to study the safety of the structure, the self-weight has been increased up to collapse. The load factor obtained at the collapse of the structure is not exactly a safety factor as the structure will never be subjected to an extra vertical load with these characteristics. However, it gives a qualitative idea about the safety of the structure. In the case of Santa Maria del Mar Church, the structure would collapse for almost 3 times the self-weight of the structure (figure 4.13). This is quite a big value and it gives an idea of a large safety margin to resist vertical loads. Clemente et al. (2006) obtained a load factor of 2 for Mallorca Cathedral, using a FEA with the same constitutive model. This difference makes sense, as Mallorca cathedral is a more slender construction.

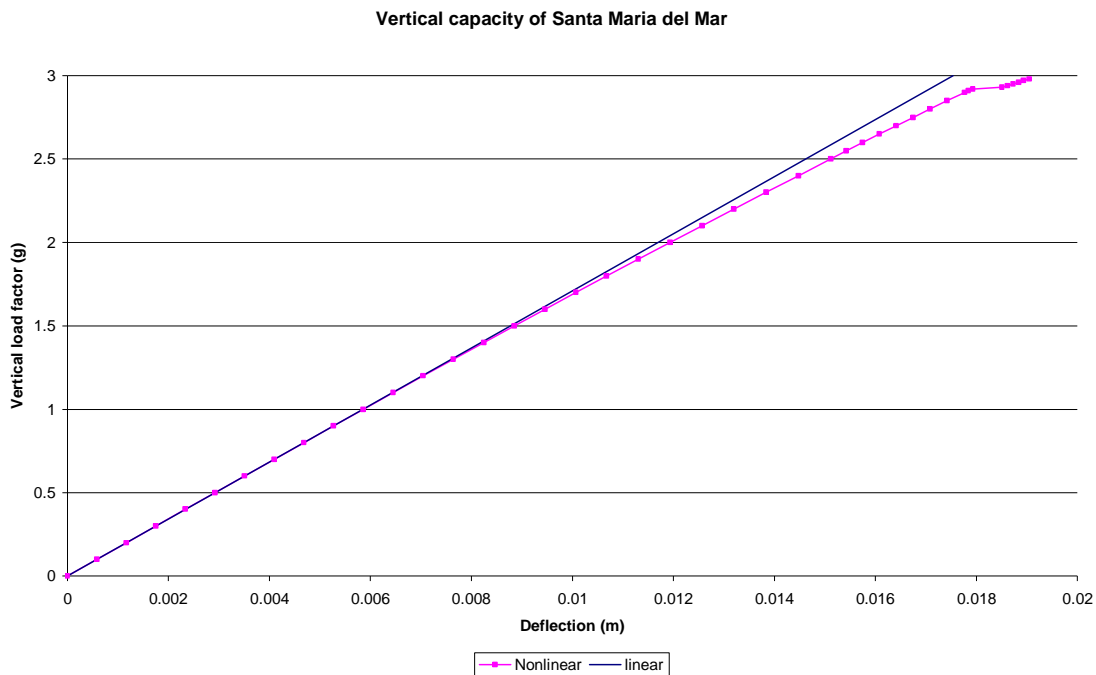


Figure 4.13 – Deflection – Vertical load factor graph up to failure

As the load is increased, the structure is damaged in a continuous way but doesn't show a clear trend to plastification. At a load factor next to 3, it was impossible to reach convergence. Just before collapse, the damage distribution is shown in figure 4.14. There is a big damage in tension in the upper side of the lateral vaults. However, there are not enough hinges to develop a collapse mechanism. What in fact leads to collapse is the fragile compressive failure of the piers, before hinges could develop. As presented in figures 4.15 and 4.16 the vertical stresses of the pier have reached the compressive strength (8MPa) in almost the whole base a generating big damage. As it is impossible to redistribute the load, the structure would collapse in a sudden way.

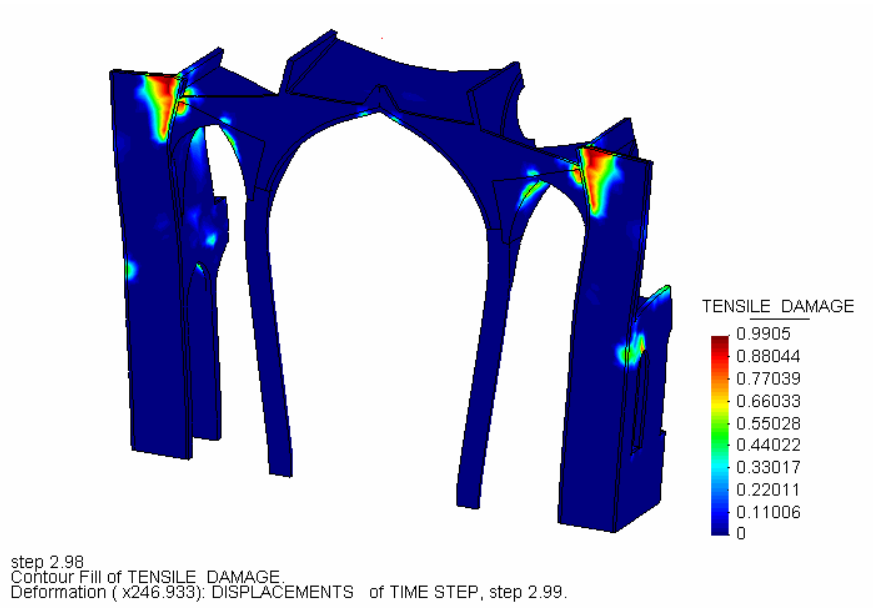


Figure 4.14 – Tensile damage distribution for LF=3

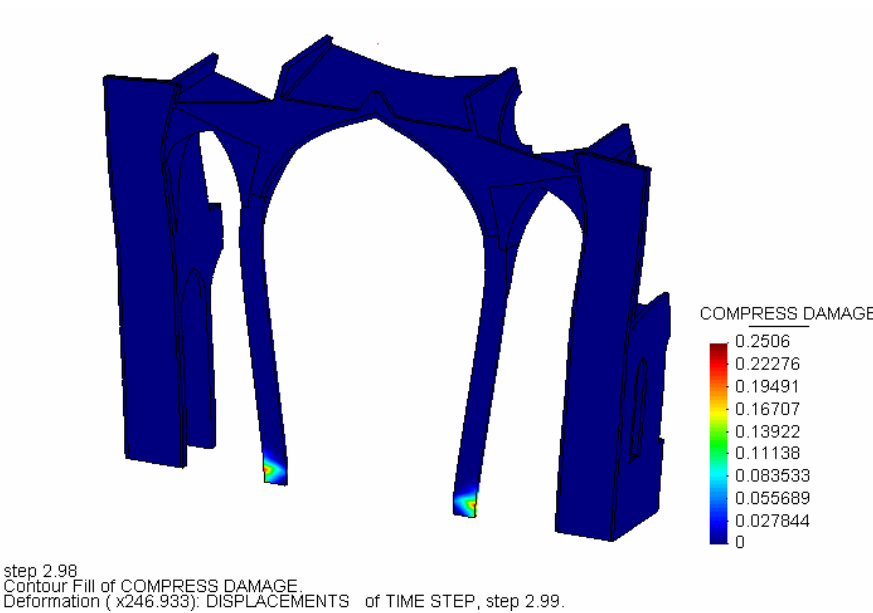


Figure 4.14 – Compressive damage distribution for LF=3

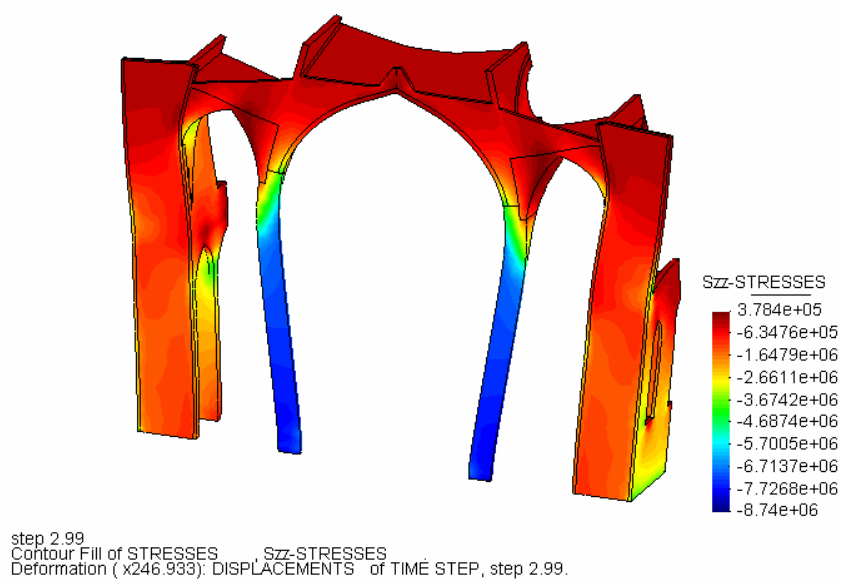


Figure 4.14 – Vertical stresses in in N/m^2 for $\text{LF}=3$

4.4 Seismic analysis: nonlinear static pushover

A pushover analysis has been done in order to assess the behaviour of the structure under a seismic load. This is a simplified analysis as it is the equivalent nonlinear static analysis of one macroelement of the structure. An accurate analysis would be a nonlinear dynamic analysis in the time-domain, introducing a time-acceleration spectrum. However, this simplified analysis is accepted to assess the seismic performance of the structure. With the pushover analysis it is possible to obtain the capacity curve that will be applied in the capacity spectrum method.

For that purpose two different horizontal actions have been studied:

1. Horizontal load proportional to the mass distribution
2. Prescription of increasing displacements according to the 1st natural mode shape, as it is the dominant vibration mode of the structure.

1. For a horizontal load proportional to the mass distribution, the obtained capacity curve is plotted in figure 4.15. Non convergence is reached for 0.105 g. As the curve becomes flat and a peak is expected for a close load. Therefore, collapse is expected for a very close value. As the pushover is load-controlled no information about the post-peak behaviour can be obtained.

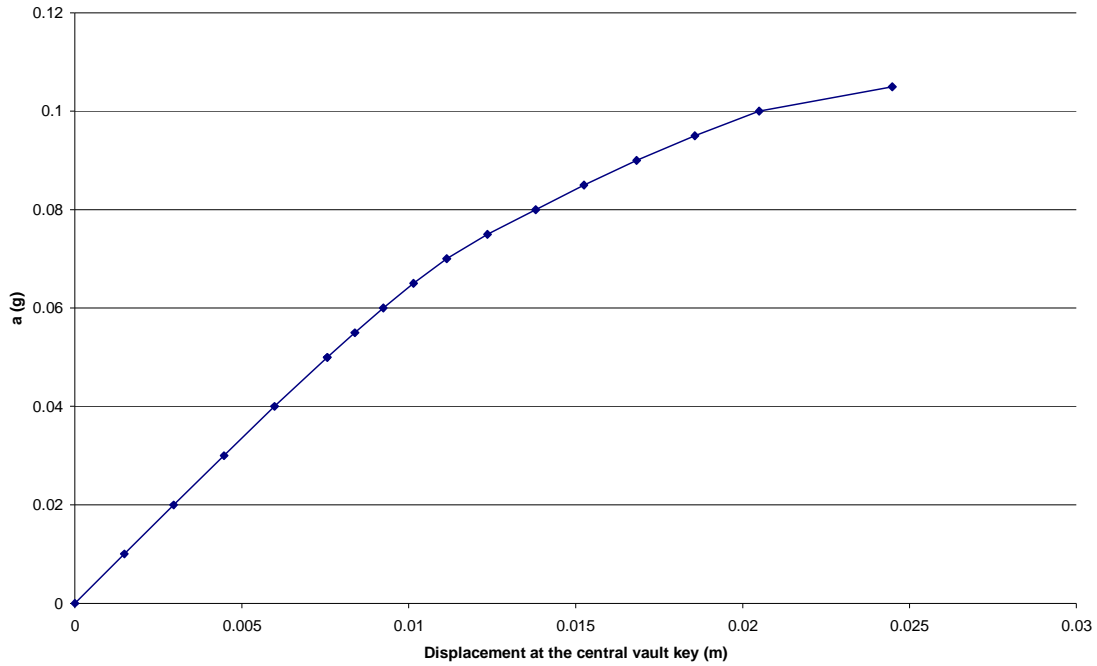


Figure 4.15 – Capacity curve for a load distributed according to the mass

In the damage distribution maps shown in figure 4.16 and 4.17, it is possible to identify cracked (tensile damage) and crushing areas (compression damage). It is possible to identify the existence of hinges (or the areas where they are about to appear) in the sections where tensile damage is significantly distributed along its depth. In this case, the cracking pattern is shown in figure 4.18 and hinges would be expected to appear in the base of the right pier and the right buttress, at the lateral vaults, at the top of the central vault and the union between the right pier and the lateral vault.

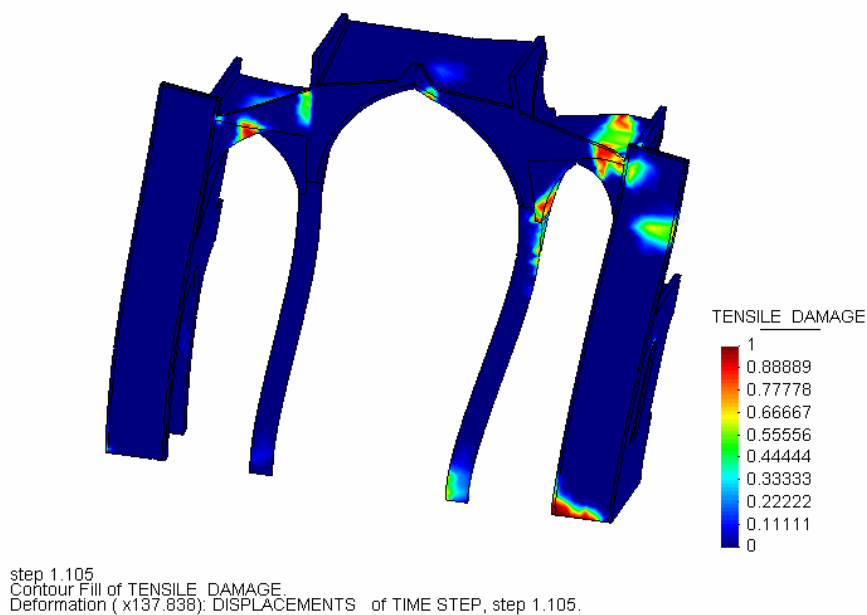


Figure 4.16 – Tensile damage distribution for s=0.105g

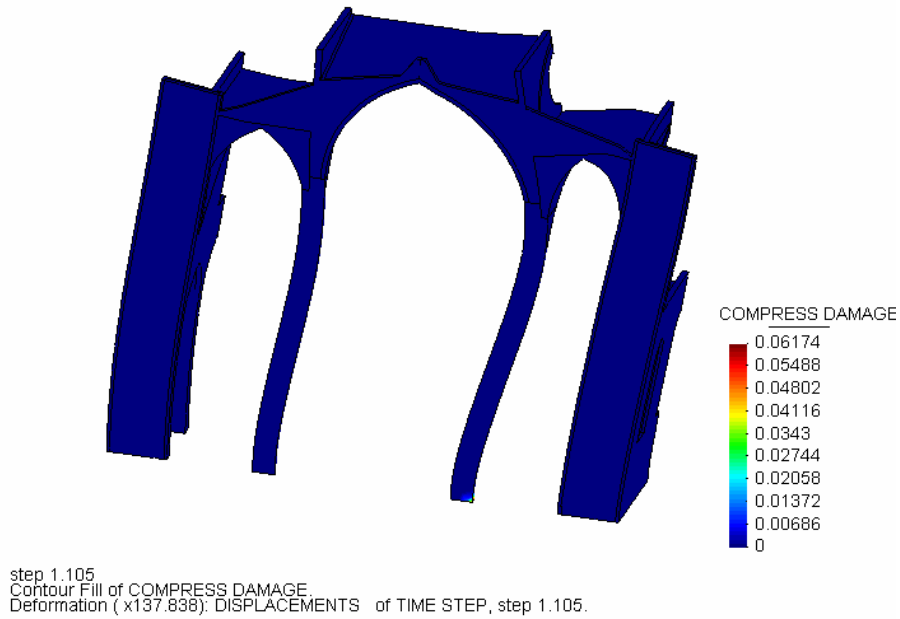


Figure 4.17 – Compressive damage distribution for $s=0.105g$

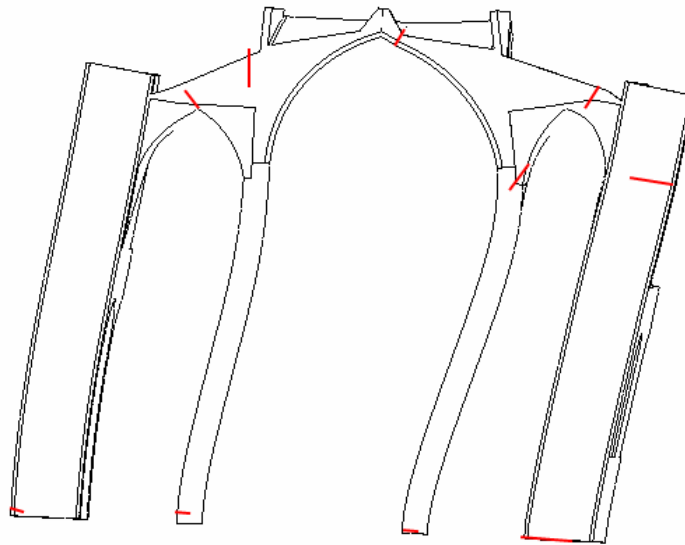


Figure 4.18 –Cracking Pattern

2. For a displacement distribution according to the 1st mode shape, the obtained capacity curve is plotted in figure 4.19. In this case the seismic coefficient is obtained as the ratio between the shear base and the self weight. Only the effective mass contributing in that mode has to be taken into account. Then, the force has to be divided by the mass participation ratio (73.5%). The original and corrected curves are plotted in figure 4.19. Now, it is possible to obtain the post-peak behaviour as it is a displacement-controlled loading. Therefore the peak can be identified. A peak is found at 0.12g and a softening curve is found loading to collapse (as it is displacement-controlled it is possible to obtain post-peak behaviour). Non convergence is

reached for a displacement of 3.6cm. Even though it cannot be identified as the collapse displacement, it is possible to see that this situation is close with the damage map (figure 4.20).

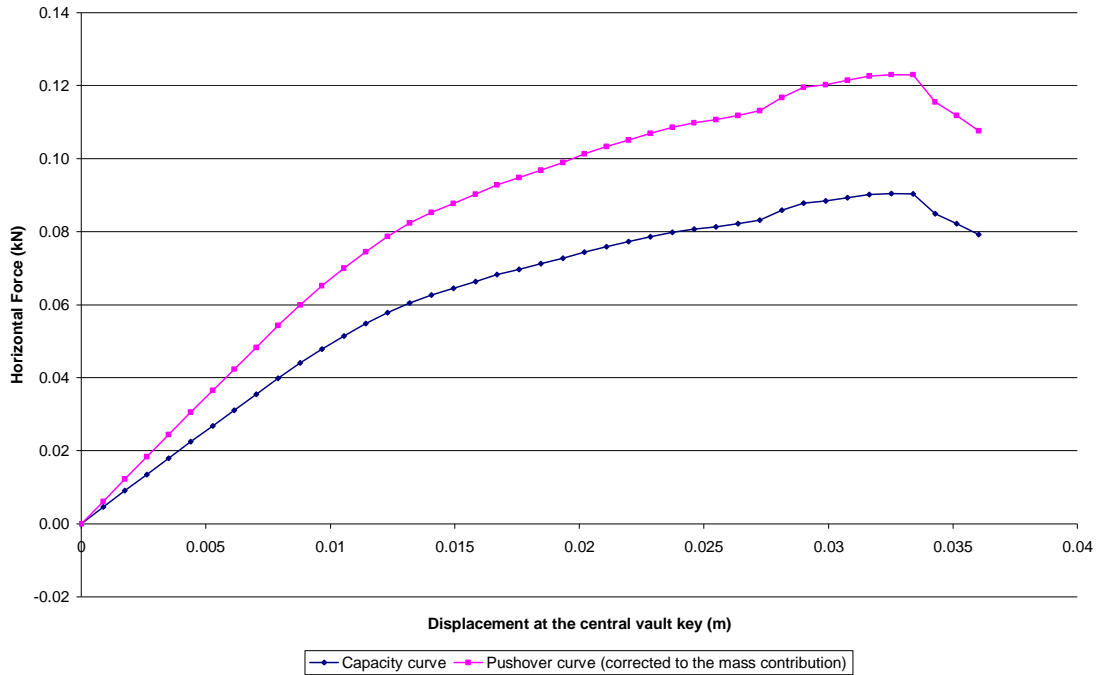


Figure 4.19 – Capacity curve for a load distributed according to the 1st mode

Again, the deformed shape and the damage distribution give an idea of appearing hinges and a collapse mechanism. The trends are similar to the obtained for the load distributed uniformly with the mass, but the damage is also distributed in other areas, due to the different imposed deformation (figures 4.20 and 4.21). As it is possible to obtain the post-peak behaviour, a more damaged structure is found where hinges are easier to identify.

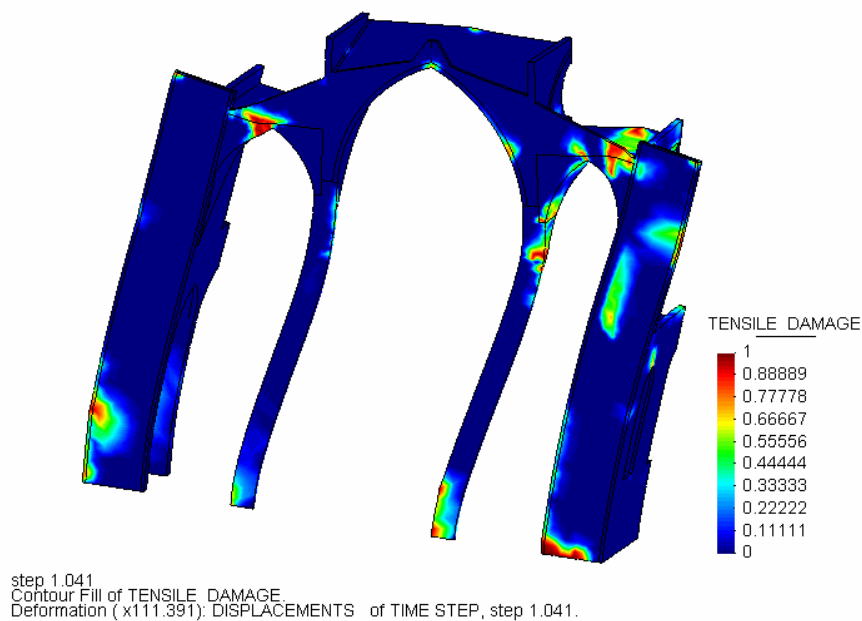


Figure 4.20 – Tensile damage distribution for s=0.12g

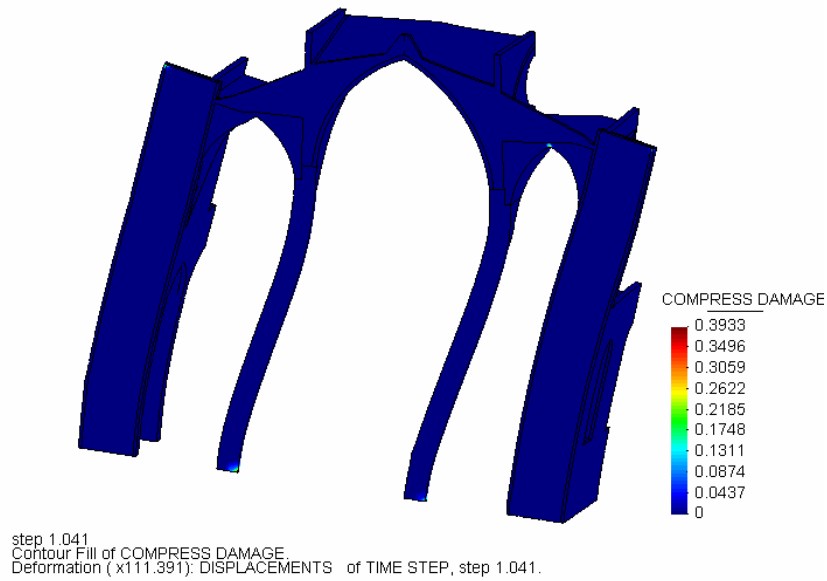


Figure 4.21 – Compressive damage distribution for $s=0.12g$

Comparing the different capacity curves (figure 4.22), we observe similar results between both methods. The difference is that with the 1st mode displacements increment we reach the peak and post-peak behaviour and with the horizontal loading proportional to the mass increase we don't reach that peak. The seismic coefficient would be between 0.105g and 0.12g, but the later value seems more realistic.

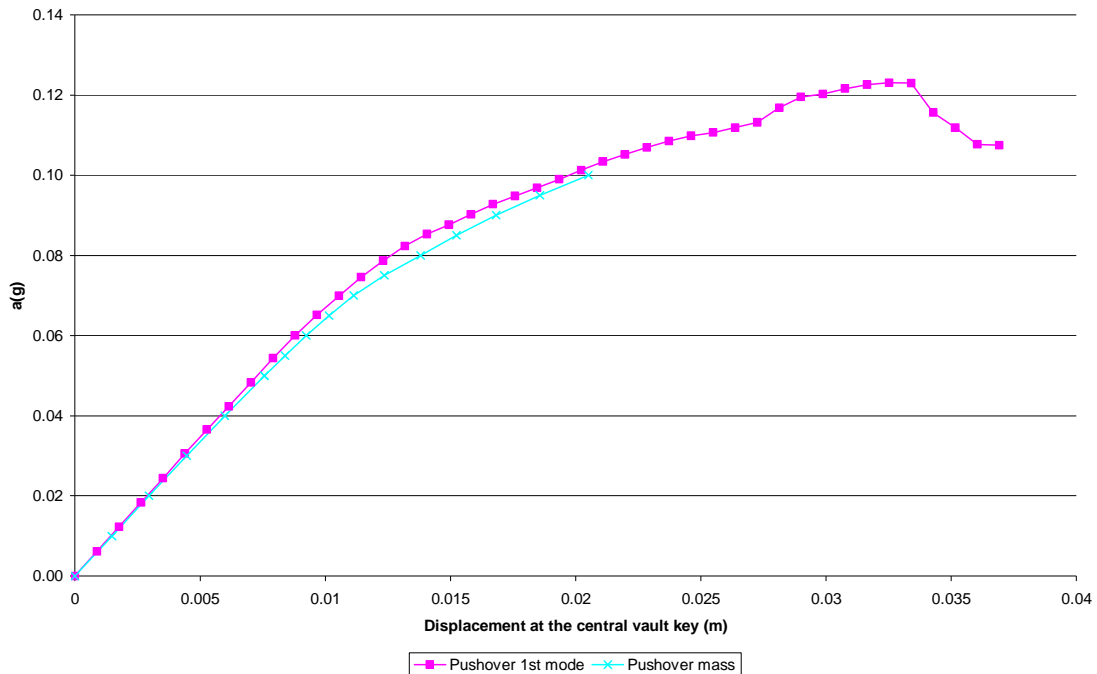


Figure 4.22 – Comparison between capacity curves

The values obtained by Irizarry (2003) for the capacity curve obtained by FEA, using a load proportional to the mass, show similar trends. In this work, the capacity is evaluated as 0.14g.

However, it takes into account the vertical and horizontal load at the same time. When considering the history of loads, problems of non convergence are encountered for 0.12g. Therefore, the damage distribution in the structure is not realistic: the first model is not loaded in the right way and the second doesn't converge. The limit analysis shows also a resistance of 0.12g. In addition, in this study the infill of the vaults has not been considered. This means a big quantity of mass in a high position. Not considering it, leads to more optimistic results, as it is proofed.

Roca (2007) obtained values between 0.09g and 0.12g using static analysis limit for different load distribution (proportional to mass and 1st mode) and infinite/finite compression. For the kinematic limit analysis the seismic coefficient was around 0.095g and 0.11g depending on the hypothesis in the vault fill. For the nonlinear FEA done by Roca the seismic coefficient is around 0.12g (correcting to the participating mass: 0.15g), obtaining a descendent flat curve that doesn't converge for a big displacement 14cm.

The values obtained in the current study match very well with the Limit Analysis results of Roca (2007). They are a little bit higher as a tensile capacity is assumed with FEA. The different values obtained for the seismic coefficients by different authors and methodologies are shown in table 4.3. The associated capacity curves are plotted in figure 4.23.

Table 4.3 – Seismic coefficients obtained with different methodologies and by different authors

Current study	FEA (load 1 st mode)	0.09/ 0.12 (corrected)
	FEA (load mass)	0.105
Roca (2007)	FEA (load 1 st mode)	0.12/ 0.15 (corrected)
	FEA (load mass)	0.13
	Static limit analysis (load 1 st mode)	0.09 /0.12
	Static limit analysis (load mass?)	0.10
	Kinematic limit analysis	0.10
Irizarry (2004)	FEA (no fill)	0.13-0.14
	Kinematic limit analysis (no fill)	0.11-0.12

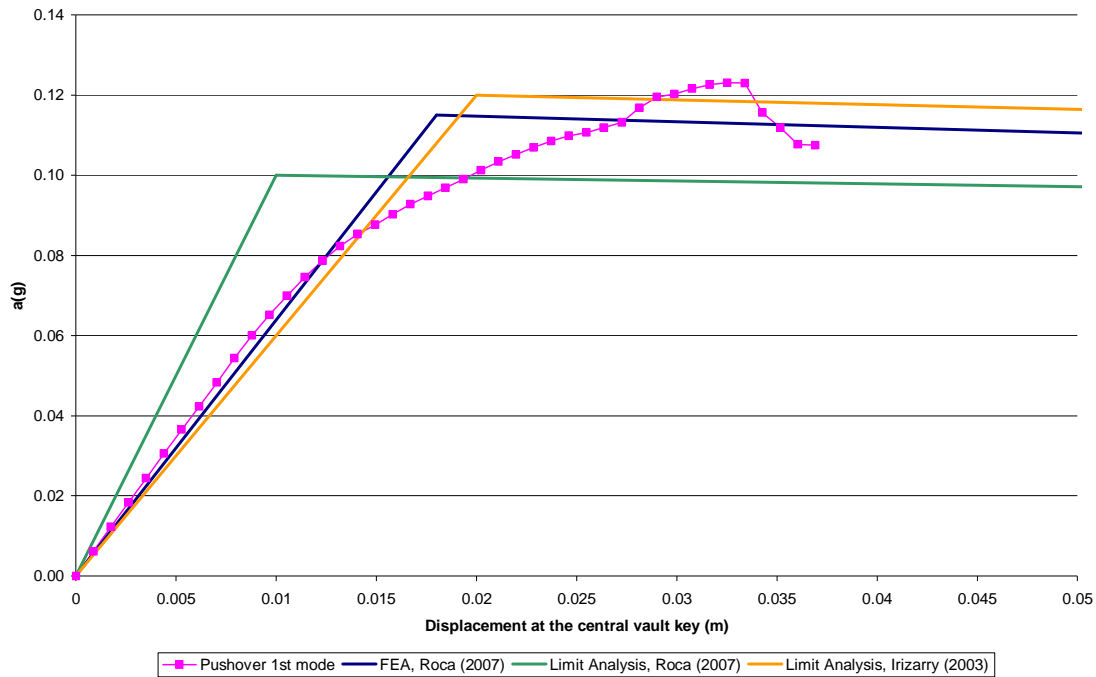


Figure 4.23 – Comparison between capacity curves obtained by different authors

The capacity curve obtained with the FEA doesn't give enough information about the collapse situation. Even though the damage maps help to identify coming hinges that will lead to a collapse mechanism, it is not possible to reach it and complete the softening curve, as done with the kinematics approach in Limit Analysis. Convergence problems are encountered before that, because the structure is modelled as a continuum. Therefore, the discharge curve obtained with the interaction of blocks cannot be found in this case. In any case, the predicted collapse mechanism is shown in figure 4.24. It matches quite well with the hypothesis of Irizarry (2004) and Roca (2007), as shown in figures 4.25 and 4.26. The main difference is that in this case, there is damage concentrated at the top of the piers instead that in the central vault, that would work as a single solid.

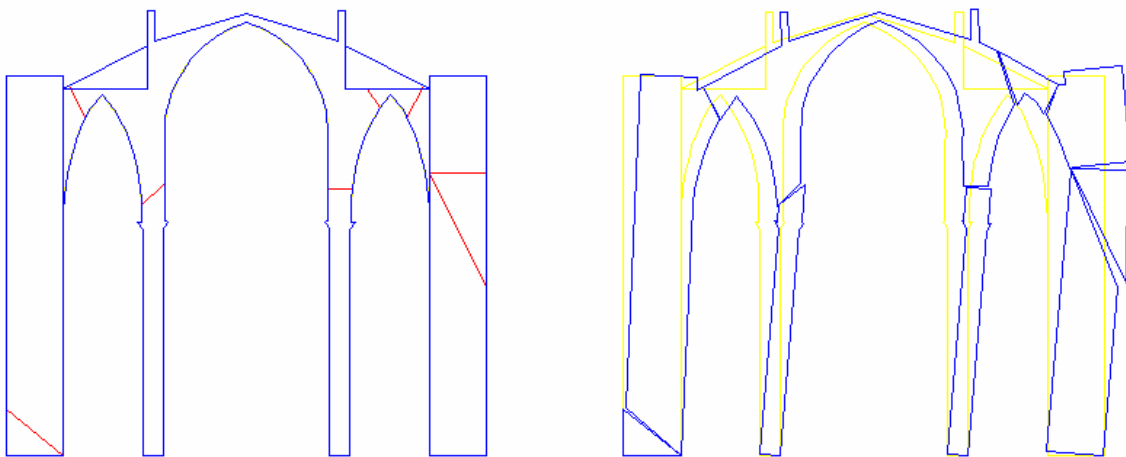


Figure 4.24 – Predicted crack pattern and collapse mechanism

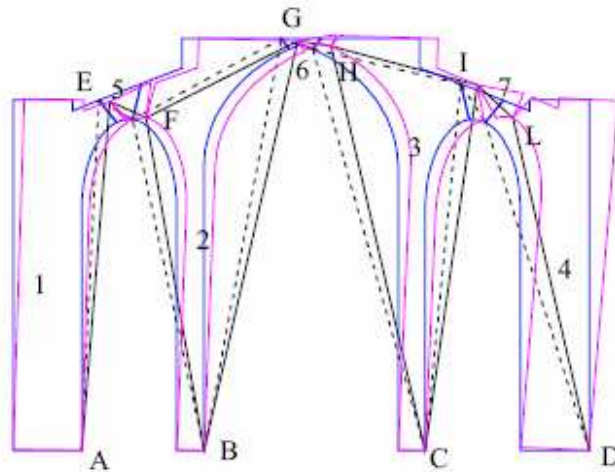


Figure 4.25 – Possible collapse mechanism defined by Irizarry (2004), $s=0.11g$

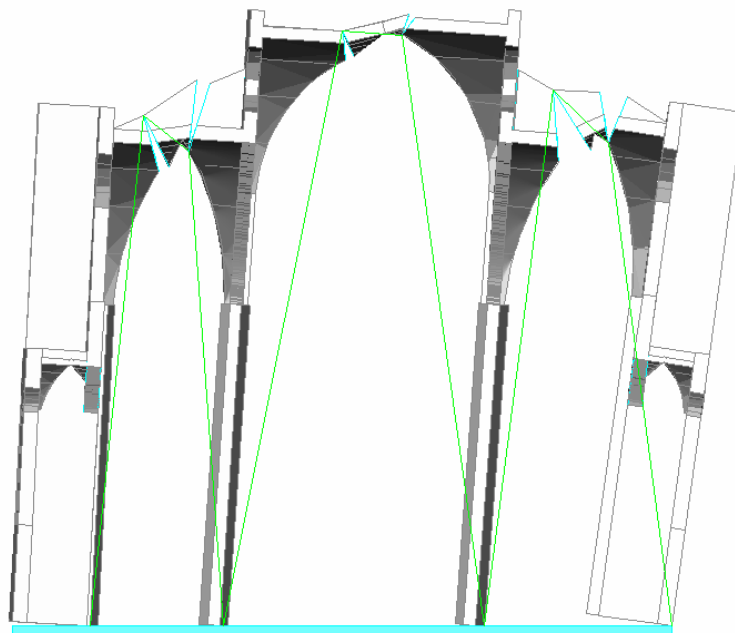


Figure 4.26 – Possible collapse mechanism defined by Roca (2007), $s=0.10g$

4.5 Sensitivity analysis

A sensitivity analysis of the model with respect to the main nonlinear mechanical parameters has been carried out. The tensile strength, compressive strength and fracture energy have been varied for a gravity load analysis and a pushover analysis (with loading pattern according to the 1st mode).

Gravity load and vertical capacity

The model is not sensible to the variation of the different studied parameters for gravity load, as almost all the structure remains in the linear range. The differences appear as damage increases and approaching collapse risk. For instance, the fracture energy has a big influence in defining the collapse situation for vertical load. Considering infinite fracture energies, as done by

some authors, makes easier numerical convergence. However, this leads to an overestimation of the capacity of the structure. For Santa Maria del Mar church it means a load factor of 3.80 for gravity load, while considering a realistic G_f (0.1Nmm/mm^2) the result was 3.0. As shown in figure 4.27, the deflection – load curve becomes flat for infinite G_f .

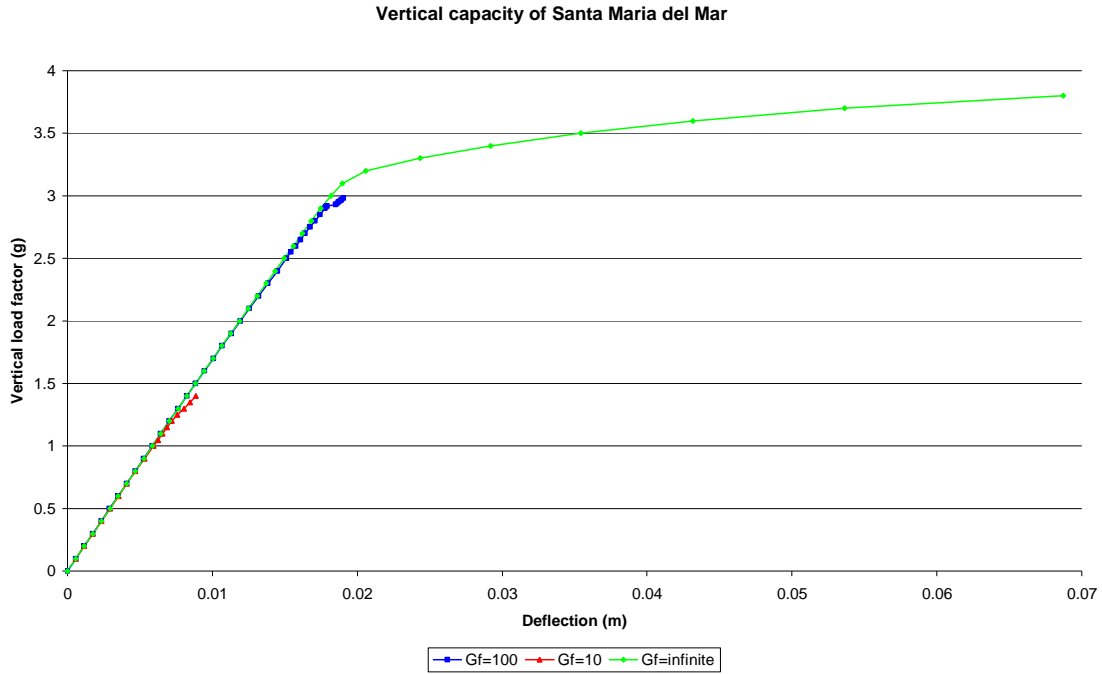


Figure 4.27 – Deflection – vertical load factor plots obtained with different G_f

This ductility associated to infinite G_f is due to the assumption of capacity to stand tension while damages, which is not a realistic hypothesis. As shown in figure 4.28 and 4.29, for both $G_f=0.01\text{Nmm/mm}^2$ and infinite G_f the origin of the collapse takes place in the crushing of the piers. The difference is that in the latter case the structure is able to accept more damage before collapse thanks to the assumed ductility (displacements are increased a 350%, while the load “only” a 26%).

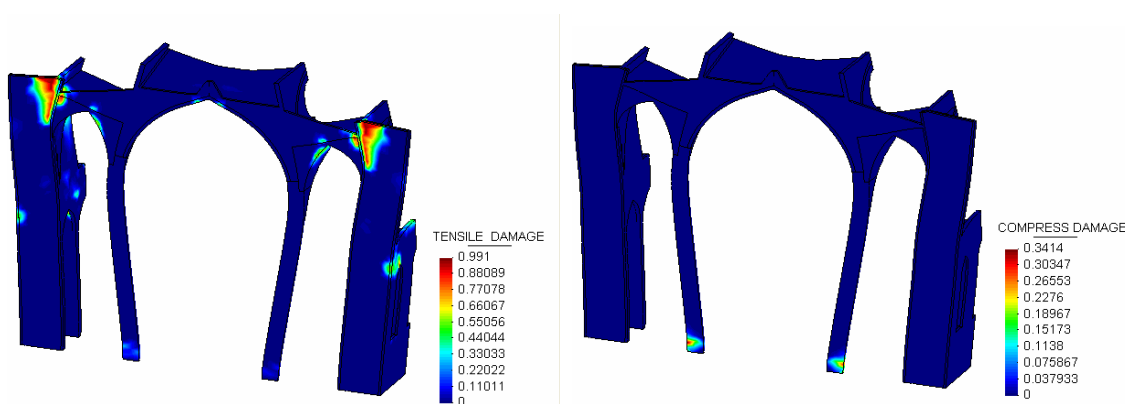


Figure 4.28 – Damage map for $G_f = 0.01\text{Nmm/mm}^2$ at LF=3

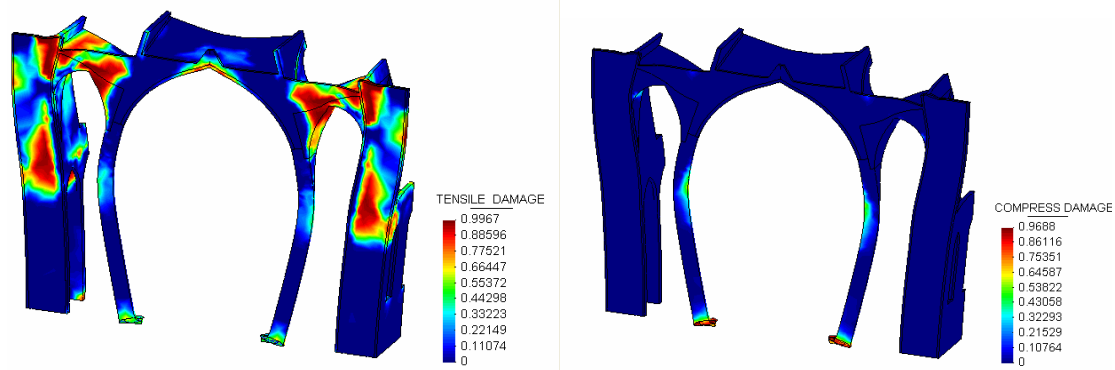


Figure 4.29 – Damage map for infinite G_f at $LF=3.8$

On the other hand, considering low G_f can give numerical problems. Assuming a lower bound for the fracture energy of masonry ($G_f = 0.01 \text{Nmm/mm}^2$), numerical problems are encountered for a load factor of 1.40. This value cannot be defined as the collapse load because no trends seem to indicate so: small change of slope in the curve (figure 4.27) and not collapse mechanism visible in the damage maps (figure 4.30): small tensile damage and no damage in compression (piers are still far away from the compressive strength).

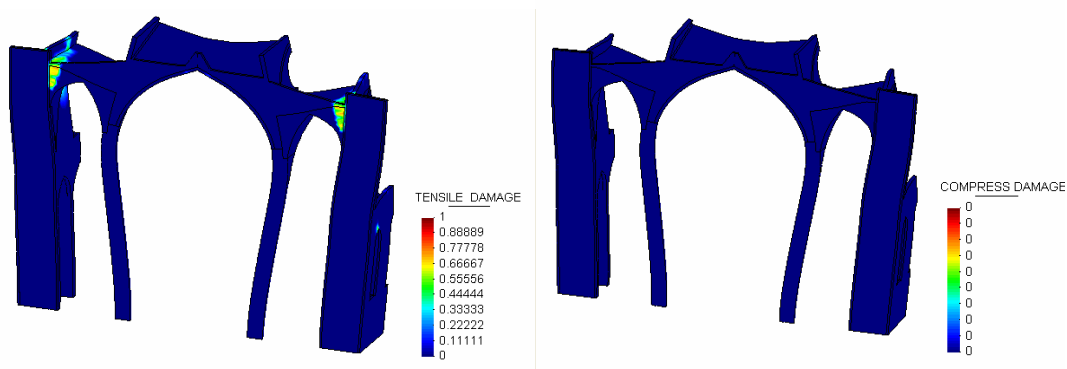


Figure 4.30 – Damage map for $G_f = 0.1 \text{Nmm/mm}^2$ at $LF=1.4$

The value of the compressive strength has a big influence in the collapse load, as failure was controlled by the crushing of the columns (figure 4.31 and 4.32). Considering half compressive strength (4MPa), the capacity of the structure is also halved (1.5), as the collapse mode is maintained. By reducing the strength until zero, the maximum load factor would also decrease linearly to zero. Increasing the compressive strength to 16MPa and infinite values, the capacity gets stuck in 3.9 and 4.0, respectively. This could be due to numerical problems but hinges are being developed. Therefore, with a high range variation, the failure mode changes and the variation of the compressive strength has no influence any more. There is not crushing of the columns, instead a mechanism associated to the formation of enough hinges would lead to collapse (figure 4.33).

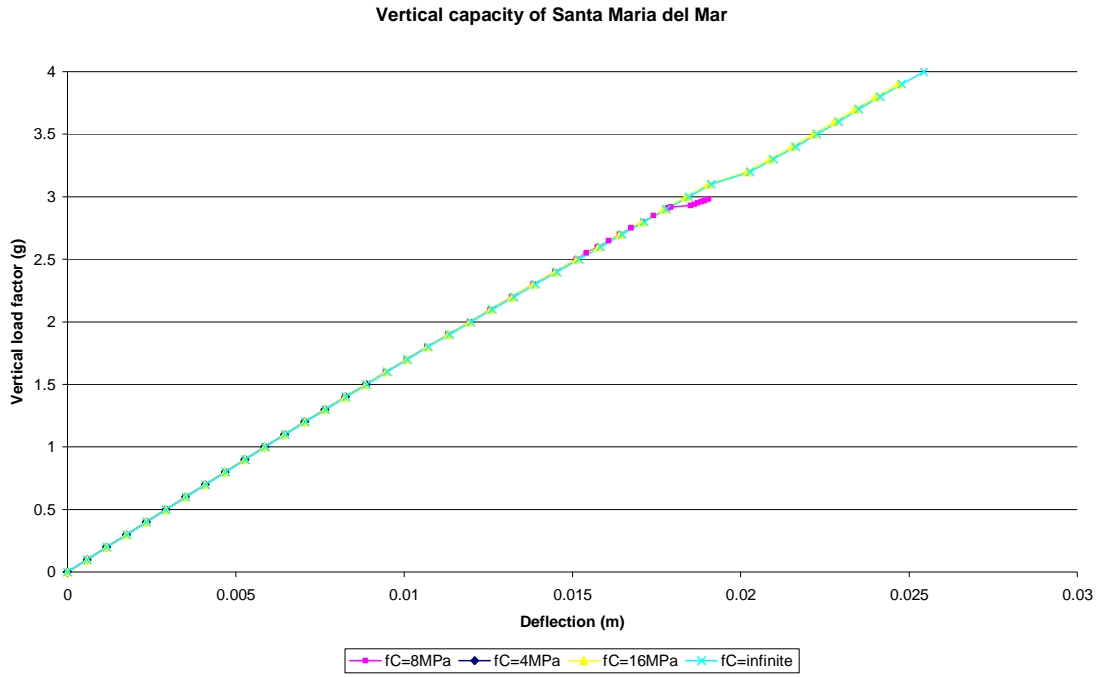


Figure 4.31 – Deflection – vertical load factor plots obtained with different f_c

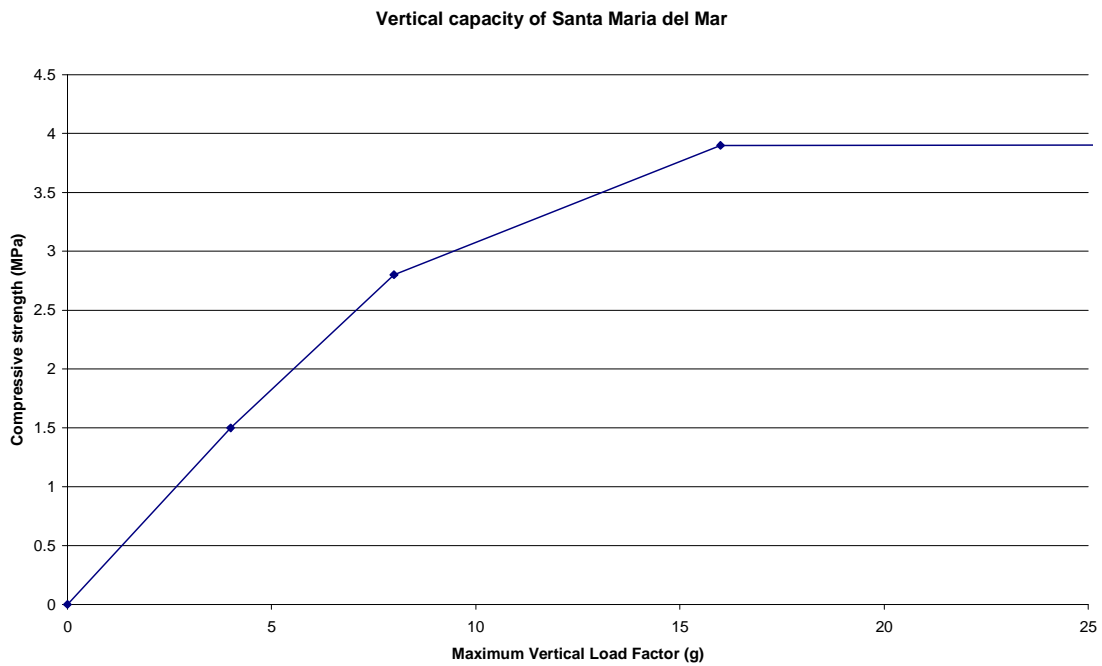


Figure 4.32 – Maximum load factor obtained with different f_c

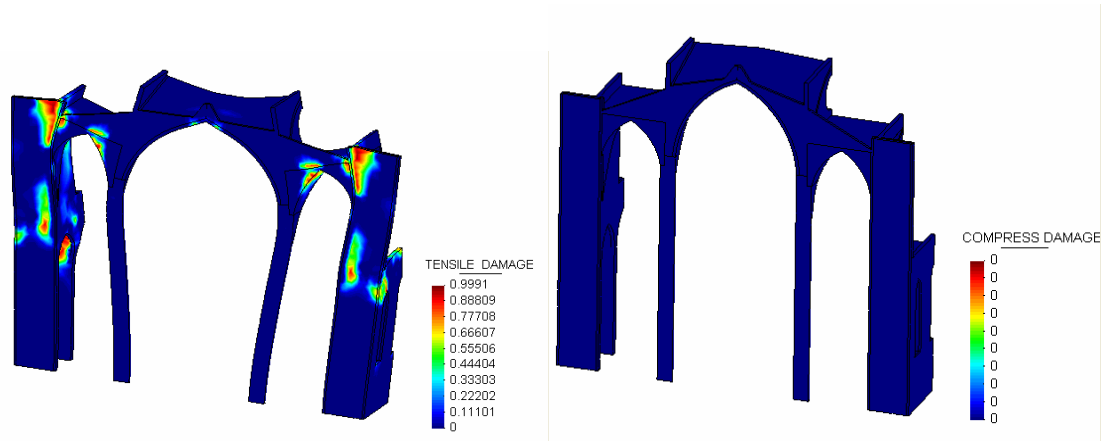


Figure 4.33 – Damage map for infinite f_c

Regarding tensile strength, it has a very small influence in the result (figure 4.34). For the range of values valid for the compressive strength, failure is controlled by this parameter and the tensile capacity is not so important.

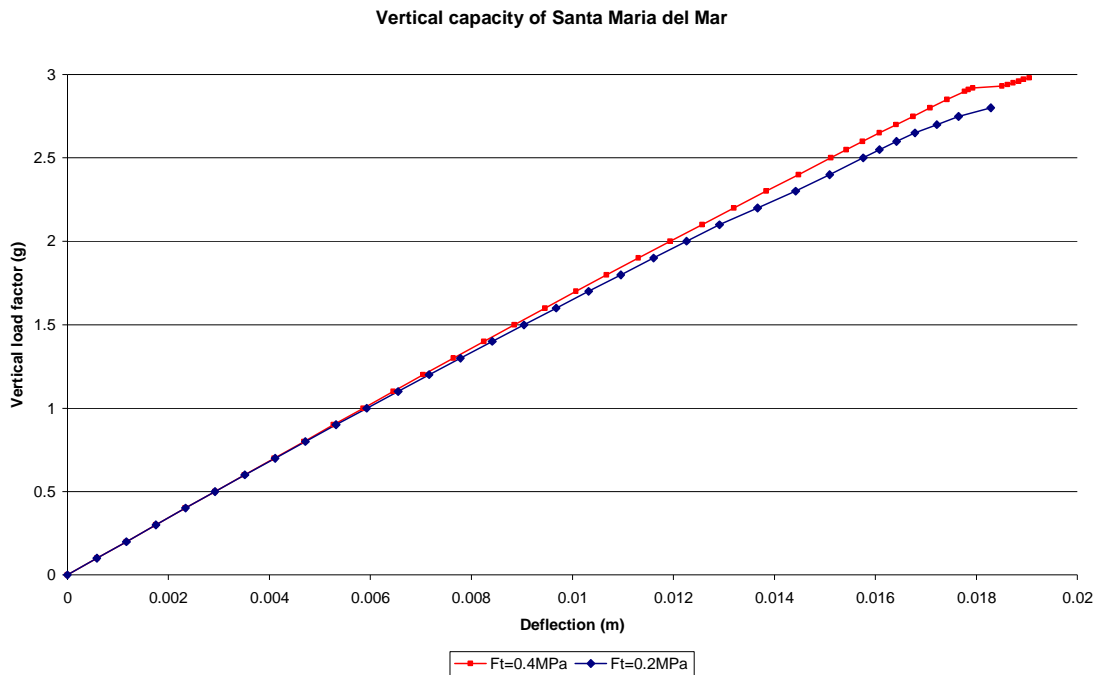


Figure 4.34 – Deflection – vertical load factor plots obtained with different f_t

Table 4.4 is a summary of the vertical capacity of Santa Maria del Mar Church (as a multiplier of the gravity load) for different mechanical parameters. The vertical capacity of the structure obtained from the numerical model is sensible to the compressive strength and fracture energy and not very much to the tensile strength. However, the structure will never be subjected to that level of load. Therefore, the main conclusion of the analysis is that assuming $G_f = 0.1 \text{ Nmm/mm}^2$, being an upper bound of the masonry fracture energy, seems to be a good equilibrium between reality and numerical efficiency.

Table 4.4 vertical capacity of Santa Maria del Mar Church for different mechanical parameters

Model	G _f	F _c	F _t	Load Factor
Reference model	100	8Mpa	0.4MPa	2.99
Infinite fracture energy	1.00E+30	8Mpa	0.4MPa	3.80
Low fracture energy	10	8Mpa	0.4MPa	1.40
Tensile strength x 0.5	100	8MPa	0.2MPa	2.80
Compressive strength x 0.5	100	4MPa	0.4MPa	1.50
Infinite compressive strength	100	INFINITE	0.4MPa	4.00
Compressive strength x 4	100	16Mpa	0.4MPa	3.90

Pushover

The study of the influence of the nonlinear mechanical parameters is even more important for the definition of the seismic capacity of the structure, as this is a more realistic hazard. Defining appropriate fracture energy is again essential. Using an infinite value can have numerical advantages but leads to an overestimation of the seismic coefficient. In this case, to a value of 0.135g instead of 0.12g for $G_f = 0.1\text{Nmm/mm}^2$. In both cases a maximum seismic coefficient is reached and a softening behaviour is observed (figure 4.35). However, the softening for infinite fracture energy is very small due to the ductility of the structure, as the structure accepts bigger damage before collapse (figures 4.36 and 4.37). On the other hand, using a very small value for G_f (0.01Nmm/mm^2) causes numerical problems as non convergence is reached for a factor of 0.045g. Again, no collapse is expected for this value as the peak is not reached (figure 4.35) and the damage is small (figure 4.38).

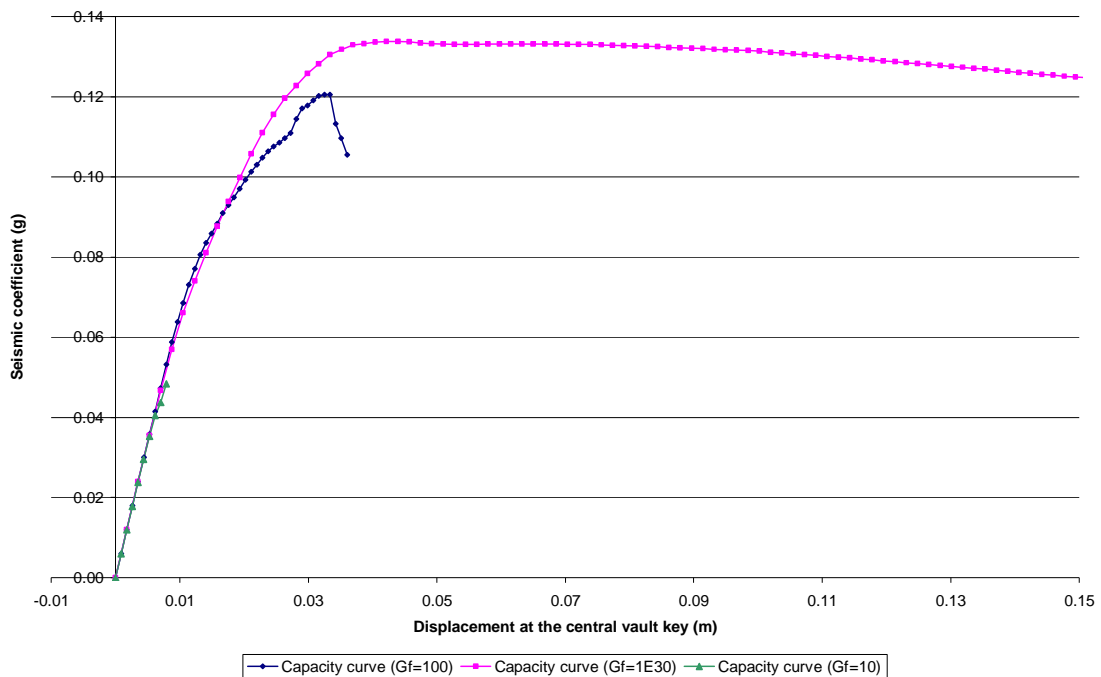


Figure 4.35 – Capacity curve obtained with different G_f

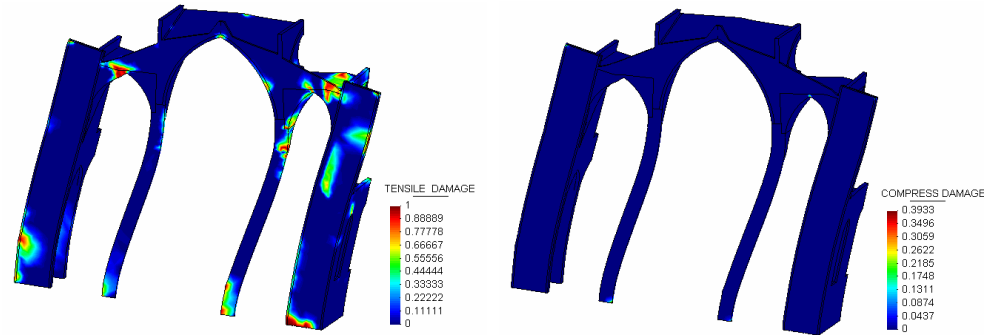


Figure 4.36 – Damage map for $G_f = 0.01 \text{ Nmm/mm}^2$ at $d = 0.035 \text{ m}$

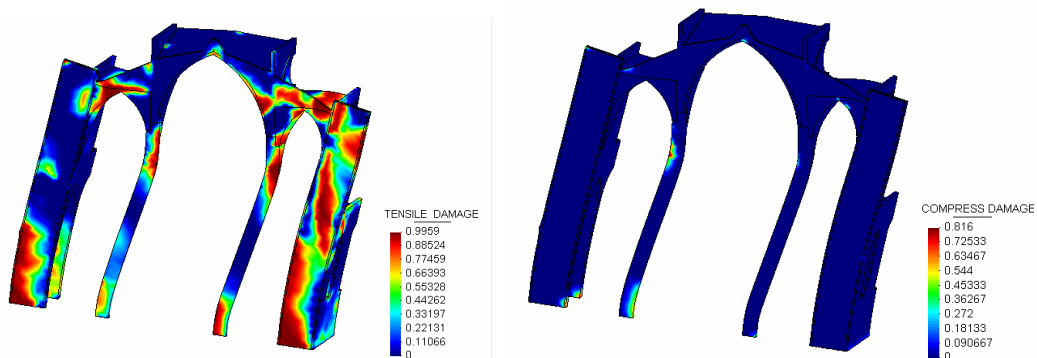


Figure 4.37 – Damage map for $G_f = 0.01 \text{ Nmm/mm}^2$ at $d = 0.15 \text{ m}$

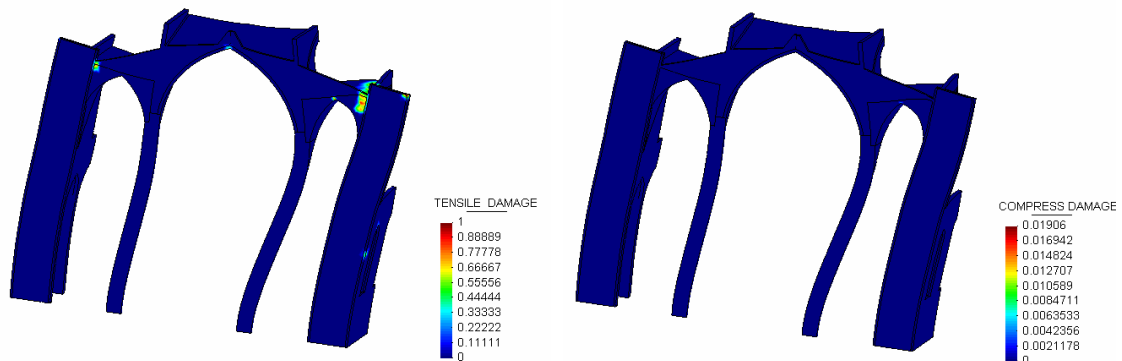


Figure 4.38 – Damage map for $G_f = 0.1 \text{ Nmm/mm}^2$ at $d = 0.008 \text{ m}$

The influence of the compressive strength in the seismic capacity of the structure has also been studied. Variations around the reference value (8MPa) have almost no influence in the capacity curve (figure 4.39), as the collapse mechanism is controlled by the formation of hinges due to cracking. Only for compressive strengths below 6MPa the seismic coefficient would be affected, as shown in figure 4.40. For example, for $f_c = 3 \text{ MPa}$ a sudden failure would be caused by crushing in the base of one of the columns for $s = 0.042 \text{ s}$ (figure 4.41). For $f_c < 2.8 \text{ MPa}$ collapse would take place for gravity load because the expected average compressive stress in the base of the piers would be higher than the strength (as a result the seismic coefficient would be 0).

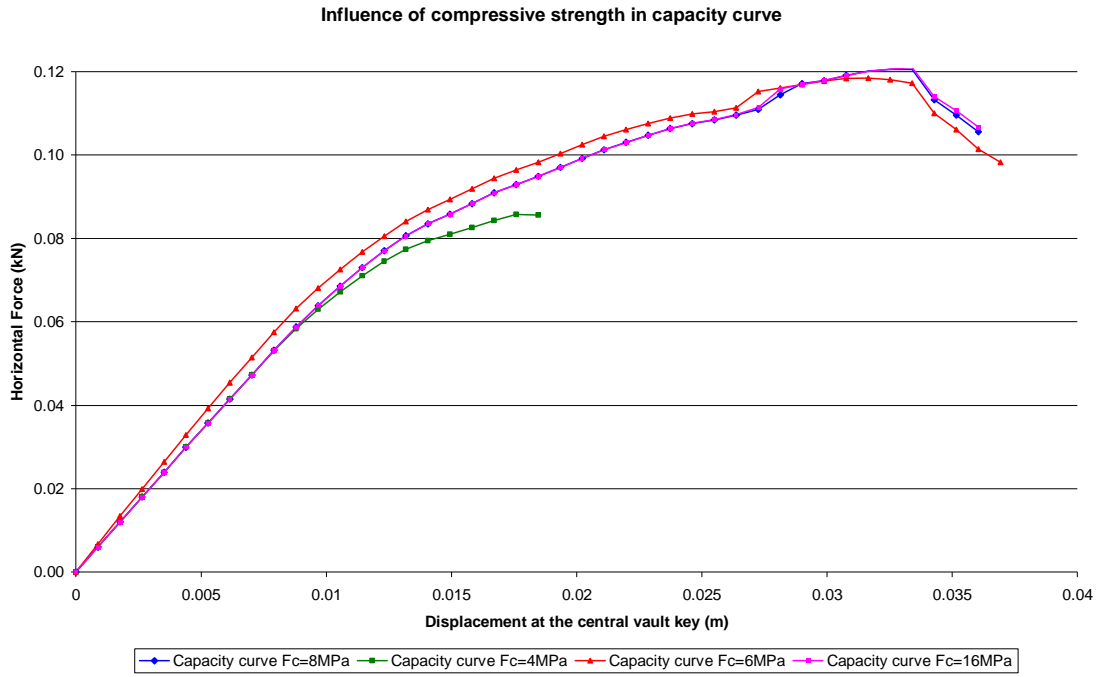


Figure 4.39 – Capacity curve obtained with different f_c

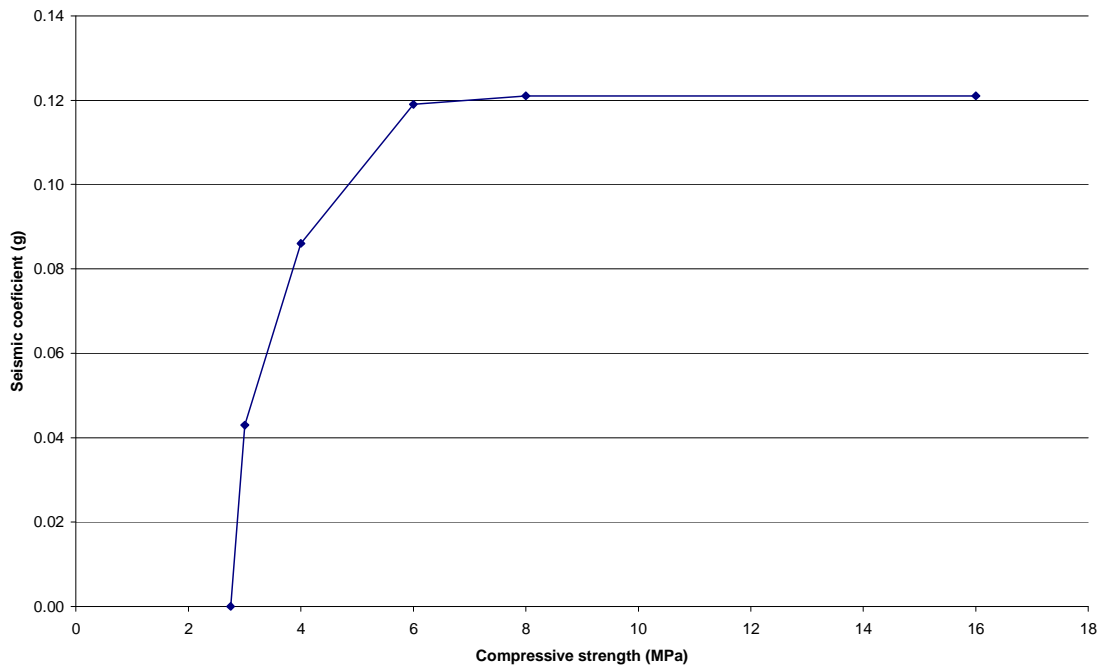


Figure 4.40 – Seismic coefficient obtained with different f_c

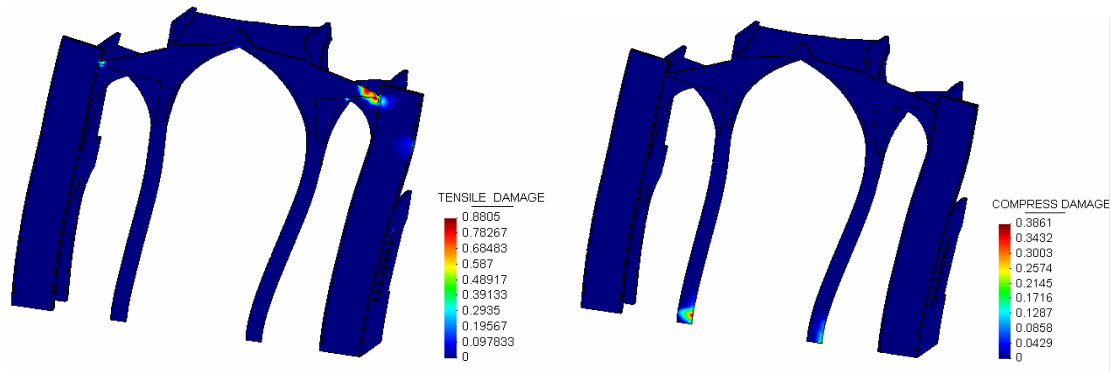


Figure 4.41 – Damage map for $f_c = 3\text{MPa}$ at $s=0.04g$

Regarding the tensile strength, it has little influence in the seismic coefficient. Dividing it by two the seismic coefficient is reduced to $0.11g$ (figure 4.42). Dividing it by four, no peak is found but should be close to $0.10g$ as the damage map shows a widespread damage (figure 4.43). Ideally, assuming $f_t = 0$, the results would be the same as the obtained from limit analysis: Roca (2007) obtained $0.10g$ using the kinematics approach. However, as this value is reduced in FEA the numerical problems are encountered. In addition, assuming some tensile capacity is a realistic hypothesis.

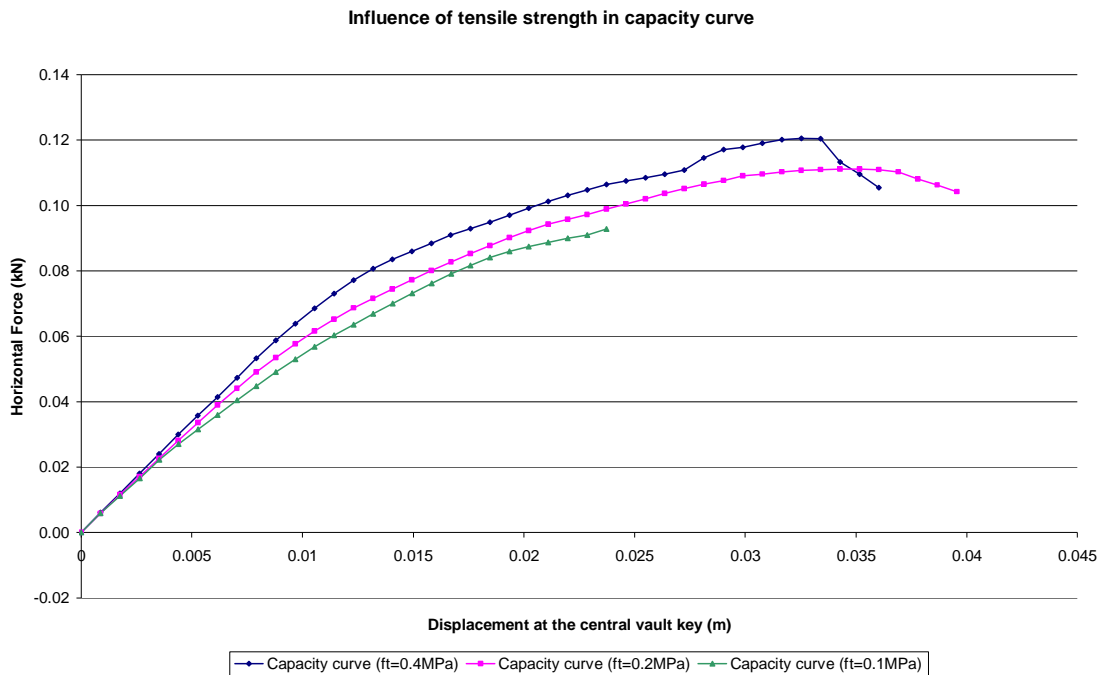


Figure 4.42 – Capacity curve obtained with different f_t

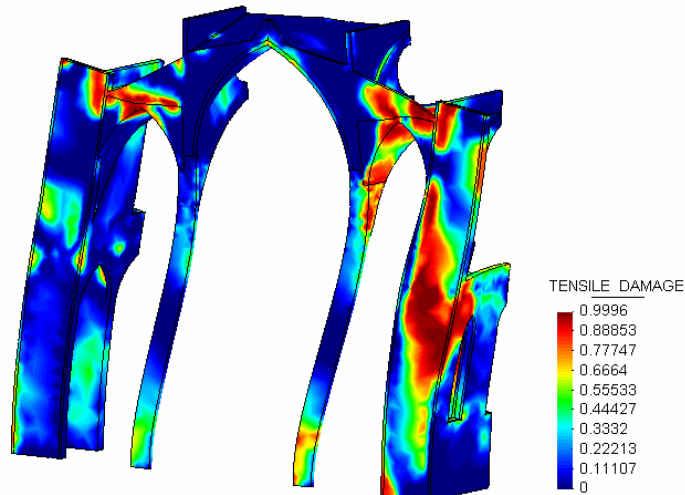


Figure 4.43 – Damage map for $f_t = 0.1\text{MPa}$ at $s=0.09g$

Table 4.5 is a summary of the seismic capacity of Santa Maria del Mar Church for different mechanical parameters. The seismic coefficient of the structure obtained from the numerical model is not very sensible to the compressive and tensile strength, in the range of possible values for the used masonry. Again, assuming $G_f = 0.1\text{Nmm/mm}^2$, being an upper bound of the masonry fracture energy, seems to be a good equilibrium between reality and numerical efficiency.

Table 4.5 Seismic capacity of Santa Maria del Mar Church for different mechanical parameters

	Gf	Fc	Ft	Seismic coef.
Reference model	100	8Mpa	0.4MPa	0.121
Infinite fracture energy	1.00E+30	8Mpa	0.4MPa	0.134
Low fracture energy	10	8Mpa	0.4MPa	0.048
Tensile strength x 0.5	100	8MPa	0.2MPa	0.111
Compressive strength x 0.5	100	4MPa	0.4MPa	0.086
Compressive strength x 4	100	16Mpa	0.4MPa	0.121
Compressive strength x 0.75	100	6MPa	0.4MPa	0.119
Compressive strength x 0.375	100	3MPa	0.4MPa	0.043
Tensile strength x 0.25	100	8MPa	0.1MPa	0.093

4.6 Simulation of possible reinforcement techniques

Three different strengthening techniques have been simulated numerically to evaluate their effectiveness to improve the seismic behaviour of the structure of Santa Maria del Mar church. The selected techniques follow the principles of conservation and the modern criteria for the analysis and restoration of historical structures have been taken into account, as recommended in the EU-India project “IMPROVING THE SEISMIC RESISTANCE OF CULTURAL HERITAGE BUILDINGS” (2006). These criteria include the well-know requirements for minimum

intervention, reversibility, non-invasiveness, durability and compatibility with the original materials and structure.

In particular the selected techniques are the following:

Injection of the buttress infill: Injection of mortar through holes previously drilled in the external parameters of the wall in order to fill existing cavities and internal voids and sealing possible cracks. This is a typical intervention to improve mechanical properties while respecting the authenticity, as long as the injected materials have proven compatibility with the original material. A lime-based mortar injection would be preferred for stone masonry structures. In the case of Santa Maria del Mar church the injection would be only beneficial in the buttress infill (figure 4.44). The columns are already massif and changing the weight in the vaults could be dangerous for the equilibrium of the structure.

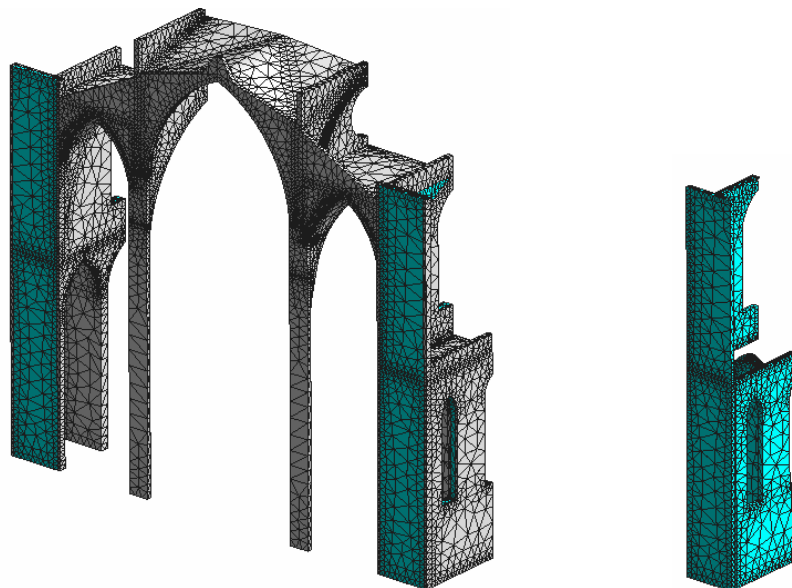


Figure 4.44 – Injected volume (buttress infill)

Prestressing: Providing a controlled compressive stress by means of cables in order to avoid the opening of cracks due to the seismic load. The transversal section would be compressed by tensioned exterior cables anchored in the upper part of the buttresses (with deviators in the central vault), as shown in figure 4.45. The use of a light steel structure (cable prestressing) makes this intervention fully reversible. In addition, the aesthetics of the interior of the church would no be altered.

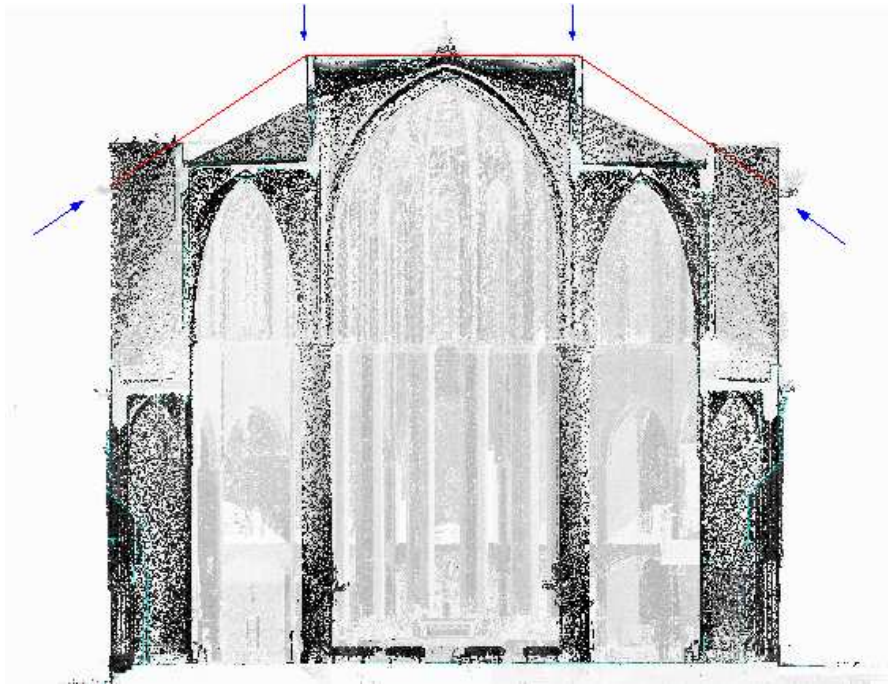


Figure 4.45 – Prestressing cables and equivalent forces

Tying triangular walls: Reinforcement of the triangular walls by means of a light steel beam or tie (figure 4.46). These triangular walls above the lateral vaults have been identified as essential elements to provide seismic strength to the structure. Their strengthening by means of metal elements able to carry tensions could improve the seismic capacity. The use of a light steel structure (beam or tie) makes this intervention fully reversible. In addition, the aesthetics of the interior of the church would no be altered. Another possibility would be to raise the triangular walls with masonry (this alternative was not tested, but the principle would be similar) as shown in figure 4.47.

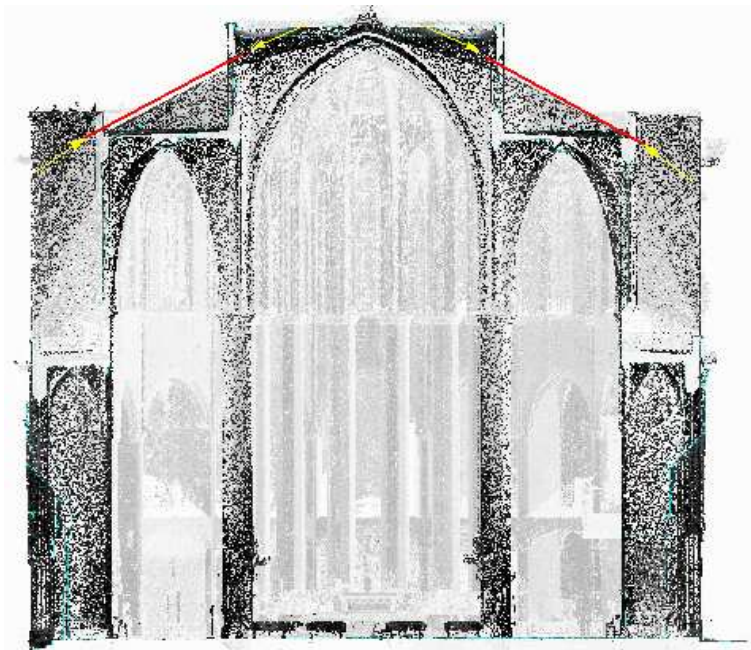


Figure 4.46 – Reinforcement of triangular walls

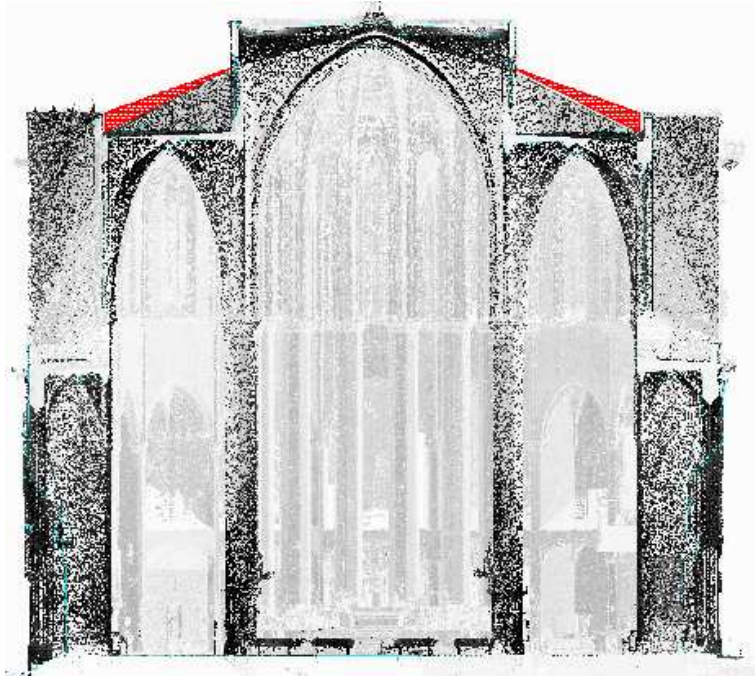


Figure 4.47 - Rise of triangular walls

The capacity curves of the original and the strengthened structure with different techniques are shown in figure 4.48. According to the simulations, the only effective technique is the injection, but the improvement of the seismic coefficient is low.

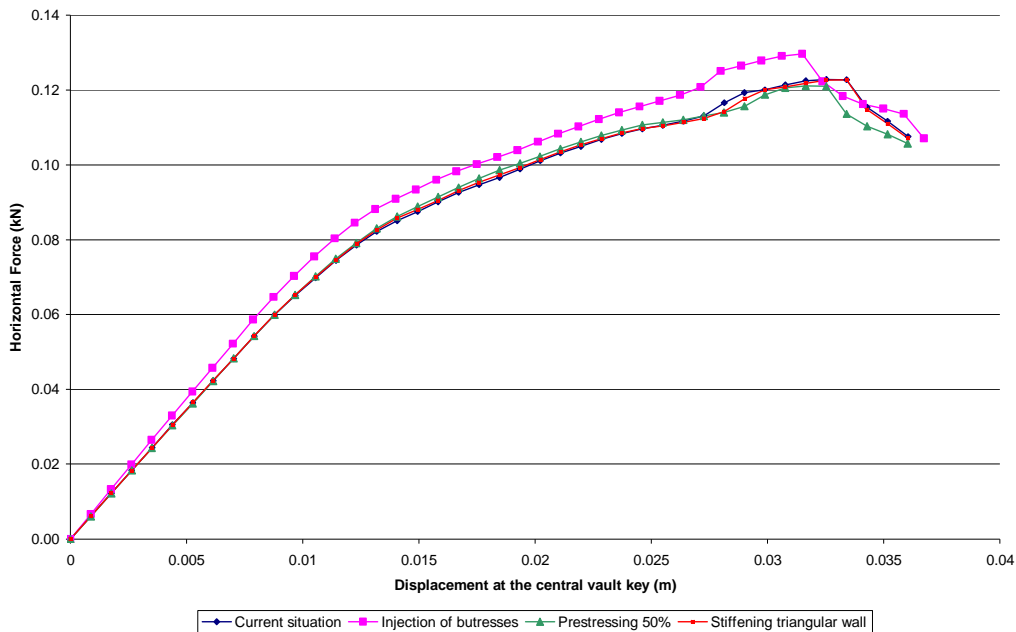


Figure 4.48 – Capacity curve for reinforced structure

The injection of buttresses has been simulated as an improvement of the mechanical properties of the wall infill. It is difficult to estimate how much the stiffness and strength are increased, but optimistic hypothesis are assumed to obtain a qualitative idea of the effect of this measure. The E-modulus, the tensile and compressive strength have been increased a 50% (lower

improvements are usually expected). In addition, the density has been increased a 25% due to the addition of mortar. A big improvement of the infill properties has shown a small influence in the results: the seismic coefficient has been increased only a 5% (0.13g). The failure mode is the same as in the original situation, but the buttress needs a higher load to achieve the same damage.

The prestressing technique was not able to provide a higher seismic capacity. Different prestressing levels were simulated as an external force: 25%,40%,50%,75% of the thrust of the vault due to self-weight. For lower prestressing levels the seismic coefficient is the same as in the original structure (0.12g). The damage pattern changes a little bit with respect with the original situation: damage appears near the anchorage areas (figure 4.49). For higher prestressing levels, this technique is even worse due to the damage introduced in the anchored area.

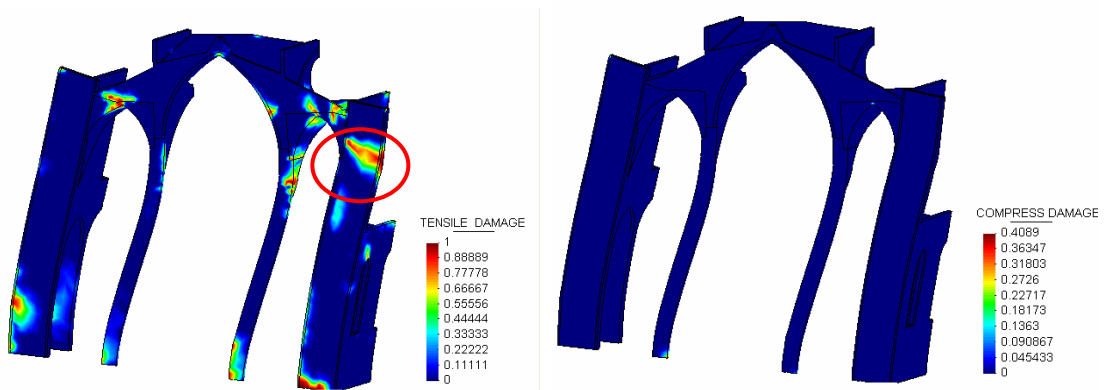


Figure 4.49– Damage map for prestressed section

Tying the triangular walls is not an efficient technique, according to the numerical analysis. Tying has been simulated in a simple way, as an equivalent external force (increasing force until yielding value). The resistance of the structure remains constant. Due to the tension capacity of the ties, the hinges will not appear in the wall. However, they will appear where the ties are anchored: as shown in figure 4.50 the damage is redistributed to the upper part of the buttresses.

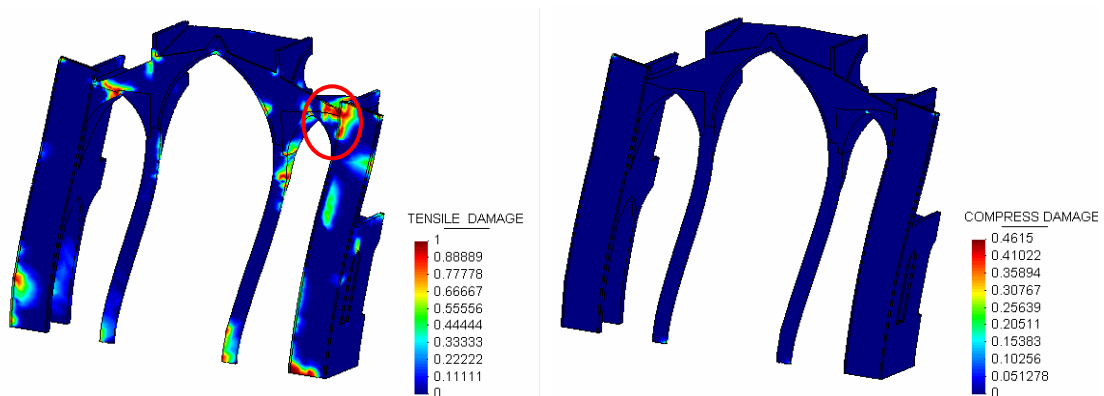


Figure 4.50 – Damage map for section strengthened with tie

CHAPTER 5

Capacity Spectrum Method applied to Santa Maria del Mar Church

In this chapter the Capacity Spectrum Method is applied to the typical bay of Santa Maria del Mar Church. First, the basis of the method and the calculation procedure are presented. Then, the capacity spectrum of the structure and the earthquake demand spectra are derived. Finally, both curves are compared in order to obtain the performance point of the structure and estimate the expected level of damage.

5.1 Capacity Spectrum Method

The capacity spectrum method was developed by Freeman et al (1975) as a simplified method to evaluate seismic performance of structures. Based in a graphical procedure, it compares the capacity of a structure with the demand of an earthquake ground motion on the structure (figure 5.1). The capacity of the structure is obtained by non-linear static pushover analysis as a force-displacement curve. The base shear forces and displacements are converted respectively to the spectral accelerations and spectral displacements of an equivalent SDOF system in order to obtain the capacity spectrum. The demands of the earthquake ground motion are usually defined by a 5% damped elastic spectra. The Acceleration Displacement Response Spectrum (ADRS) format is used, in which spectral accelerations are plotted against spectral displacements (with the periods represented by radial lines).

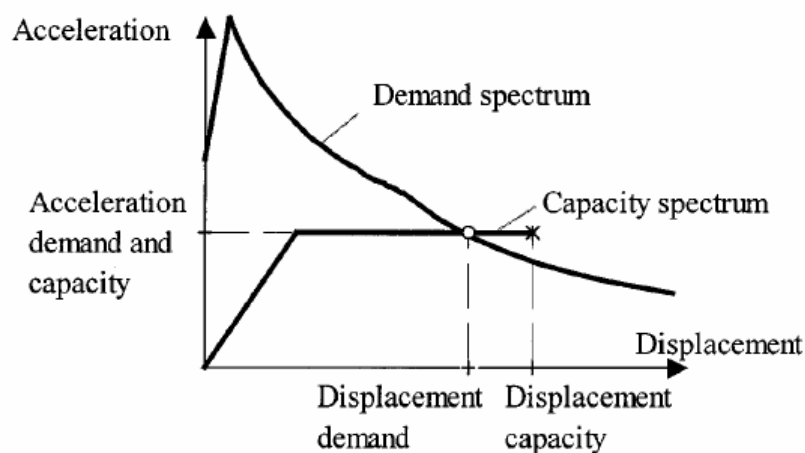


Figure 5.1- Capacity spectrum method, Fajfar (1999)

When the structure shows inelastic behaviour, hysteretic damping in the structure is produced in addition to the viscous damping. In this case, the seismic demand spectrum must be reduced to take into account the inelastic deformations. The intersection of the capacity spectrum and the reduced demand spectrum (performance point) provides an estimation of the expected damage level of the structure. The methodology presented by Irizarry (2004) will be followed to apply this method. It consists in the following steps:

1. Obtain the capacity spectrum of the structure. From the capacity curve obtained from the pushover analysis, the top displacement and shear base coordinates (V,d) are converted into the spectral displacement and spectral acceleration coordinates (S_d,S_a) by means of the following transformations:

$$S_a = \frac{V}{\alpha M g} \quad (5.1)$$

$$S_d = \frac{d_{top}}{\phi_{top} PF_\phi} \quad (5.2)$$

Where M is the total mass of the structure, α is the mass participation ratio used in the SDOF (associated to the 1st mode), ϕ_{top} is the 1st mode shape in the top and PF_ϕ the participation factor of the 1st mode. The values of α and PF_ϕ are calculated as follows:

$$\alpha = \frac{\left(\sum_{i=1}^N m_i \phi_{i,1} \right)^2}{M \sum_{i=1}^N m_i \phi_{i,1}^2} \quad (5.3)$$

$$PF_\phi = \frac{\sum_{i=1}^N m_i \phi_{i,1}}{\sum_{i=1}^N m_i \phi_{i,1}^2} \quad (5.4)$$

2. Convert the capacity spectrum curve into an equivalent bilinear function, to simplify the process to obtain performance point.

3. Plot the 5% damped elastic demand spectrum (S_{ae},S_d) and the simplified capacity spectrum (S_a,S_d) in the same graph.

4. Choose a trial point ($S_{d,tr}, S_{a,tr}$) in the capacity spectrum as the intersection with the unknown reduced demand spectrum.

5. For the trial point chosen define the associated ductility μ_{tr} as the ratio between the maximum displacement and the yield displacement of the bilinear function:

$$\mu_{tr} = \frac{S_{d,tr}}{S_{dy}} \quad (5.4)$$

The structural period T_{tr} and the strength reduction factor $R_{\mu,tr}$ are defined as follows:

$$T_{tr} = 2\pi \sqrt{\frac{S_{d,tr}}{S_{ae,tr}}} \quad (5.5)$$

$$\begin{aligned} R_{\mu,tr} &= (\mu_{tr} - 1) \frac{T_{tr}}{T_c} + 1 && T_{tr} < T_c \text{ acceleration range} \\ R_{\mu,tr} &= \mu_{tr} && T_{tr} \geq T_c \text{ velocity range} \end{aligned} \quad (5.6)$$

6. Calculate the reduced demand spectra by reducing the damped elastic demand spectrum by the reduction factor:

$$S_a = \frac{S_{ae}}{R_{\mu,tr}} \quad (5.7)$$

7. Find the intersection between the capacity spectrum and the reduced demand spectrum ($S_{d,new}$, $S_{a,new}$).

8. If $S_{d,new}$ equals $S_{d,tr}$ (with a tolerance margin) the performance point has been found. On the contrary, the process should be repeated until reaching it.

Once found the performance point, the expected level damage in the structure can be estimated. Different damage classifications exist based on damage threshold limits defined using the spectral displacement at the performance point. The damage thresholds established this criterion to the capacity spectrum of Santa Maria del Mar, as shown in figure 5.2.

Table 5.1 – Damage threshold limit definition from RISK-UE project (Lagomarsino et al., 2003)

Damage limit state	Damage level	Damage threshold limit (Sd)
Limit state 1	no damage	0.7S _{dy} (can be modified)
Limit state 2	slight damage	S _{dy} (intersection with nonlinear curve)
Limit state 3	moderate damage	1/8 S _u (S _u = ultimate displacement)
Limit state 4	extensive damage	S _d = 1/4 S _u
Limit state 5	complete damage	S _d = 1/2 S _u .

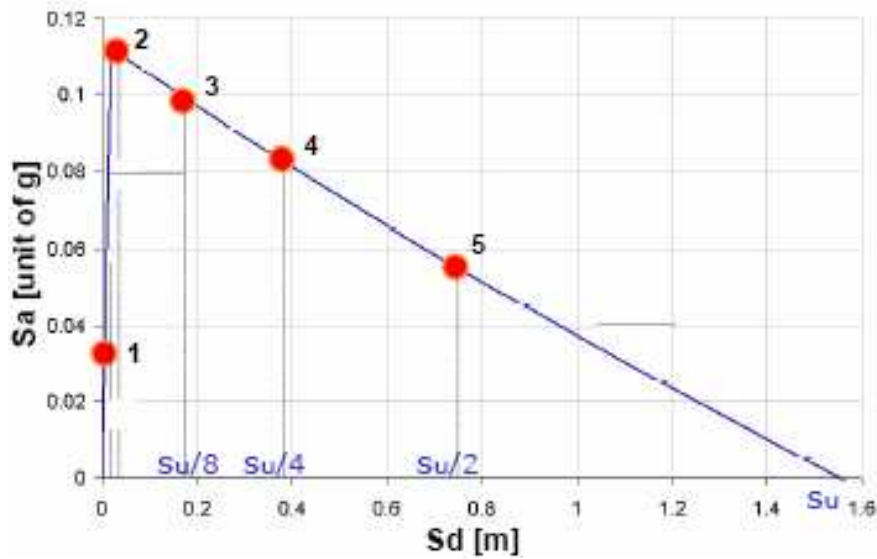


Figure 5.2 – Damage thresholds used by Irizarry (2004) for Santa Maria del Mar Church

5.2 Capacity spectrum

The capacity spectrum will be built from the capacity curve obtained in the static nonlinear pushover analysis, using a loading pattern according to the 1st mode of the structure. This curve is plotted in figure 5.3.

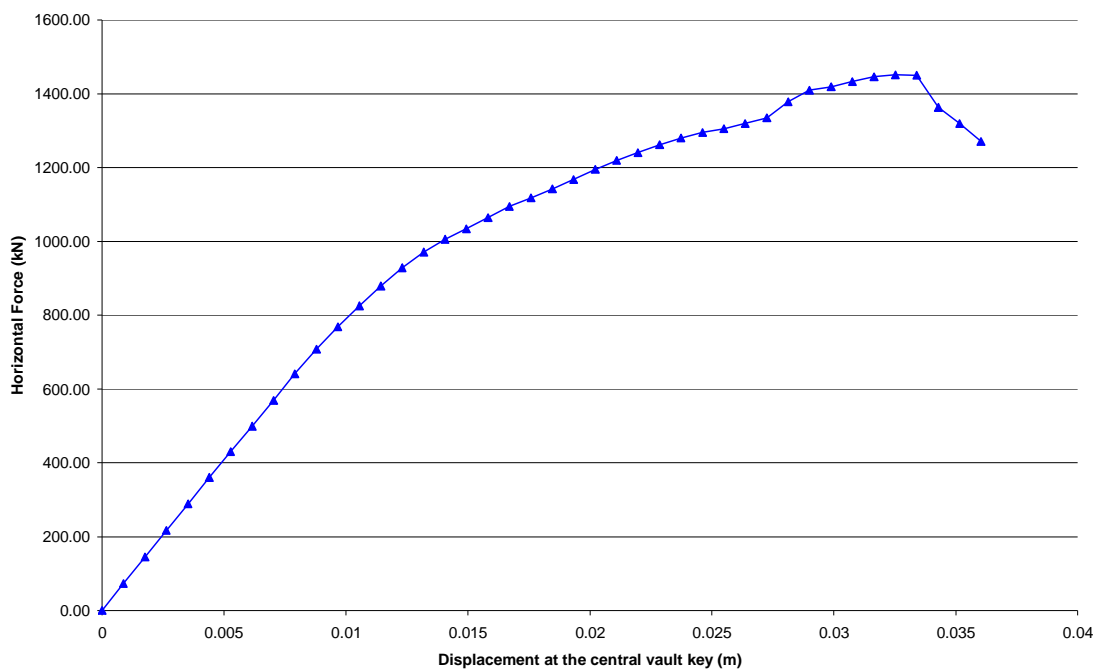


Figure 5.3 – Capacity curve of Santa Maria del Mar obtained with FEA

In order to transform it, the parameters were found for the 1st mode: $\alpha = 0.736$ and $PF\phi = 1.25$ $\phi = 0.89$. This curve is simplified to a bilinear relationship, trying to keep the same fracture energy (that is making the area integrated between both functions equal to 0). The resulting capacity spectrum, the simplified bilinear spectrum are plotted in figure 5.4. The capacity spectrum obtained by Roca (2007) is also plot. As shown, the bilinear functions have similar elastic limit and slope but differ a little bit in the maximum spectral acceleration.

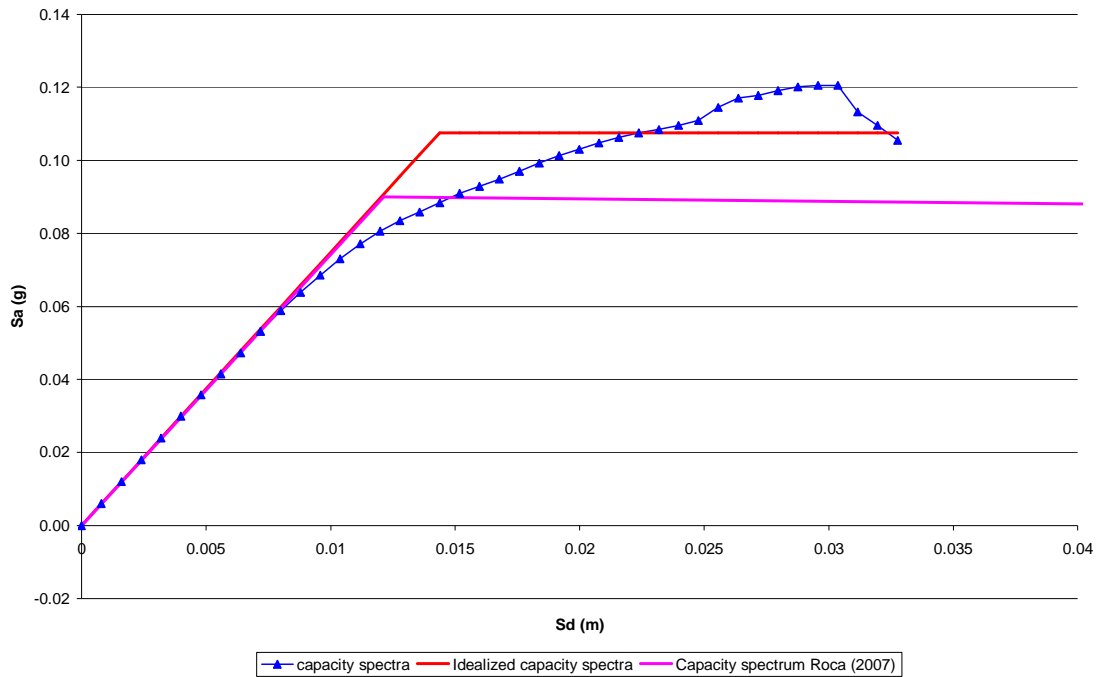


Figure 5.4 – Capacity spectrum of Santa Maria del Mar (obtained with FEA and simplified)

5.3 Demand spectra

Sta. Maria del Mar Church is located in an area of moderate earthquake hazard. In order to characterize the seismic demand for Sta. Maria del Mar the current Spanish Seismic Code (NCSE-02, 2002) has been considered. The same values assumed by Roca (2007) were used. The specific soil conditions of the location and a factor of 1.3 due to the importance of the building have been considered. Therefore, the basic acceleration corresponds to 0.04g while the acceleration for calculations reaches 0.18g in the elastic demand spectrum.

In addition, the demand spectra obtained by Irizarry (2004), using deterministic and probabilistic approaches, have been considered. These demand spectra are plotted in the following figure in terms of pseudoaccelerations (g) and pseudodisplacement (cm) for a return period T=500 years. All the demand spectra are plotted in figure 5.5.

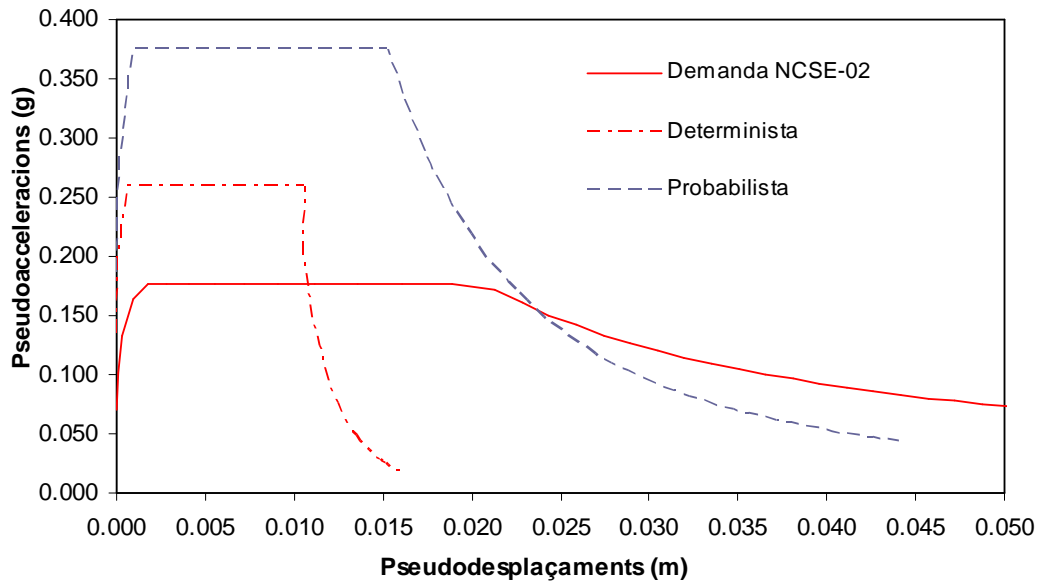


Figure 5.5 – Elastic demand spectra for Santa Maria del Mar location (Roca, 2007)

5.4 Performance point and damage estimation

The performance point was found for the three different demand spectra, by reducing the elastic demand spectra by the appropriate ductility, as shown in figures 5.6 to 5.8. The resulting displacements, associated ductility and expected damage are listed in table 5.2.

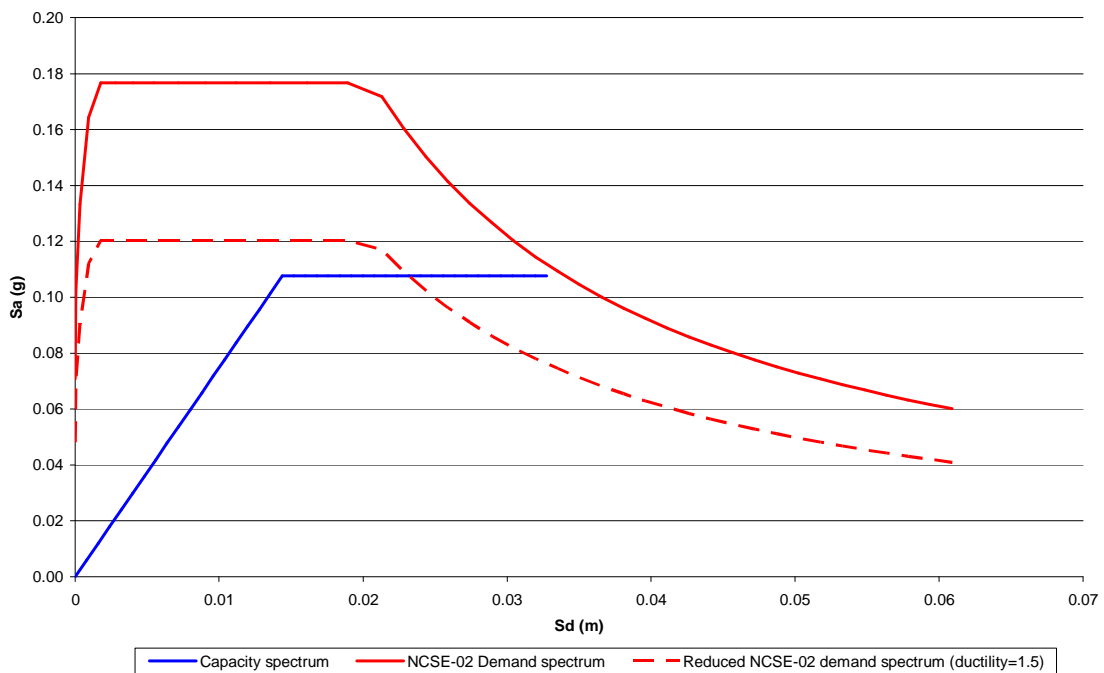


Figure 5.6 – Performance point for NCSE-02 demand spectrum

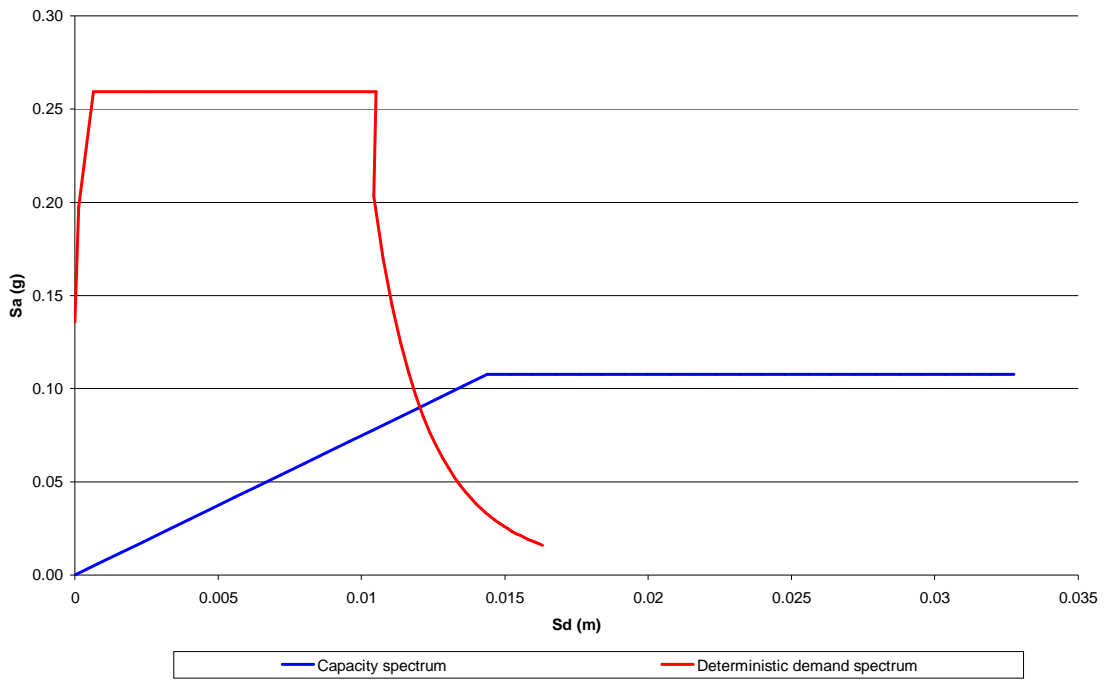


Figure 5.7 – Performance point for deterministic demand spectrum

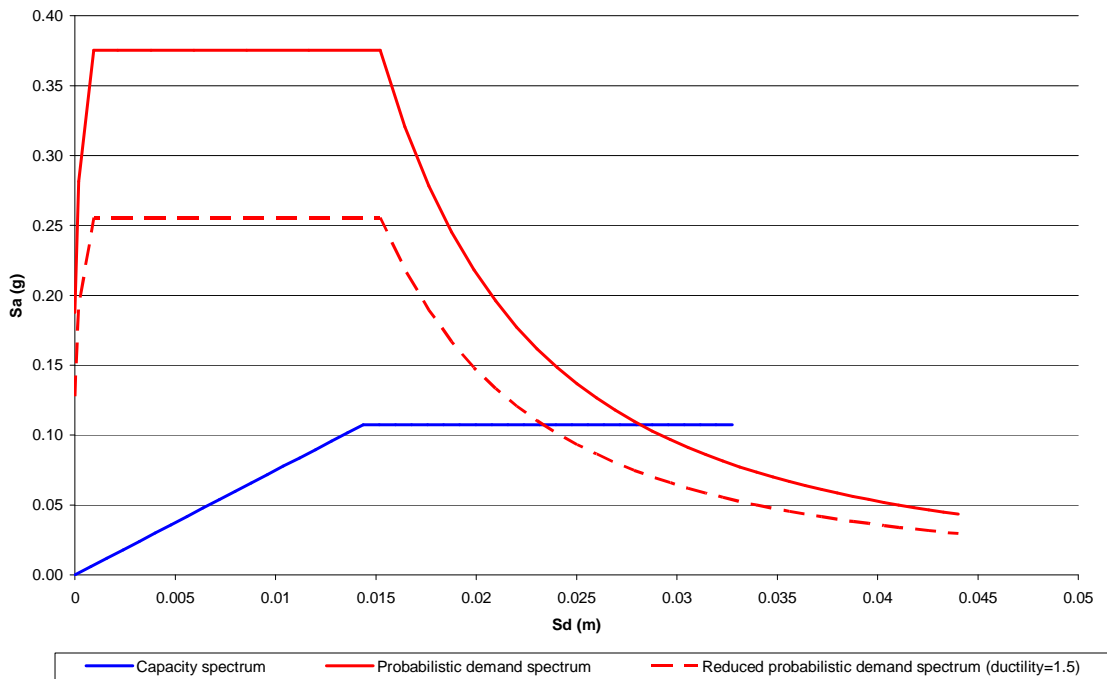


Figure 5.8 – Performance point for probabilistic demand spectrum

Table 5.2 – Spectral displacement, ductility and expected damage level

Demand spectrum	Spectral Displacement (m)	Ductility	Damage level For FEA $d_u=3.6\text{cm}$	Damage level For kinematic limit analysis $S_{du}=d_{K,0}=151\text{cm}$ (Roca, 2007)
NCSE-02	0.023	1.5	Severe ($S_d=0.64S_{du}$)	Moderate ($S_d=0.02S_{du}$)
Deterministic	0.012	-	Slight ($S_d=0.85S_{dy}$)	Slight ($S_d=0.85S_{dy}$)
Probabilistic	0.023	1.5	Severe ($S_d=0.64S_{du}$)	Moderate ($S_d=0.02S_{du}$)

The spectral displacement varies between 1.2 cm and 2.3cm, depending on the demand curve assumed. For the deterministic demand spectrum, the damage would be considered slight, as it is next but below the nonlinear range (no ductility associated). In the rest of cases, the damage level depends on the ultimate displacement of the structure. In this sense, the results obtained from FEA have a limitation as explained in chapter 4: it is not possible to reach the ultimate displacement numerically. Considering collapse at the last record before non convergence, the value for the displacement would be really low and not realistic, as the structure would still be able to rotate as a mechanism once damaged. In this case, the damage would be considered as severe. This makes no sense as it would be an enormous difference with the obtained result with the deterministic curve. Therefore, it is only possible to compare it with the ultimate displacements found by kinematics limit analysis $d_{K,0}$ (even if the model was a little bit different). In this case, the performance point would be far away from it, and the damage would be classified as moderate. Lagomarsino (2006) suggests assuming collapse at a 40% of the ultimate displacement found by kinematics limit analysis ($d_{K,0}$). The obtained performance point would be far away from that situation, the spectral displacement is less than a 4% than the collapse displacement.

Roca (2007) obtained very similar results for the performance point, using the NCSE-02 spectrum. For the limit analysis capacity spectrum the spectral displacement was 2.2 cm and the ductility 1.8. For the FEA capacity curve, the spectral displacement was 1.5 cm and the ductility 1.5. In both cases it meant slight to moderate damage. Irizarry (2004) obtained between 1.22 and 1.68 cm depending on the assumed demand spectrum (and an associated ductility between none to 3.0). Damages were also expected to be moderate.

The FEA showed a clear limitation to provide capacity curves to be applied in the Capacity Spectrum Method. The treatment of the structure as a continuum didn't permit to monitor the capacity curve when the structure is already a mechanism that rotates. In fact, this method is prepared for limit analysis where it is possible to obtain the complete curve.

In addition, there is a big scattering in the values, as the method is very sensible to the capacity and the demand spectra assumed. However, the results of this method have to be evaluated in a qualitative way. Therefore, the main conclusion is that there is coincidence among the

different studies in the qualitative estimation of damage: expected to be slight to moderate, and probably easily repairable.

The conclusions about the expected level of damage of the structure are in good agreement with the historical information. There is no evidence of important damages in the structure. It is true that the Church suffered some damage due to earthquakes: in 1373 the Eastern tower partially collapsed and in 1428 the rose window of the façade fell down. However, this damage is not related to the studied macro-element: the typical bay. From the current damage that the structure presented, there is no evidence of significant damage due to an earthquake. The main problems are related to weathering and past fires. Probably, earthquakes didn't cause important damage or the damaged was repaired in the past.

CHAPTER 6

Conclusions

A study of the seismic performance of the structure of Santa Maria del Mar Church has been done. This work has mainly involved a numerical analysis of the structure. However, additional evidence provided by History, inspection and monitoring of the structure have been taken into account. The conclusions extracted from each research level are presented in this chapter. Then, a final statement about the seismic performance of the structure is drawn. Finally, further developments to improve the knowledge on this structure are proposed.

6.1 State of the art in the study of the structure

Santa Maria del Mar church has a very important cultural value as it is a magnificent example of the Southern Gothic architecture. This building is characterized by having 3 naves and no transept, creating a very big internal space due to very slender columns and large span vaults. In addition, it is a slightly buttressed construction. The existing buttresses are thin and are integrated in the building, creating spaces for little chapels. No flying arches can be found in the structure. Instead, the lateral vaults are high enough to assumed their function and transfer the thrust from the central vault to the buttresses. As a result, they need of a load-resistant infill, made of medieval concrete. The central vault, in its turn, has a light infill made by ceramic pieces to reduce this thrust and the vertical load to the columns. These columns are very slender and have a massif ashlar masonry section. The walls and buttress are three-leaf elements, having an important rubble infill intermediate layer. The structure is founded in a poor soil, and shows some heterogeneity due to the pre-existence of some construction under the ground level.

Santa Maria del Mar Church started to be built in 1329 and was finished in 1383. There is evidence of two events causing damage in the structure during construction. In 1373 an earthquake caused the partial collapse of the Eastern tower. In 1378 there was an important fire that caused important damages in the interior of the church. In addition, the structure was damaged by an earthquake in 1427 (the rose window of the façade collapsed) and a fire in 1936, that affected some piers.

The most important damage nowadays visible in the structure are cracks and loss of material in the piers, related to the past fires. Beside the collapse of very specific elements (the rose window and the upper part of a tower), the structure is not thought to have suffered

considerable damage due to earthquake. Some crack patterns are visible in the façade and in the walls probably related to seismic action. The building is thought to have resisted an earthquake of VI (MSK) intensity, which could be associated to a ground peak acceleration of 0.04g (defined as the design PGA for Barcelona by the Spanish Seismic Code). However, this information is obtained indirectly and is not very reliable.

The studies carried out by Irizarry (2004) and Roca (2007) concluded that the structure is safe in terms of seismic hazard. By means of Limit Analysis and Finite Element Analysis, the seismic coefficient of the structure (maximum base shear / mass) was found to be between 0.09g and 0.14g. Slight to moderate damages would be expected in the structure due to an earthquake, from the application of the Capacity Spectrum Method. Roca (2007) carried out the study with more accurate information of the geometry, materials and the morphology. This data put the structure in a worse situation as the soil conditions were found to be poor and the existing infill of the lateral vaults contributed in a negative way to the seismic capacity of the structure. It was also found that the triangular walls above the lateral vaults contribute in a significant way to the seismic capacity of the structure.

6.2 Finite Element Analysis

The main contribution of this work to the study of Santa Maria del Mar Church is the numerical simulation of the seismic performance of the structure. A tension-compression damage model has been used to carry out a nonlinear Finite Element Analysis. Based in the theory of continuum damage, it takes into account the different behaviour of masonry under tension and compression. This model has already been satisfactorily used in similar studies and it is considered to be sufficiently accurate and relatively inexpensive in terms of computational cost for such a complex models. A controversial aspect of this model is the definition of the fracture energy associated to the softening behaviour of the material. Traditionally, very high values were used to ensure numerical convergence, but they can lead to an overestimation of the capacity of the structure. Instead, realistic values of fracture energy have to be assumed in order to obtain accurate results, and the use of numerical techniques should help to improve convergence.

A model of the typical bay of the structure has been analysed, using the data obtained Roca (2007). The model was calibrated using modal analysis, by adjusting the 1st mode of the structure to the experimental value. There was an attempt to adjust the following modes but it was not possible. This showed that the FEM it is just an approximation of the reality and there are limitations to take into account complex phenomena. On the other hand, the stresses in the piers matched well with the values obtained from the NDT "hole drilling" test.

The FEA of the structure subjected to gravity load revealed that the structure shows almost no damage and that it has an elevated safety margin (it could stand a load up to 3 times its self weight). The seismic behaviour of the structure was studied by means of a static nonlinear pushover. The structure was able to stand up to a seismic coefficient of 0.12g. This value is lower than the values found with FEA by Irizarry (2004) and Roca (2007), but is very close to the values obtained by Roca (2007) with Limit Analysis. A collapse mechanism was identified and a capacity curve was obtained to use it in the Capacity Spectrum Method. Their appearance was similar to the ones obtained by Irizarry (2004) and Roca (2007). But in this case, the central vault would not face important problems and would work as a solid, concentrating the damages in the top of the piers.

A sensitivity analysis of the model was carried out to define the influence of the different mechanical parameters. The compressive stress was found to be a determinant value when defining the vertical capacity of the structure, as the collapse was controlled by the crushing of the piers. However, in the range of possible values for the compressive strength (8MPa or more), the safety margin remains very big. It is exactly the same conclusion for the seismic capacity, for compressive strengths higher than 6MPa this parameter has no influence in the results. In the same way, the variability of the tensile strength has a small influence in the results. On the other hand, a realistic value for the fracture energy has to be assumed. Assuming an infinite value, practice done to ensure good numerical behaviour, leads to an overestimation the seismic capacity of the structure of 11%. However, it is not necessary to use very small values as numerical problems can appear.

Possible strengthening strategies were simulated numerically in a simplified way. The techniques follow quite well the modern principles of conservation (minimum intervention, respect to authenticity, non-invasiveness, etc). No seismic improvement was found in the used of an external transversal prestressing. The same result was obtained for the reinforcement with a metal beam of the triangular walls on top of the lateral vaults (these elements were found to be essential for the seismic behaviour of the structure). The only improvement was found by injecting the walls and buttresses with a lime mortar. However, the use of this technique cannot be justified because it provides a very small improvement, at most a 5% of the seismic coefficient.

6.3 Capacity Spectrum Method

The Capacity Spectrum Method was applied in order to evaluate the expected damage of the structure. The capacity spectrum obtained from the FEA was crosses with demand spectra obtained by previous studies. Different values for the performance point were found depending on the demand curve used: between 1.2 cm and 2.3cm. This scattering of values is common, as the method is sensible to little changes in the curves. The important point is the resulting

classification of the expected damage, based on displacement thresholds. In this sense, the FEA didn't work well for applying this method as it didn't provide a complete capacity spectrum up to the ultimate displacement. The treatment of the structure as a continuum didn't permit to monitor the capacity curve when the structure is already a mechanism that rotates.

Comparing the displacement spectrum with the ultimate displacements obtained by Irizarry (2004) and Roca (2007) using kinematic limit analysis, the damage would be expected to be slight to moderate. This is the same conclusion obtained this authors. The important point is that similar performance point and ductility level were obtained.

Finally, the conclusions about the expected level of damage of the structure are in good agreement with the historical information. Beside the problems with the rose window and one of the towers in the past, there is no evidence of important damages in the structure

6.4 Final conclusion on the seismic performance of the structure

The structure of Santa Maria del Mar Church can be considered safe and strong enough to resist the seismic action with acceptable levels of damage. The historical evidence and the inspection reflect not important damages due to earthquakes in the past. The numerical analysis showed that the structure could resist perfectly the seismic action in Barcelona, and the damage would be slight to moderate.

It has not been possible to find any light and respectful reinforcement in the structure that is able to provide an extra seismic capacity. Probably, only by doing a hard intervention the structure would be able to improve significantly its seismic performance. However, it is more convenient to accept and repair the slight to moderate damage caused by an earthquake, than assuming the elevated cultural cost of a hard intervention. It is only recommended to repair some currently damaged structural elements. Piers showing loss of material should recover their original cross-section. It is also recommended to ensure the integrity and proper connection of the triangular walls above the lateral walls, by doing punctual injections. They proper performance is important because they have been found to be important in the seismic capacity of the structure.

The FEA using a tension – compression damage model has been an accurate tool to analyse the structure with a nonlinear static pushover analysis. However, this is still a simplified analysis and didn't work well combined with the Capacity Spectrum Method.

6.5 Future developments

Future studies of Santa Maria del Mar church should investigate in more in depth the interaction between the different macro-elements and the soil conditions, in order to obtain more accurate perspective of the structural behaviour. In addition, the seismic performance should be evaluated by using more accurate and complex tools. For instance, nonlinear dynamic analysis should be done to validate other simplified results, as it is the only possibility to model the seismic action in a realistic way. Therefore, a possible study could be the nonlinear dynamic analysis of the complete structure including the soil conditions. This has to be combined with the use of more powerful computational tools, as the analysis can be very time-consuming nowadays.

Regarding the material constitutive model, the tension – compression damage model could be improved to represent better the masonry behaviour. The use of a tracking algorithm to represent better the cracking phenomena has already been implemented in other studies. Other features could also be added, as the anisotropic nature of masonry in the damage definition or the influence between compression and tension damage in reverse cycles.

References

CEN, European Committee for Standardisation (2005). Eurocode 6: Design of masonry structures. EN 1996-1-2:2005.

Cervera, M., Agelet de Saracibar, C., Chiumenti, M. (2002). COMET Data Input Manual v. 5.0. CIMNE, Barcelona.

Cervera, M. (2003). Viscoelasticity and rate-dependent continuum damage models. Monografía CIMNE. M79. CIMNE, Barcelona.

Clemente, R., (2006). Análisis estructural de edificios históricos mediante modelos localizados de fisuración. *Ph.D. Thesis*. Civil Engineering School of Barcelona, Technical University of Catalonia.

Clemente, R., Roca, P., Cervera, M. (2006). Damage model with crack localization. Application to historical buildings. *Structural Analysis of Historical Constructions V*, New Delhi.

Fajfar, P. (1999). Capacity Spectrum Method based on inelastic demand spectra. *Earthquake Engineering and Structural Dynamics*, 28.

Freeman, S. A. , Nicoletti, J.P. and J.V. Tyrell (1975). Evaluations of existing buildings for seismic risk - A case study of Puget Sound Naval Shipyard, Bremerton, Washington. *Proceedings of the 1st US National Conference on Earthquake Engineering*, Berkeley.

ICOMOS (2003). Recommendations for the Analysis, Conservation and Structural Restoration of Architectural Heritage. ISCARSAH Committee.

Irizarry, J., Modesta, S., Resemini, S. (2003). Curvas de capacidad para edificios monumentales: la iglesia Santa María del Mar de Barcelona. *2º Congreso Nacional de Ingeniería Sísmica*, Málaga.

Irizarry, J. (2004). An advanced approach to seismic risk assessment. Application to the cultural heritage and the urban system of Barcelona. *PhD. Thesis*. Civil Engineering School of Barcelona, Technical University of Catalonia.

Lagomarsino, S., Giovinazzi, S., Podestà, S., Resemini, S. (2002). WP5: Vulnerability assessment of historical and monumental buildings. *RISKUE: An advanced approach to earthquake risk scenarios with application to different European cities*. European Union Project.

Lagomarsino, S. (2006). On the vulnerability assessment of monumental Buildings. *Bull Earthquake Eng.*, 4:445–463.

Lourenço, P. (1996). Computational strategies for masonry structures. *Ph.D. Thesis*. Delft University.

Massanas, M. (2003). Análisis estructural de la Mezquita Pequeña Santa Sofía de Estambul. *Master Thesis*, Civil Engineering School of Barcelona, Technical University of Catalonia.

Massanas, M., Roca, P., Cervera, M., Arun, G. (2004). Damage model with crack localization. Application to historical buildings, Structural analysis of Küçük Ayasofya Mosque in İstanbul. *Structural Analysis of Historical Constructions IV*, Balkema, Amsterdam.

Mendoza, J. (2002). Análisis estructural de los pórticos tipo de la Catedral de Girona. *Master Thesis*. Civil Engineering School of Barcelona, Technical University of Catalonia.

NCSE-02 (2002). Normativa de Construcción Sismorresistente Española. Comisión Permanente de Normas Sismorresistentes, Real Decreto 997/2002. Boletín Oficial del estado 244.

Roca,P. (2007). Basílica de Santa Maria del Mar: estudi de l'estructura. Technical University of Catalonia.

UE-India Project: Improving the seismic resistance of Cultural Heritage Buildings (2006). Identification of Strengthening Strategies. EU-India Economic Cross Cultural Programme, Universidade do Minho.

Vendrell, M., Giràldez, P., Caballé, F., González, R., Roca, P. (2007). Estudi històrico-constructiu, materials de construcció i estabilitat estructural de Santa Maria del Mar. Departament de Cultura i Mitjans de Comunicació, Generalitat de Catalunya.

